CHEMICAL REVIEWS

Predictive Molecular Thermodynamic Models for Liquid Solvents, Solid Salts, Polymers, and Ionic Liquids

Zhigang Lei, Biaohua Chen, Chengyue Li, and Hui Liu

More About This Article

Additional resources and features associated with this article are available within the HTML version:

- Supporting Information
- Access to high resolution figures
- Links to articles and content related to this article
- Copyright permission to reproduce figures and/or text from this article

View the Full Text HTML

ACS Publications
High quality. High impact.

Predictive Molecular Thermodynamic Models for Liquid Solvents, Solid Salts, Polymers, and Ionic Liquids

Zhigang Lei,* Biaohua Chen,* Chengyue Li, and Hui Liu

State Key Laboratory of Chemical Resource Engineering, Beijing University of Chemical Technology, Box 35, Beijing, 100029 China

Contents

1. Introduction

Generally, molecular thermodynamic models for treating the phase equilibria of solutions can be classified into two categories: activity coefficient relations and equations of state. The term "predictive molecular thermodynamic models" has no unified definition thus far, although many researchers use it in their papers. In this context, it means the types of models that phase equilibria can be described as, provided that molecular structures or physical properties of pure components in the mixture are known. The models of this type include the activity coefficient model:

(i) Solvent−solvent systems with low molecular weight: the UNIFAC model and its revisions; MOSCED model, SPACE model; DISQUAC model; Pierotti−Deal−Derr model; Weimer−Prausnitz model; Prausnitz and Anderson theory;

(ii) Solvent−solid salt systems: the improved UNIFAC model; scaled particle theory;

(iii) Solvent−polymer systems: entropic-FV/UNIFAC model; UNIFAC-FV model, GK-FV model; UNIFAC-ZM model; FH/Hansen model;

(iv) Solvent−ionic liquid system: the COSMO-RS model and the equations of state;

(v) Solvent−solvent systems with low molecular weight: PSRK model; MHV2 model; LCVM model, W−S model; UNIWAALS model; GCEOS model; and

(vi) Solvent−polymer systems: GC-Flory EOS model; GCLF EOS model.

For solvent−polymer systems, equations of state are preferred over activity coefficient models because equations of state can disclose the dependence of phase volume on

* To whom correspondence should be addressed. Tel: +86 10 64433695. Fax: +86 10 64419619. E-mail: leizhg@mail.buct.edu.cn; chenbh@mail.buct.edu.cn.
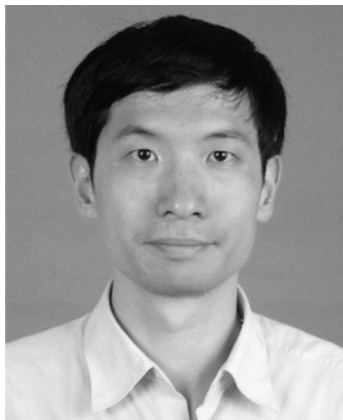
Professor Zhigang Lei was born in Hubei province (China) in 1973. He received his B.S. degree in 1995 from Wuhan Institute of Technology, and his Ph.D. degree in 2000 from Tsinghua University. Later, he was a postdoctoral member at Beijing University of Chemical Technology working with Professor Chengyue Li. In 2003–2005, he worked as a researcher at the Research Center of Supercritical Fluid Technology (Tohoku University, Sendai, Japan). In 2005–2006 he received the world-famous Humboldt Fellowship and carried out his research as the Chair of Separation Science and Technology (Universität Erlange-Nürnberg, Erlangen, Germany). In 2006, he gave up the world-famous JSPS Fellowship and came back to China. He is now a Professor in the State Key Laboratory of Chemical Resource Engineering (BUCT, China). His current research interests include process intensification in chemical engineering and its molecular thermodynamics. He has contributed to more than 30 papers as the first author or corresponding author in international journals and to one book entitled *Special Distillation Processes*.

Professor Biaohua Chen was born in Jiangxi province (China) in 1963. He is a member of the Standing Committee of the Beijing Chemical Industry Association and a member of the Editorial Board of the *Journal of Petrochemical Universities* (China). In 2000, he was a visiting scholar at Washington University in St. Louis and the University of Washington. He has received two National Science and Technology Progress Prizes (second class), and one Natural Science Progress Prize. His main research interests are industrial catalysis, new reactor technology, and green chemistry and technology. He has contributed to about 100 papers in national and international journals.

Professor Chengyue Li is a prestigious scientist who continues to work at Beijing University of Chemical Technology. His main research interests are chemical reactor unsteady-state operations and reactor dynamics, green chemical technology, and structured catalysts and reactors. He has received a National Science and Technology Progress Prize (second class), a State Prize for Outstanding Educational Achievement (first class), two Ministry Science and Technology Prizes (first class), and a Chinese Universities Natural Science Prize (second class). He has contributed to about 250 papers in national and international journals. He has edited one monograph and translated one book into Chinese. He was formerly an Executive Editor of *Journal of Chemical Industry and Engineering* (China) and a member of the Academic Committees of the State Key Laboratories of Fundamental Catalysis, Chemical Engineering and Heavy Oil Processing (China).

Professor Hui Liu was born in Gansu Province (China) in 1964. He received his B.S. degree in 1984, M.S. degree in 1989, and Ph.D. in 1996, all from the Chemical Engineering Department of Tianjin University. He has been working in the College of Chemical Engineering of BUCT since 1998. He was awarded a Chinese Higher Education Institution Prize for Natural Science (second class). His main research interests are multiphase reaction engineering, including experimental investigation and performance modeling of bubble column reactors and multiphase ejecting type bioreactors, measurement of multiphase flow and mass transfer properties in low- and high-pressure trickle beds, hydrogenation kinetics of gasoline, and theory and measurement of intracrystalline diffusion in zeolites, etc. He has contributed to more than 20 papers in international journals.

pressure, which is especially important in estimating the solubility, swelling degree, and crystallinity of polymers in polymer processing.

Undoubtedly, predictive molecular thermodynamic models are very important in separation processes and polymer processing. In the separation processes (e.g., extractive distillation, liquid−liquid extraction, absorption, etc.), a third solvent is commonly needed to add into the components to be separated so as to improve the separation factor.[1,2] So the solvent (entrainer or separating agent) is the core, and a

suitable solvent plays an important role in the economical design of separation processes. However, it is tiresome to choose the best solvent from thousands of different substances for a given system through experiments. We should identify the relation between molecular structure of the solvent and separation performance. In this case, predictive molecular thermodynamic models are used as a screening tool to find out the best suited solvent rapidly. Only on this

basis is the best suited solvent synthesized so as to largely reduce the amount of experimental work. By means of predictive molecular thermodynamic models, the materials including liquid solvents, solid salts, polymers, and ionic liquids can be regarded as "designer solvents" in separation processes. That is to say, the molecules are split into groups, and once a potential molecular satisfying the property specifications is screened, the chemists are required to synthesize it for a given separation task. It is beyond our scope to review how to synthesize the specified liquid solvents, solid salts, polymers, and ionic liquids.

In polymer processing (e.g., microcellular foam production, plasticization in blending and injection molding, surface modification, dyeing, and PGSS (particles from gas-saturated solutions) process),[3-11] gas (e.g., carbon dioxide (CO_2)) is being used as a physical blowing agent. The thermodynamic properties, such as gas solubility in the polymer, polymer density, and polymer crystallinity, play an important role in controlling the nature of the functional materials, since these affect, for instances, particle size distribution and shape in PGSS process and thermal conductivity, weight, and impact strength or toughness in foaming processing. For such processes, the thermodynamic properties sometimes are difficult to measure experimentally, especially under extreme conditions (very high pressure and very low temperature), and thus, a predictive model is indispensable.

The predictive molecular thermodynamic models also can be classified into two categories: the models with relation to experimental data; for example, the UNIFAC model in which the interaction parameters are correlated from experimental data and prediction of thermodynamic properties is made on the basis of existing parameters for the constituent atomic groups of the molecules present in the mixture; and the models with no relation to experimental data (or called priori predictive models); for example, the COSMO-RS model in which only atom-specific parameters are required and prediction of thermodynamic properties is made on the basis of unimolecular quantum chemical calculations that provide the necessary information for the evaluation of molecular interactions in liquids. The COSMO-RS model is a novel and efficient method for the priori prediction of thermophysical data of liquids and has been developed since 1994. It is especially suitable for solvent−ionic liquid systems.

This review is devoted to the systematic introduction of predictive molecular thermodynamic models for different systems. The contents are arranged in the series of solvent−solvent systems with low molecular weight, solvent−solid salt systems, solvent−polymer systems, and solvent−ionic liquid systems step by step. In Section 2. we first introduce the well-known UNIFAC model, which is especially suitable for simple solvent molecules with low molecular weight and is incorporated into CAMD, where the UNIFAC groups provide building blocks for assembling molecules. Then, the extension of the UNIFAC model to solvent−solid salt systems, as well as scaled particle theory, which is an a priori predictive model and related to salt effect, is introduced in Section 3. There are many predictive molecular thermodynamic models available for the prediction of the thermodynamic properties of polymer−solvent systems. But the group-contribution lattice−fluid equation of state (GCLF EOS) has unique features. The only input required for this model is the molecular structures of the polymer and solvent in terms of their functional groups. It does not require accurate density

data for the solvent and polymer and can predict the pressure effect. Therefore, the GCLF EOS and its applications in polymer processing are emphasized in Section 4. Afterward, the COSMO-RS model is introduced to tailor the suitable ionic liquid for the separation of nonpolar, polar, and polar−weakly polar systems in Section 5. Since both the COSMO-RS model and UNIFAC model are suitable for the prediction of phase equilibria for solvent−solvent systems, the comparison of the predictive results between these two models is interesting. Finally, the conclusion remarks are given in Section 6.

2. Solvent−Solvent Systems with Low Molecular Weights

2.1. UNIFAC Models

From the classic thermodynamics, we know that the activity coefficient is introduced as the revision and judgment for the nonideality of the mixture.[12-20] If the activity coefficient is equal to unity, it means that the interactions between dissimilar or same molecules are always identical, and the mixture is in the ideal state; if the activity coefficient is away from unity, the mixture is in the nonideal state. The concept of activity coefficient is often used for the liquid phase. The activity coefficient in the liquid phase must be determined so as to derive the equilibrium ratio, K_i, and relative volatility, α_{ij}, and thus establish the mathematical models of chemical engineering processes. the liquid-phase activity coefficient models are set up on the basis of excess Gibbs free energy. The relation of the activity coefficient, γ_i, and excess Gibbs free energy, G^E, is given below:

$$\left[\frac{\partial(nG^E)}{\partial n_i}\right]_{T,P,n_j} = RT \ln \gamma_i \qquad (2.1)$$

$$n = \sum_i n_i \qquad (2.2)$$

The liquid-phase activity coefficient models are divided into two categories: (1) The models are suitable for the nonpolar systems; for instance, hydrocarbon mixture, isomers, and homologues. Those include regular solution theory (RST) and the Flory−Huggins no-heat model.[21-26] (2) The models are suitable for nonpolar and polar systems. Those models are commonly used to predict the liquid-phase activity coefficient and include the Margules equation, van Laar equation, Wilson equation, NRTL (nonrandom two liquids) equation, UNIQUAC (universal quasichemical) equation, UNIFAC (UNIQUAC Functional-group activity coefficients) equation, and so on.

Among those, the Wilson, NRTL, UNIQUAC, and UNIFAC models are the most widely used for binary and multicomponent systems because of their flexibility, simplicity, and ability to fit many polar and nonpolar systems. In addition, one outstanding advantage of those equations is that they can be readily extended to predict the activity coefficients of a multicomponent mixture from the corresponding binary-pair parameters. In fact, in most separation processes, a multicomponent mixture is often involved.

However, in the Wilson, NRTL, and UNIQUAC models, the experimental data must be given to correlate the binary-pair parameters. Therefore, they are not purely predictive

models, as defined above. But the UNIFAC model, in which no binary data are required, is a widely used predictive model. This model is currently very popular and can be used to predict the liquid phase activity coefficient of binary or multicomponent systems, even when the experimental phase equilibrium data are unavailable. It has several advantages over the Wilson, NRTL, and UNIQUAC equations: (1) Size and binary interaction parameters are available for a wide range of types of function groups (more than 100 function groups). (2) Extensive comparisons with experimental data are available. (3) It is an open system, and more function groups and more parameters will be filled in the UNIFAC list in the future. But it still has a problem; that is, the ions (cation and anion groups) are not complete in the UNIFAC menu. In particular, in the recent years, ionic liquids have attracted more attention in separation processes, which will be mentioned later. (4) Experimental measurements of vapor−liquid phase equilibrium are very time-consuming and therefore expensive. For example, if measurements are performed for a 10-component system at just one constant pressure (e.g., atmospheric pressure) in 10% mole steps and an average number of 10 data points can be experimentally determined daily, the measurements (in total, 92 378 data points) will take more than 37 years.[27] Therefore, with the view to multicomponent mixtures, the UNIFAC model is more advantageous than the Wilson, NRTL, and UNIQUAC models in saving the measurement time. That is why it was very popular and desirable in the synthesis, design and optimization of separation processes over the past few years.[340] The UNIFAC model is still developing, and by far, there are three versions for solvent−solvent systems with low molecular weights.

2.1.1. History of Group Contribution Methods

The earliest group-contribution method for predicting activity coefficients is the ASOG (analytical solution of groups) model that was proposed by Deal and Derr[28−32] and used the Wilson model to represent the group activity coefficients. The ASOG model treats a solution as a mixture of various structural groups, as opposed to a mixture of two or more distinct compounds. This treatment has the inherent advantage that there are significantly fewer structural groups than compounds; hence, fewer parameters are needed for a large number of binary and multicomponent mixtures. However, by far, the group interaction parameters for only 43 groups and 341 group pairs are available in the parameter matrix of ASOG model, which frequently cannot meet the requirement for the systems in which the group interaction parameters are missing.

An original UNIFAC model that combines the functional group concept with a model for activity coefficients based on an extension of the quasi chemical theory of liquid mixtures (UNIQUAC) was proposed by Fredenslund et al. in 1975.[33] This model can be applied at infinite dilution and finite concentrations and was the most widely used before several revisions and extensions were developed.[34−40] The activity coefficient is expressed as functions of composition and temperature. The model has a combinatorial contribution to the activity coefficient, , that is, $\ln \gamma_i^C$, essentially due to differences in size and shape of the molecules, and a residual contribution, , that is, $\ln \gamma_i^R$, essentially due to energetic interactions:

$$\ln \gamma_i = \ln \gamma_i^C + \ln \gamma_i^R \qquad (2.3)$$

I. Combinatorial part.

$$\ln \gamma_i^C = 1 - V_i + \ln V_i - 5q_i\left(1 - \frac{V_i}{F_i} + \ln\left(\frac{V_i}{F_i}\right)\right) \qquad (2.4)$$

$$F_i = \frac{q_i}{\sum_j q_j x_j}, \qquad V_i = \frac{r_i}{\sum_j r_j x_j} \qquad (2.5)$$

The pure component parameters r_i and q_i are, respectively, relative to molecular van der Waals volumes and molecular surface areas. They are calculated as the sum of the group volume and group area parameters, R_k and Q_k,

$$r_i = \sum_k v_k^{(i)} R_k, \qquad q_i = \sum_k v_k^{(i)} Q_k \qquad (2.6)$$

where $v_k^{(i)}$, always an integer, is the number of groups of type k in molecule i. Group parameters R_k and Q_k are normally obtained from van der Waals group volumes and surface areas, V_k and A_k, given by Bondi.[41]

$$R_k = \frac{V_k}{15.17}, \qquad Q_k = \frac{A_k}{2.5 \times 10^9} \qquad (2.7)$$

II. Residual Part.

$$\ln \gamma_i^R = \sum_k v_k^{(i)}[\ln \Gamma_k - \ln \Gamma_k^{(i)}] \qquad (2.8)$$

Γ_k is the group residual activity coefficient, and $\Gamma_k^{(i)}$ is the residual activity coefficient of group k in a reference solution containing only molecules of type i.

$$\ln \Gamma_k = Q_k[1 - \ln(\sum_m \theta_m \psi_{mk}) - \sum_m (\theta_m \psi_{km}/\sum_n \theta_n \psi_{nm})] \qquad (2.9)$$

$$\theta_m = \frac{Q_m X_m}{\sum_n Q_n X_n}, \qquad X_m = \frac{\sum_i v_m^{(i)} x_i}{\sum_i \sum_k v_k^{(i)} x_i} \qquad (2.10)$$

X_m is the fraction of group m in the mixture.

$$\psi_{nm} = \exp[-(a_{nm}/T)] \qquad (2.11)$$

The parameter a_{nm} characterizes the interaction between groups n and m. For each group−group interaction, there are two parameters: $a_{nm} \neq a_{mn}$.

Equations 2.9 and 2.10 also hold for $\ln \Gamma_k^{(i)}$, except that the group composition variable, θ_k, is now the group fraction of group k in pure fluid i. In pure fluid, $\ln \Gamma_k = \ln \Gamma_k^{(i)}$, which means that as $x_i \to 1$, $\gamma_i^R \to 1$. γ_i^R must be close to unity because as $x_i \to 1$, $\gamma_i^C \to 1$ and $\gamma_i \to 1$.

2.1.2. The Modified UNIFAC Model

The modified UNIFAC model can be applied at infinite dilution and finite concentration.[42−46,339] As in the original UNIFAC model, the activity coefficient in the modified UNIFAC model is also the sum of a combinatorial and a residual part (see eq 2.3).

The combinatorial part is changed in an empirical way to make it possible to deal with compounds very different in size:

$$\ln \gamma_i^C = 1 - V_i' + \ln V_i' - 5q_i\left(1 - \frac{V_i}{F_i} + \ln\left(\frac{V_i}{F_i}\right)\right) \quad (2.12)$$

The parameter V_i' can be calculated by using the relative van der Waals volumes R_k of the different groups:

$$V_i' = \frac{r_i^{3/4}}{\sum_j x_j r_j^{3/4}} \quad (2.13)$$

All other parameters are calculated in the same way as in the original UNIFAC model:

$$V_i = \frac{r_i x_i}{\sum_j x_j r_j} \quad (2.14)$$

$$r_i = \sum v_k^{(i)} R_k \quad (2.15)$$

$$F_i = \frac{q_i x_i}{\sum_j x_j q_j} \quad (2.16)$$

$$q_i = \sum v_k^{(i)} Q_k \quad (2.17)$$

The residual part can be obtained by using the following relations:

$$\ln \gamma_i^R = \sum_k v_k^{(i)}(\ln \Gamma_k - \ln \Gamma_k^{(i)}) \quad (2.18)$$

$$\ln \Gamma_k = Q_k\left(1 - \ln(\sum_m \theta_m \psi_{mk}) - \sum_m \frac{\theta_m \psi_{km}}{\sum_n \theta_n \psi_{nm}}\right) \quad (2.19)$$

whereby the group area fraction, θ_m, and group mole fraction, X_m, are given by the following equations:

$$\theta_m = \frac{Q_m X_m}{\sum_n Q_n X_n} \quad (2.20)$$

$$X_m = \frac{\sum_j v_m^{(j)} x_j}{\sum_j \sum_n v_n^{(j)} x_j} \quad (2.21)$$

In comparison to the original UNIFAC model, the van der Waals properties are changed slightly, and at the same time, temperature-dependent parameters are introduced to permit a better description of the real behavior (activity coefficients) as a function of temperature.

$$\psi_{nm} = \exp\left(-\frac{a_{nm} + b_{nm}T + c_{nm}T^2}{T}\right) \quad (2.22)$$

Thus, to calculate the activity coefficient, such parameters

as R_k, Q_k, a_{nm}, b_{nm}, c_{nm}, a_{mn}, b_{mn}, and c_{mn} should be predetermined. Since the existing parameters of the modified UNIFAC model are extended with the help of the Dortmund Data Bank (DDB) and the integrated fitting routines, even the values of R_k and Q_k are possibly different from those in the original UNIFAC model. As the group parameters are replenished step by step, this model has the tendency to substitute the original UNIFAC model because of its better predictions of the real behavior of nonelectrolyte systems and its importance in chemical process development. The present status of all research concerning the modified UNIFAC model (Dortmund) is always available via the Internet at http://www.uni-oldenburg.de/tchemie/consortium or http://www.unifac.org.

Gmehling et al.[42] compared the calculated results between the ASOG and the UNIFAC models; however, the number of main groups and available group interaction parameters is very different for these models. There is also a difference in the total number of systems that can be predicted by the different methods. With the original and the modified UNIFAC models, more systems can be predicted than with the ASOG model. Therefore, the comparison was limited to the number of systems that could be calculated by all of the models. From the results, it was found that the modified UNIFAC model gives the best results; the original UNIFAC model, the second; and the ASOG model, the last.

2.1.3. The $\gamma\infty$-Based UNIFAC Model

This UNIFAC model is appropriate only at infinite dilution (therefore called the γ^∞-based UNIFAC model).

A UNIFAC parameter table exclusively based on γ^∞ data is presented by Bastos et al.[47] It aims at the improvement of the general accuracy and range of applicability of the UNIFAC model as far as the calculation for γ^∞ and S^∞ values is involved. Therefore, it can be regarded as a useful supplement to the existing vapor−liquid equilibrium (VLE) and liquid−liquid equilibrium (LLE) parameters.

The 190 pairs of parameters of 40 different groups have been estimated from ∼8000 data points on the basis of experimental γ^∞ data, with an average relative error of 20%. The equation forms, as well as the values of R_k and Q_k, are the same as in the original UNIFAC model. The difference between these two models is only the interaction parameters of the UNIFAC groups. However, the weakness of the UNIFAC models (including three versions) is that the proximity effects cannot be distinguished in the calculated results, which does not conform to the real situation.

2.2. MOSCED and SPACE Models

The MOSCED and the SPACE models do not adopt the group concept, but instead, use only pure component parameters to predict liquid-phase activity coefficients. The MOSCED (modified separation of cohesive energy density) model is an extension of RST (regular solution theory) to mixtures that contain polar and hydrogen-bonding components.[48−53] The cohesive energy density is separated into dispersion forces, dipole forces, and hydrogen bonding, with small corrections made for asymmetry. The dipolarity and hydrogen bond basicity and acidity parameters are correlated on the basis of a limited database of activity coefficients. By using the expression for the cohesive energy density and accounting for the asymmetry effect, the activity coefficient at infinite dilution for component 2 in solvent 1 is written as

$$\ln \gamma_2^\infty = \frac{v_2}{RT}\left[(\lambda_1 - \lambda_2)^2 + \frac{q_1^2 q_2^2(\tau_1 - \tau_2)^2}{\psi_1} + \right.$$
$$\left. \frac{(\alpha_1 - \alpha_2)(\beta_1 - \beta_2)}{\xi_1}\right] + d_{12} \quad (2.23)$$

where λ is a measure of a molecule's polarizability; τ represents its polarity; α and β are, respectively, acidity and basicity parameters; q is a measure of the dipole−induced dipole energy; ψ and ξ interpret the asymmetry effect; v is molar volume; and d_{12} is a Flory−Huggins term that is usually minor anyway. The outstanding characteristic of this model is that it can predict activity coefficients at infinite dilution using only pure component parameters, which are available in the parameter table.

The SPACE (solvatochromic parameters for activity coefficients estimation) method, proposed by Hait et al.,[54−56] uses a much larger database and recently established scales of solvent and solute dipolarity and hydrogen bonding.[57−60] The SPACE equation assumes additivity and independence of the various contributions to the cohesive energy density: (1) dispersion, (2) dipolar interactions, (3) hydrogen-bonding interactions, and (4) size differences:

$$\ln \gamma_2^\infty = \frac{v_2}{RT}[(\lambda_1 - \lambda_2)^2 + (\tau_1 - \tau_{2\text{eff}})^2 + $$
$$(\alpha_1 - \alpha_{2\text{eff}})(\beta_1 - \beta_{2\text{eff}})] + d_{12} \quad (2.24)$$

where the meanings of physical quantities refer to eq 2.23. But the SPACE model uses effective values for solute parameters ($\tau_{2\text{eff}}$, $\alpha_{2\text{eff}}$, $\beta_{2\text{eff}}$), which are calculated by a linear interpolation of the SPACE solvent (1) and solute (2) parameters. Unfortunately, the complete SPACE parameters for all compounds studied are provided only in the supplementary material that must be ordered from the specified institution.[54]

Castells et al.[56] investigated five kinds of liquid-phase activity coefficient models (three versions of UNIFAC model mentioned above, MOSCED, and SPACE models) for predicting infinite dilution activity coefficients γ^∞ of five linear, four branched, and two cyclic alkanes in 67 solvents at 25 °C, and the results were compared with experimental data. For a database of 737 limiting activity coefficients, the SPACE model gives an average absolute error of 8.1%, and in only 13.3% of the cases are the errors worse than 15%. The modified UNIFAC model gives an absolute average error of 9.8%, and 32% of the predicted γ^∞ have errors larger than 15%. On the whole, the UNIFAC and γ^∞-based UNIFAC models perform comparably. Although it is created specifically for the task of estimating γ^∞, the γ^∞-based UNIFAC model does not give as good a prediction as might be expected.

We applied three versions of UNIFAC model (the original UNIFAC model, the modified UNIFAC model, and the γ^∞-based UNIFAC model) to estimate the liquid-phase activity coefficients of the key components of n-butane and 1-butene at infinite dilution in the solvent DMF (N,N-dimethylformamide) and compared the calculated and experimental values at different temperatures (see Figure 1). It shows that the calculated values of the modified UNIFAC model correspond the best to the experimental data, with the average relative deviation (ARD) of 3.06%. The ARDs of the original UNIFAC model and the γ^∞-based UNIFAC model are up to 11.84 and 17.17%, respectively.

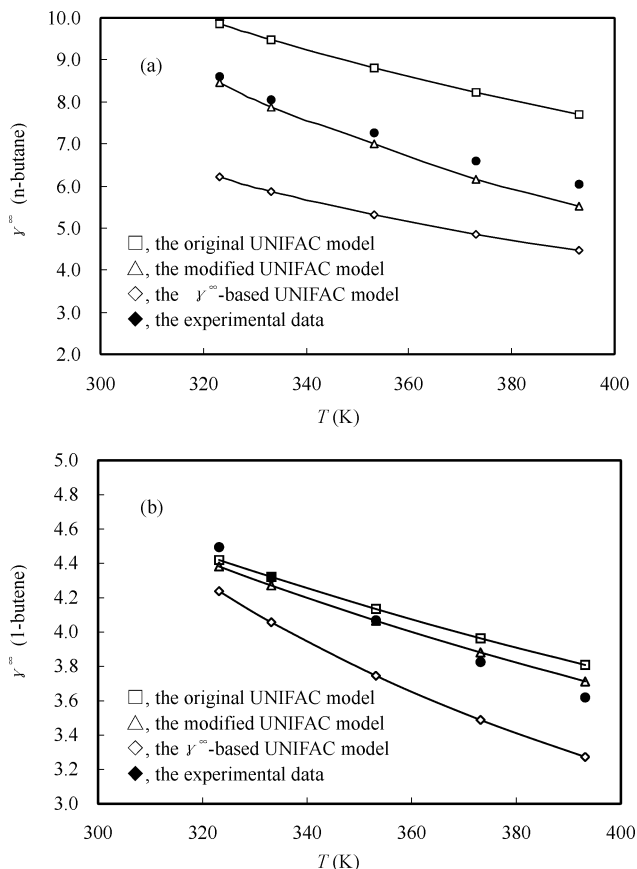**Figure 1.** Activity coefficients of n-butane (a) and 1-butene (b) in DMF (N,N-dimethylformamide) at infinite dilution at different temperatures. The calculated results from three versions of UNIFAC model are compared with those from experiments.[333]

None of these models is sensitive enough to deal with the experimental difference of γ^∞ between branched and linear isomers in polar solvents.

2.3. CAMD

In separation processes, the ease of separation of a given mixture with key components i and j is given by the relative volatility:

$$\alpha_{ij} = \frac{y_i/x_i}{y_j/x_j} = \frac{\gamma_i P_i^0}{\gamma_j P_j^0} \quad (2.25)$$

where x is molar fraction in the liquid phase, y is molar fraction in the vapor phase, γ is the activity coefficient, and P_i^0 is the pure component vapor pressure.

The solvent is often introduced to change the relative volatility as far away from one as possible when the components of the mixture to be separated have similar boiling points or form an azeotrope. Since the ratio of P_i^0/P_j^0 is constant for small temperature changes, the only way that the relative volatility is affected is by introducing a solvent that changes the ratio γ_i/γ_j. This ratio, in the presence of the solvent, is called selectivity, S_{ij}:

$$S_{ij} = \left(\frac{\gamma_i}{\gamma_j}\right)_s \quad (2.26)$$

In some cases, a significant change in the operation temperature and pressure alters a_{ij} enough to eliminate an

Table 1. Attachment Type Characterization of UNIFAC Groups

attachment type	groups			
(N, 0)	CH_3OH	CH_3NO_2	H_2O	CH_3NH_2
	CF_3	CH_3SH	CH_3CN	furfural
	$HCOOH$	$DMSO$	$(CH_2OH)_2$	CH_2Cl_2
	$CHCl_3$	$ACRY$	DMF	NMP
	CH_3NH_2	CS_2	CCl_3F	$CHCl_2F$
	$CHClF_2$	$CClF_3$	CCl_2F_2	C_4H_4S
	morph	$AmHCH_3$	$Am(CH_3)_2$	
(M, 1)	(CH_3)			
(J, 2)	(CH_2)			
(L, 1)	(CH_2Cl)			
(L, 2)	$(CHCl)$			
(K, 1)	$(CH_2$=$CH)$	(OH)	(CH_3CO)	(CHO)
	(CH_3COO)	$(HCOO)$	(CH_3O)	(CH_2NH_2)
	(CH_3NH)	(C_5H_4N)	(CH_2CN)	$(COOH)$
	$(CHCl_2)$	(CCl_3)	(CH_2NO_2)	(CH_2SH)
	(I)	(BR)	(CHC)	$Cl-(C$=$C)$
	(SiH_3)			

attachment type	groups			
(K, 2)	$(CH$=$CH)$	$(CH_2$=$C)$	(CH_3N)	(C_5H_3N)
	(CCl_2)	$(CHNO_2)$	(CC)	$(DMF\text{-}2)$
	(COO)	(SiH_2)	(SiH_2O)	
(K, 1), (L, 1)	(CH_2CO)	(CH_2COO)	(CH_2O)	
	(CH_2NH)	(FCH_2O)		
(I, 1)	(ACH)	(ACF)		
(H, 1)	$(ACCH_3)$	$(ACOH)$	$(ACNH_2)$	$(ACCl)$
	$(ACNO_2)$			
(H, 1), (M, 1)	$(ACCH_2)$			
(H, 1), (J, 2)	$(ACCH)$			

azeotrope, so the solvent (called entrainer or separating agent) is the core in the separation processes, and a suitable solvent plays an important role in the economical design of separation processes.

However, it is tiresome to experimentally choose the best solvent from thousands of different substances for a given system. The computer-aided molecular design (CAMD) developed in the 1980s may break new ground in this aspect by largely reducing the amount of experimental work. The application of CAMD in separation processes is mostly based on the UNIFAC group contribution. Incalculable molecules would be formulated by simply joining UNIFAC groups if they were without any constraint. In accordance with certain combination rules, however, the size of the combinatorial problem can be greatly reduced, and only then are the chemically feasible molecules generated. Furthermore, in terms of given target properties, the desired molecules are screened from chemically feasible molecules. The groups of UNIFAC provide building blocks for assembling molecules. CAMD is essentially the inverse of property prediction by group contribution. Given a set of desirable properties, it is proposed to find a combination of structural groups satisfying the property specifications. In most cases, more than one solution is produced. Thus, a screening is needed, since only one of the alternatives may be chosen for the specified problem. Finally, such factors as corrosion, prices, source, azeotrope, and so on should be taken into consideration. Of course, it is a procedure after CAMD.

Now CAMD is widely used in the separation processes such as gas absorption, liquid−liquid extraction, extractive distillation and so on,[61−83] which is an important application of the UNIFAC model for the design of materials with low molecular weights.

2.3.1. CAMD Program

CAMD is conducted in the following four steps:

(a) Group Sorting and Preselection. Groups are the basis of CAMD, and molecular design makes full use of the group concept raised by Franklin,[84] which is built on the UNIFAC groups. The groups must be systematically ordered to facilitate their use. The approach proposed by Gani et al.[85−87] and Pretel et al.[88] to sort the groups is often adopted. That is, a certain group is characterized by the number of attachments present in a given group (or the valence number of the group) and the degree of difficulty that the group combines other groups (or the type of attachment). The

UNIFAC groups are sorted and listed in Table 1. If a group belongs to several different classes, it means that this group takes on different types of characterization in different molecules.

The attachment types are indicated as ordered pairs (i, j), where i is the type of attachment and j is the number of i attachment. Five types of attachments are put forward for nonaromatic groups:

N = single molecules as a group having no attachment with other groups, such as H_2O;

K = severely restricted attachment, such as OH;

L = partially restricted attachment, such as CH_2Cl;

M = unrestricted carbon attachment in linear dual-valence or single-valence groups, such as CH_3; and

J = unrestricted carbon attachment in radial dual valence groups, such as CH_2.

For aromatic molecules, two new attachments are introduced:

I = aromatic carbon ring attachment, such as ACH, and

H = substituted aromatic carbon ring attachment, such as ACCl.

Type M and J attachments are extended to aromatic groups:

M = unrestricted attachment in a carbon linked to an aromatic carbon, such as $ACCH_2$, and

J = unrestricted attachment in a radial carbon linked to an aromatic carbon, such as ACCH.

The chemically feasible molecules will be generated from the characterized UNIFAC groups in terms of combination rules. Not all of the UNIFAC groups need to be used in CAMD. The groups may be prescreened according to the criteria: availability of binary parameters for the synthesis group and elimination of unsteady, corrosive, or toxic compounds. For instance, some groups, , that is, Cl^- or F^-, may cause corrosion to the equipment and must be avoided in the process design.

(b) Combination of Groups. The greatest difficulty in CAMD is assembling groups into one molecule. To generate chemically stable molecules, the assembly must fit to the following rules:

(i) The chemical valence of a molecule must be zero. (ii) The neighborhood effect of groups must be avoided. Fortunately, many researchers[17−20] have discussed this rule from different perspectives and given the corresponding restriction conditions. Their work is helpful for us to program CAMD.

Table 2. Results of CAMD for the Separation of *n*-Heptane (1) and Benzene (2) at *T* = 303.15 K

no.	molecular structure	MW	T_b/K	α_{12}^{∞}	S_{12}^{∞}	SP	azeotropic judgment	
							1 and solvent	2 and solvent
1	DMSO	78.1	462.2	9.782	19.938	0.318	yes	no
2	CH_2CN-CH_2CN	80.0	495.3	8.759	17.853	0.312	yes	no
3	$CH_3COO-CH_2-CH_2CN$	113.0	474.3	7.026	14.321	0.354	no	no
4	DMF	73.1	426.15	5.767	11.754	0.686	yes	no
5	$CH_2NH_2-CH_2CN$	70.0	442.9	5.604	11.422	0.468	yes	no
6	NMP	99.1	477.2	5.552	11.317	0.756	no	no
7	$CH_2NH_2-CH_2-COOH$	89.0	486.3	5.242	10.685	0.543	no	no
8	ACN	41.0	354.8	5.134	10.465	0.621	yes	yes
9	$CH_3COO-CH_2-CH_2-CH_2CN$	127.0	497.2	5.086	10.366	0.417	no	no
10	$OH-CH_2-CH_2CN$	71.0	462.5	5.067	10.328	0.210	yes	no

(iii) In general, a molecule is composed of not more than eight groups, and the number of polar groups cannot be over three. The groups in a molecule must agree with the following attachment criterion: K ≤ M + J/2 + 2 for aliphatic compounds; I + H = 6, H ≤ 2 or H ≤ 3 for aromatic compounds. For aliphatic−aromatic compounds, these restrictions must be satisfied simultaneously. Otherwise, this molecule is unsteady under normal conditions.

(iv) The group parameters and group interaction parameters must be known in advance. The combination procedure is carried out in such a manner that the only combinations considered are those resulting in the generation of chemically feasible structures. The combinations from a preselected number of groups and testing for their chemical feasibility take place simultaneously.

(c) Prediction of Target Properties. Different problems have different sets of properties as constrains. For CAMD in separation processes, such properties as relative volatility at infinite dilution (α_{ij}^{∞}), selectivity at infinite dilution (S_{ij}^{∞}), solubility capacity (SP), molecular weight (MW), boiling point (T_b), critical properties, etc. are important. Specification of the problem type identifies the corresponding target properties. Because not all of the target properties are computable, it is convenient to classify them as explicit target properties and implicit target properties. Prediction methods for explicit target properties[89−94] are available and can be implemented automatically by computer. Prediction methods for implicit properties are not presently available, and thus, a combination of experience, information from the open references, and experiments is needed to determine them.

On the other hand, a pure component databank, which comprises extensive physical properties (e.g., molecular weight, normal boiling point, critical properties, vapor pressure constant in the Antoine equation, ideal gas heat capacity, etc.) is also necessary. If target properties can be sought in the databank, the values from the databank (not from calculation) may be regarded as the ultimate results.

(d) Sort Order and Selection of Potential Solvents. As we know, for some separation processes, the relative volatility (or selectivity) is the most important among all the explicit properties. The solvent with the highest relative volatility is always considered to be the most promising solvent for a given separation task. For this reason, solvents are normally ranked in the order of relative volatility (or selectivity).

Additionally, it is necessary to evaluate such implicit properties as toxicity, cost, stability, and material source. The solvents that do not satisfy the requirement of implicit properties are crossed out from the order. The remaining solvents ranked in the front are possibly the potential solvents we seek.

The CAMD program has been proposed by Lei et al.[95] and Chen et al.[96] For the solvent mixture, one is the main solvent, and the other is additive. In CAMD, the first step is to find the main solvent; when the basic solvent is determined, the next step is to find the additive in the same way as a single solvent.

2.3.2. Case Study

(1) Hydrocarbon Systems. We have investigated the systems of propane/propylene, *n*-butane/1-butene, and *n*-heptane/benzene because their separations are commonly encountered in the chemical industry.[97−102] The mixtures have similar boiling points or form azeotropes, and thus, a third solvent, which is screened by means of CAMD, is needed to add into the mixture. The separation mechanism for separating hydrocarbons is similar. Therefore, for instance, for the system of *n*-heptane/benzene, the restrictions for solvents in CAMD are listed as follows:

(i) Preselected group types: CH_3, CH_2, CH_3COO, CH_3CO, COOH, OH, CH_2CN, CH_2NH_2, ACH, $ACCH_3$, $ACNH_2$, ACOH, H_2O, CH_3OH, $(CH_2OH)_2$, acetonitrile (ACN), *N,N*-dimethylformamide (DMF), *N*-methyl-2-pyrrolidone (NMP), morpholine (Morph), furfural, dimethyl sulfoxide (DMSO);

(ii) Expected group number; 1−6;

(iii) Maximum molecular weight: 150;

(iv) Minimum boiling point: 323.15 K;

(v) Maximum boiling point: 503.15;

(vi) Temperature: 303.15 K;

(vii) Minimum relative volatility at infinite dilution: 5.0;

(viii) Minimum solubility capacity: 0.10.

By means of CAMD, the design results are obtained and listed in the order of decreasing relative volatility at infinite dilution, as shown in Table 2. Note that molecules nos. 3, 5, 7, 9, and 10 are difficult buy in chemical markets (or are bought only at very expensive prices). From this perspective, they are excluded as the potential solvents. Furthermore, after considering such implicit properties as toxicity (excluding molecules nos. 2 and 4), boiling point (excluding molecule no. 8), and chemical stability (excluding molecule no. 1), only molecule no. 6, NMP, remains. NMP has many outstanding advantages as the solvent, such as nontoxicity, noninjurious, facility of ecological treatment, and high separation ability.

The reliability of NMP as the solvent has already been verified by our experiments and simulations,[96,102] but CAMD goes a step further to provide the theoretical foundation for the selection of NMP. This also indicates that the designed results from CAMD are acceptable in this regard.

Braam and Izak[103] studied the system of cyclohexane/benzene by means of CAMD and found that aniline is possibly the best solvent, resulting in a relative volatility of 2.65 with cyclohexane in the distillate. The only solvent not to result in a higher relative volatility is acetonyl acetone, which has a higher boiling point than aniline. However, NMP is common in both cases. Unfortunately, DMF as a commonly used solvent is neglected by Braam and Izak. The reason may be that DMF forms minimum-boiling-point azeotropes with nonaromatic hydrocarbons having 6−8 carbon atoms (e.g., cyclohexane and heptane),[104] which causes solvent losses with the distillate. To decrease the solvent losses, the addition of stream to the distillation column above the solvent feed has been recommended. The stream breaks the DMF−hydrocarbon azeotrope, and DMF entrained by the distillate can be recovered by washing it with water or ion exchange.

(2) Separation of Ethanol and Water. This mixture forms a minimum-boiling azeotrope, and thus, a third solvent is needed to add into the mixture. The solvent for this system proposed by Lei et al.[105,106] and Li et al.[107] is ethylene glycol. This solvent will allow the recovery of ethanol in the distillate with a predicted relative volatility of 2.54. However, Braam and Izak[103] found that the first solvent generated by CAMD for this system is hexachlorobutadiene, which causes a relative volatility more than 3 times higher. This solvent was tested and performed very well.

The solvents to reverse the relative volatility of the system were also generated to facilitate the recovery of water in the distillate. In this case, the best solvent generated by CAMD is dodecane for this interesting separation.

(3) Other Systems. Separation of the systems of acetone/methanol, ethanol/ethyl acetate and methanol/methyl acetate has also been studied by Braam and Izak[103] by means of CAMD. For separating acetone and methanol, dimethyl sulfoxide (DMSO) generated by CAMD is assumed to be the best alternative to water that is commonly used in industry. For separating ethanol and ethyl acetate, diethylene glycol and DMSO generated by CAMD were tested experimentally to be the potential alternatives. For separating methanol and methyl acetate, tetrachloroethylene generated by CAMD was tested and performed very well. Therefore, it is suggested that tetrachloroethylene should replace 2-methoxyethanol, which is now used as the industrial solvent.

Gani et al.[87] studied the separation of the systems of ethanol/water; acetic/water; and styrene/xylene, which forms azeotropes, and the best solvents as entrainers in liquid−liquid extraction and extractive (or azeotropic) distillation were selected by means of CAMD. But it is pointed out that the choice of these solvents strongly depends on the conditions under which the separations are performed (e.g., separation temperature and pressure).

Only some typical and important systems are covered here, but there are still too many applications of CAMD in separation processes to be summarized. Interested readers may refer to the references listed in this section. However, CAMD based on UNIFAC models is very desirable in material design. By means of CAMD, the experiment working is greatly decreased in a search for the best solvents. CAMD as a useful tool plays an important role in finding the solvent and shortening the search time.

Unfortunately, for liquid solvents with low molecular weights, there are still about 54% of the UNIFAC group interaction parameters missing because experimental data are needed to fill them. This is where CAMD is limited. For the development of calculation techniques, it is thought that, in addition to the efforts to influence the computation methods of target properties with the screening of potential solvents and replenish the group parameters, were CAMD combined with other software (e.g., Excel, PRO/II, ASPEN PLUS), its functions would become stronger, and the designed results would be more reliable. It is believed that with the development of CAMD, it could be extended and applied in many more fields.

2.4. DISQUAC Model

In the family of group-contribution methods, apart from the UNIFAC models, the DISQUAC (dispersive-quasichemical group-contribution) model[108−143] also can be used to predict the liquid-phase activity coefficients, but not as extensively as the UNIFAC models.

The main features of DISQUAC are as follows: (i) The total molecular volumes, r_i; surfaces, q_i; and molecular surface fractions, α_i; of the compounds present in the mixture are calculated additively on the basis of the group volumes, R_G, and surfaces, Q_G, similar to the UNIFAC models. As volume and surface units, the volume, R_{CH_4}, and surface, Q_{CH_4}, of methane are taken arbitrarily.[132] (ii) The partition function is factorized into two terms in such a way that the excess functions are calculated as the sum of three contributions: a dispersive (DIS) term, which represents the contribution from the dispersive forces; a quasichemical (QUAC) term, which arises from the anisotropy of the force fields created by the solution molecules; and a combinatorial term, which is represented by the Flory−Huggins equation.[132] Thus,

$$G^E = G^{E,COMB} + G^{E,DIS} + G^{E,QUAC} \qquad (2.27)$$

$$\ln \gamma_i = \ln \gamma_i^{COMB} + \ln \gamma_i^{DIS} + \ln \gamma_i^{QUAC} \qquad (2.28)$$

(iii) The interaction parameters are assumed to be dependent on the molecular structure. (iv) The value $z = 4$ for the coordination number is used for all of the polar contacts. This represents one of the more important shortcomings of the model and is partially counteracted via the hypothesis of considering structure-dependent interaction parameters.

The equations used to calculate the DIS and QUAC contributions to γ_i are described in detail by Gonzalez et al.[132−138] The temperature dependence of the interaction parameters is expressed in terms of the DIS and QUAC interchange coefficients $C_{st,l}^{DIS}$ and $C_{st,l}^{QUAC}$, where $s \neq l$ are two contact surfaces present in the mixture and $l = 1$ (Gibbs energy), $l = 2$ (enthalpy), and $l = 3$ (heat capacity). In the DISQUAC model, the proximity and steric effects are taken into account, which is different from in the UNIFAC models.

Kehiaian et al.[139−143] first proposed the DISQUAC model and applied it to the prediction of solid−liquid equilibria in the mixtures of n-alkylbenzene and n-alkane and thermodynamic behavior of binary liquid organic mixtures. The research group of Gonzalez et al.[115−129,132−138] are always engaged in a systematic study on the ability of DISQUAC model to predict SLE (solid−liquid equilibria), LLE, VLE, and excess enthalpy, H^E, of the mixtures. Systematic comparison between the results from DISQUAC model and those from the modified UNIFAC model has been done for the systems in which the interaction parameters are available

in both models. It was concluded that the DISQUAC model provides a more reliable prediction than the modified UNIFAC model, especially in the case of linear, branched, and cyclic isomers.

The DISQUAC model is not popularly used for predicting liquid-phase activity coefficients in that the equations of the DISQUAC model are more complicated than those of the UNIFAC models, so many parameters have to be determined, and some of them are not directly available. Additionally, the group interaction parameters in the DISQUAC model are not as complete as in the UNIFAC models, although the DISQUAC model improves the prediction of the UNIFAC models.

2.5. Pierotti–Deal–Derr Model

The Pierotti−Deal−Derr model[144] is one of those models that use only pure component parameters to predict liquid-phase activity coefficients at infinite dilution and thus deduce relative volatility at infinite dilution in separation processes.[145−157]

Activity coefficients at infinite dilution are correlated to the number of carbon atoms of the solute and solvent (n_1 and n_2). For the members of homologous series $H(CH_2)_{n1}X_1$ (solute) in the members of the homologous series $H(CH_2)_{n2}Y_2$,

$$\lg \gamma_1^\infty = A_{12} + \frac{F_2}{n_2} + B_2 \frac{n_1}{n_2} + \frac{C_1}{n_1} + D_0(n_1 - n_2)^2 \quad (2.29)$$

where the constants are functions of temperature, B_2 and F_2 are functions of the solvent series, C_1 is a function of the solute series, A_{12} is a function of both, and D_0 is independent of both.

For zero members of a series, for example, water for alcohol, no infinite value for γ^∞ is obtained. Instead, by convention, any terms containing an n for the zero members are incorporated in the corresponding coefficient. So for n-alcohols in water,

$$\lg \gamma_1^\infty = K + B_2 n_1 + C_1/n_1 \quad (2.30)$$

Notice that the term $D_0(n_1 - n_2)^2$ is incorporated into the K constant because D_0 is smaller than the other coefficients by a factor of 1000. Therefore, this term is insignificant. In eq 2.30, only K is a function of the solute and solvent. B_2 is always the same when water is the solvent, and C_1 is the same for n-alcohol solutes. This is shown better from the following homologous series in water at 100 °C:

$$n\text{-alcohols: } \lg \gamma_1^\infty = -0.420 + 0.517n_1 + \frac{0.230}{n_1} \quad (2.31)$$

$$n\text{-aldehydes: } \lg \gamma_1^\infty = -0.650 + 0.517n_1 + \frac{0.320}{n_1} \quad (2.32)$$

where the coefficient B is the same in both cases.

2.6. Parachor Model

Activity coefficients at infinite dilution are obtained from the following relationship,

$$\lg \gamma_1^\infty = \frac{1}{2.303RT} [U_1^{1/2} - CU_2^{1/2}]^2 \quad (2.33)$$

$$U_i = \Delta H_i^V - RT \quad (2.34)$$

where U_i is the potential energy of component i; ΔH_i^V is the enthalpy of evaporation; C is a constant, a function of temperature, the parachor ratio of the two components, and the number of carbon atoms in the solute and solvent molecules; T is the absolute temperature; and R is the gas constant. The same variety of systems covered in the Pierotti−Deal−Derr method is also included in this approach.

2.7. Weimer–Prausnitz Model

Starting with the Hildebrand−Schatchard model for nonpolar mixtures, Weimer and Prausnitz[147] developed an expression for evaluating values of hydrocarbons in polar solvents,

$$RT \ln \gamma_2^\infty = V_2[(\lambda_1 - \lambda_2)^2 + \tau_1^2 - 2\psi_{12}] + RT\left[\ln \frac{V_2}{V_1} + 1 - \frac{V_2}{V_1}\right] \quad (2.35)$$

where V_i is the molar volume of pure component i, λ_i is the nonpolar solubility parameter, τ_i is the polar solubility parameter, T is the absolute temperature, and R is the gas constant. The subscript 1 represents the polar solvent and subscript 2 is the hydrocarbon solute with

$$\psi_{12} = k\tau_1^2 \quad (2.36)$$

Later, Helpinstill and Van Winkle[148] suggested that eq 2.35 is improved by considering the small polar solubility parameter of the hydrocarbon (olefins and aromatics):

$$RT \ln \gamma_2^\infty = V_2[(\lambda_1 - \lambda_2)^2 + (\tau_1 - \tau_2)^2 - 2\psi_{12}] + RT\left[\ln \frac{V_2}{V_1} + 1 - \frac{V_2}{V_1}\right] \quad (2.37)$$

$$\psi_{12} = k(\tau_1 - \tau_2)^2 \quad (2.38)$$

For saturated hydrocarbons,

$$\psi_{12} = 0.399(\tau_1 - \tau_2)^2 \quad (2.39)$$

For unsaturated hydrocarbons,

$$\psi_{12} = 0.388(\tau_1 - \tau_2)^2 \quad (2.40)$$

For aromatics,

$$\psi_{12} = 0.447(\tau_1 - \tau_2)^2 \quad (2.41)$$

The term ψ_{12} corresponds to the induction energy between the polar and nonpolar components. Since no chemical effects are considered, the correlation should not be used for solvents showing strong hydrogen bonding.

Although these three methods also declare the quantitative structure−property relationships, their parameters are very limited, which leads to their narrow application in separation processes, so these methods have been rarely reported in recent years.

2.8. Prausnitz and Anderson Theory

Separation of hydrocarbon mixtures with the polar solvents as entrainers has been practiced in industry for many years, although there has been only limited understanding of the

fundamental phase equilibria that forms the thermodynamic basis of this operation. It is known that the addition of polar solvents to a hydrocarbon mixture generally results in increased volatilities of paraffins relative to naphthenes, olefins, diolefins, and alkynes and increased volatilities of naphthenes relative to aromatics. Therefore, the addition of a polar solvent enables facile separation of certain mixtures that otherwise can only be separated with difficulty. Prausnitz and Anderson theory[158] tries to explain the selectivity of hydrocarbons from the viewpoint of molecular thermodynamics and intermolecular forces. The interaction forces between the solvent and the component are broadly divided into two types, , that is, physical force and chemical force. The true state in the solution is undoubtedly a hybrid of these two forces.

2.8.1. Physical Force

The selectivity is related to the various energy terms leading to the desired nonideality of solution and can be expressed in such a manner.

$$RT \ln S_{23} = [\delta_{1p}{}^2(V_2 - V_3)] + [V_2(\delta_{1n} - \delta_2)^2 - V_3(\delta_{1n} - \delta_3)^2] + [2V_3\xi_{13} - 2V_2\xi_{12}] \quad (2.42)$$

where subscripts 1−3 represent solvent, the light component, and the heavy component to be separated in one separation process, respectively, and V_i is the molar volume of component i.

The three bracketed terms in eq 2.42 show, respectively, the separate contributions of physical force to the selectivity, , that is, the polar effect, the dispersion effect, and the inductive effect of the solvent. It is convenient to rewrite eq 2.42 as

$$RT \ln S_{23} = P + D + I \quad (2.43)$$

where

$$P = \delta_{1p}{}^2(V_2 - V_3)$$

$$D = V_2(\delta_{1n} - \delta_2)^2 - V_3(\delta_{1n} - \delta_3)^2$$

$$I = 2V_3\xi_{13} - 2V_2\xi_{12}$$

It is found that the polar term P is considerably larger than the sum of D and I, and frequently, very much larger. Thus, eq 2.43 becomes

$$RT \ln S_{23} = \delta_{1p}{}^2(V_2 - V_3) \quad (2.44)$$

Of course, in the special case that components 2 and 3 are identical in size, the polar term vanishes. This means that the physical force cannot play a role in separating the hydrocarbon mixture. In this case, the chemical force is dominant and can be used to explain the separation phenomena, as is discussed in the following text.

Equation 2.44 not only shows the effect of molecular size but also predicts that when one separates hydrocarbons of different molar volumes, the selectivity is sensitive to the polar solubility parameter. It indicates that the effectiveness of a solvent depends on its polarity, which should be large, and on its molar volume, which should be small.

One example of separating a C4 mixture (mainly containing butane, butene, butadiene, and butyne) is given to

Table 3. The Solvents for Separating Ethane (1) and Ethylene (2)

solvent	dipole moment, μ (Debye)	relative volatility, α_{12}^∞	selectivity, S_{12}^∞
toluene	1.23	0.84	0.83
xylene	o-1.47	0.90	0.89
	m-1.13		
	p-0		
tetrahydrofuran	5.70	0.97	0.96
butyl acetate	6.14	0.95	0.94
ethyl acetate	6.27	1.01	1.00
pyridine	7.44	1.02	1.01
acetone	8.97	1.08	1.07
ACN	11.47	1.24	1.23
DMF	12.88	1.20	1.19
dimethyl sulfoxide	13.34	1.19	1.18
NMP	13.64	1.14	1.13

illustrate the physical force. It is known that the order of the molar volume of a C4 mixture is as follows:

butane > butene > butadiene > butyne
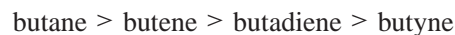
According to eq 2.44, the order of volatilities of a C4 mixture is in the same order,

butane > butene > butadiene > butyne
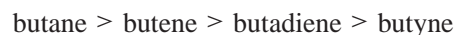
However, in order to have a much higher selectivity, the polar solubility parameter of the solvents should be as great as possible. That is why such solvents as ACN, DMF, and NMP with high polarity and small molar volume are used for this separation.

Another example deals with the separation of ethane (1) and ethylene (2).[159] The experimental results are listed in Table 3, in which the solvent polarity is characterized by the dipole moment. It can be seen that with an increase in the dipole moment, relative volatility and selectivity at infinite dilution also approximately increase, which is consistent with the Prausnitz and Anderson theory.

2.8.2. Chemical Force

For components with identical size, solvent polarity is not useful, and selectivity on the basis of a physical effect is not promising. In such cases, selectivity must be based on chemical force, which will selectively increase the interaction between the solvent and the components to be separated. However, examples of separating components with identical size are rare.

Postulated in the chemical viewpoint of solutions is that nonideality in solution arises because of association and solvation. In accordance with this concept, the true species in solution are loosely bonded aggregates consisting of two (or more) molecules of the same species (association) or of different species (solvation). That is to say, the solvent and the component can form complexes. Such complexes are believed to be the result of acid−base interactions following the Lewis definitions that a base is an electron donor and that an acid is an electron acceptor.

For example, for the separation of a C4 mixture, the fluidity of the electron cloud is different for the group C−C, C=C, C=C−C=C, C≡C and in the following order:

C−C < C=C < C=C−C=C < C≡C
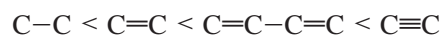
The greater the fluidity is, the easier the group is polarized.

electron donor
(base)
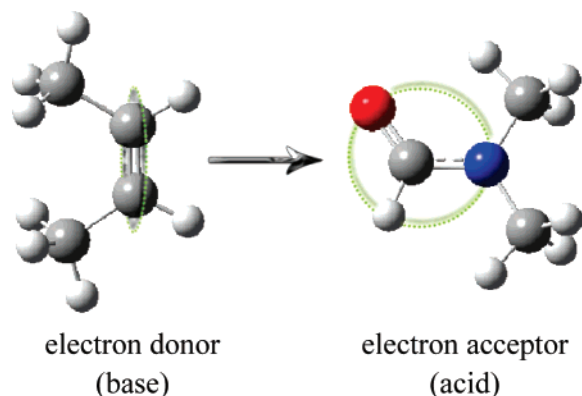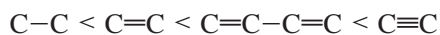
electron acceptor
(acid)

Figure 2. Schematic diagram of molecular interaction between DMF and *cis*-2-butene (arrow shows donation of electrons).

Accordingly, the base of C4 hydrocarbons is in the same order,

$$C-C < C=C < C=C-C=C < C\equiv C$$

which means that the chemical force between solvent and butyne is the greatest, whereas it is the smallest between solvent and butane.

So the volatilities of a C4 mixture are in the following order:

$$butane > butene > butadiene > butyne$$
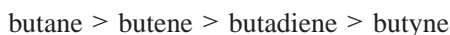
which is consistent with the results from experiments.[99,105] A schematic diagram of molecular interaction between DMF and *cis*-2-butene is shown in Figure 2, where the electron cloud of group C=C is captured by the function group of DMF. Actually, physical and chemical forces exist simultaneously in the solution. Possibly in some cases, one is predominant, and the other is minor.

The limitation of this theory is that it is suitable only for the separation of nonpolar systems. But in chemical engineering, polar−polar and nonpolar−polar systems are often encountered, and in this case, the molecular interaction may be more complicated. But the idea of physical and chemical forces is valuable and may be adopted. For instance, for the separation of acetic acid and water with tributylamine as the entrainer, the chemical force between acetic acid and tributylamine is very strong and has been verified by IR (infrared spectra) and GC−MS (gas chromatography−mass spectrometry) techniques.[160,161]

2.9. Group Contribution Equations of State

Prediction of phase equilibria for a gaseous compound (low boiling point compound) + liquid solvent systems at high temperatures and pressures is very important in many chemical processes, such as gas hydrate, purification, and refining of natural oils and derivatives by supercritical fluids.[162] Predictive molecular thermodynamic models are developing along two ways: activity coefficient models and equations of state, but under high temperature and pressure state, mixtures of a low boiling point compound (gaseous compound) and a liquid solvent show complex phase behavior because of a large difference in their physical properties, such as polarities and critical properties. Therefore, in this case, equations of state are preferred over activity coefficient models.

Since Huron and Vidal[163] proposed an approach that allowed incorporation of excess Gibbs energy, G^E, models into the mixing rules for cubic equations of state, many group-contribution equations of state have been developed. One of them is the PSRK (Predictive Soave−Redlich−Kwong) model proposed by Holderbaum and Gmehling,[164] in which the PSRK mixing rule combines the UNIFAC model with the SRK (Soave−Redlich−Kwong) equation of state.[165−175] A comparison with other group-contribution equations of state, such as the MHV2 (modified Huron−Vidal *i*th order),[176−179] LCVM (linear combination of Vidal and Michelsen mixing rules),[180] W−S (Wong−Sandler),[181] UNIWAALS (UNIFAC + van der Waals),[182] GCEOS (group-contribution equation of state),[183−191] and so on, shows that the PSRK model has some very important advantages: (i) the PSRK mixing rule has a well-defined reference state (the liquid mixture at atmospheric pressure), whereby the constant $A_0 = -0.64663$ used in the PSRK mixing rule is basically calculated using experimental liquid volumes in the saturated state of a large number of substances at atmospheric pressure; (ii) the PSRK model gives reliable results for vapor−liquid equilibria and gas solubility over a large temperature and pressure range; and (iii) the parameter matrix of the PSRK model is much larger than that of other group-contribution equations of state, which provides a larger range of applicability.

The PSRK model is based on the modified Soave−Redlich−Kwong (SRK) equation of state[192] as follows:

$$P = \frac{RT}{v - b} - \frac{a(T)}{v(v + b)} \quad (2.45)$$

where a, b, and c are equation parameters, and v is the molar volume. The pure component parameters a_{ii} and b_i are obtained from the critical data T_c and P_c of the pure components,

$$a_{ii}(T) = 0.42748 \frac{R^2 T_{c,i}^2}{P_{c,i}} \alpha_i(T) \quad (2.46)$$

$$b_i = 0.08664 \frac{RT_{c,i}}{P_{c,i}} \quad (2.47)$$

where $\alpha_i(T)$ can be obtained from pure component vapor pressures using the Mathias−Copeman parameters[193] $c_{1,i}$, $c_{2,i}$, and $c_{3,i}$ fitted to experimental vapor pressure data,

$$\alpha_i(T) = [1 + c_{1,i}(1 - \sqrt{T_{r,i}}) + c_{2,i}(1 - \sqrt{T_{r,i}})^2 + c_{3,i}(1 - \sqrt{T_{r,i}})^3]^2 \quad (2.48)$$

or the generalized form using the acentric factor ω:

$$c_{1,i} = 0.48 + 1.574\omega_i - 0.176\omega_i^2$$

$$c_{2,i} = 0, c_{3,i} = 0$$

Applying equation of state to mixtures, the parameters $a(T)$ and b can be calculated using the PSRK mixing rule. Therefore, the pure component parameters $a_{ii}(T)$, b_i and the excess Gibbs energy at a reference state (g_0^E) are required. At the reference state (the liquid at atmospheric pressure), an optimized ratio of the inverse packing fraction $u = 1.1$ and $v^E = 0$ is assumed, and the following relation is obtained,

$$\frac{a(T)}{bRT} = \sum_i x_i \frac{a_{ii}(T)}{b_i RT} + \frac{\frac{g_0^E}{RT} + \sum_i x_i \ln \frac{b}{b_i}}{\ln \frac{u}{u+1}} \quad (2.49)$$

where $g_0^E = RT \sum_i x_i \ln \gamma_{0,i}$ is calculated from the UNIFAC model at the reference state.

For the parameter b, the classical linear mixing rule is used:

$$b = \sum_i x_i b_i \quad (2.50)$$

Fischer and Gmehling[175] extended the range of application of the PSRK model in which such gases as CH_4, CO_2, CO, Ar, NH_3, H_2S, H_2, O_2, and N_2 have been introduced as new groups. The required interaction parameters for these groups were fitted to experimental vapor−liquid equilibrium data. Afterward, Gmehling et al.[173] added 10 new main groups for the gases SO_2, NO, N_2O, He, Ne, Kr, Xe, HCl, HBr, and SF_6 to the parameter matrix with the help of experimental VLE data for low-boiling-point substances. Finally, Horst-mann et al.[170] introduced additional structural groups for the gas epoxides HF, HI, COS, F_2, Cl_2, Br_2, HCN, NO_2, CF_4, O_3, and $ClNO$ and fitted the corresponding group interaction parameters to experimental VLE data. The available PSRK/ UNIFAC interaction parameter sets are more than 900 given as supplementary material (please see the online version at doi: 10.1016/j.fluid.2004.11.002.).[165]

On the other hand, the PSRK model is not limited to the description of nonpolar systems. It also can successfully be applied for the description of the systems containing polar components, supercritical components, asymmetric compo-nents, polymers, and even electrolytes with reliable results.

The PSRK model combines the SRK equation of state with the UNIFAC model in the PSRK mixing rule. Similarly, other simple cubic equation of states (e.g., PR (Peng− Robinson)) also can be combined with predictive activity coefficient models, of course. These two combinations in the mixing rule have also been proposed: PR/ASOG (PRASOG),[194,195] PR/UNIFAC.[196,197] But the study on them is very limited because the group parameters in the ASOG model are not as complete as in the UNIFAC models. In the PR/UNIFAC model, a volume translation PR equation of state is adopted to improve the prediction for saturated liquid densities for the pure compounds.

3. Solvent–Solid Salt Systems

Phase equilibria for solvent−solid salt systems are of significant interest for the separation processes in chemical industry since the presence of salt in the liquid phase may substantially influence the phase equilibrium behavior of the systems. Even small amounts of solid salt could have an appreciable effect on the boiling points, mutual solubility, and relative volatility. The salt effect is important for different industrial separation processes, such as salt distillation, extractive crystallization of salts, liquid−liquid extraction, and extractive distillation. Therefore, the predictive molecular thermodynamic models are necessary to predict phase equilibria for solvent−solid salt systems and, thus, screen the suitable salt rapidly for a given separation task.

3.1. The Extended UNIFAC Models

There are three kinds of predictive molecular thermo-dynamic models for solvent−solid salt systems based on group-contribution method (i.e., the UNIFAC model).

3.1.1. Model of Kikic et al.

Sander et al.[198] presented a model for the description of salt effects on vapor−liquid equilibria of water−solvent mixtures. This model combines a Debye−Hückel term with a modified UNIQUAC term with concentration-dependent parameters. Kikic et al.[199] modified this model in two aspects: (1) the Debye−Hückel term accounting for the long-range (LR) electrostatic forces was calculated according to the McMillan−Mayer solution theory as described by Cardoso and O'Connell;[200] (2) the UNIQUAC term was substituted by a UNIFAC term for the short-range (SR) physical interactions with concentration-independent group interaction parameters.

The activity coefficient γ_s of a solvent, s, in a solvent− solid salt mixture is calculated as

$$\ln \gamma_s = \ln \gamma_s^{D-H} + \ln \gamma_s^C + \ln \gamma_s^R \quad (3.1)$$

where γ_s^{D-H} is the Debye−Hückel term and γ_s^C and γ_s^R represent the UNIFAC combinatorial and residual contribu-tions.[201]

The Debye−Hückel term is calculated from the following equation as described by Macedo et al.,[202]

$$\ln \gamma_s^{D-H} = \frac{2AM_s d}{b^3 d_s} \left[1 + b\sqrt{I} - \frac{1}{1 + b\sqrt{I}} - 2 \ln(1 + b\sqrt{I}) \right] \quad (3.2)$$

for the solvent s, and

$$\ln \gamma_j^{LR} = -\frac{z_j^2 A I^{1/2}}{1 + b I^{1/2}} \quad (3.3)$$

for the ions that are produced by the dissociation of solid salts in the solvent mixture.

In eqs 3.2 and 3.3, M_s is the molecular weight of solvent s, I is the ionic strength, d_s is the molar density of pure solvent s calculated from the DIPPR tables ((DIPPR Tables of Physical and Thermodynamic Properties of Pure Com-pounds), d is the molar density of the solvent mixture, and A and b are the Debye−Hückel parameters.

$$A = 1.327\,757 \times 10^5 \, d_s^{1/2}/(DT)^{3/2} \quad (3.4)$$

$$b = 6.359\,696 d_s^{1/2}/(DT)^{1/2} \quad (3.5)$$

The density of the solvent mixture is described by the following empirical equation,

$$d = \sum_s v_s d_s \quad (3.6)$$

where v_s is the salt-free volume fraction of the solvent s in the liquid phase and is defined as

$$v_s = x_s' V_s / \sum_i x_i' V_i \quad (3.7)$$

where x_i' is the liquid-phase mole fraction of the solvent i on a salt-free basis, and V_i is the molar volume of solvent i. The dielectric constant, D, of the mixed solvents is obtained from the values of the pure solvents, D_s, and Oster's empirical mixing rule.[203] For a binary mixture, it can be approximated to

$$D = D_1 + [(D_2 - 1)(2D_2 + 1)/2D_2 - (D_1 - 1)]v_2 \quad (3.8)$$

The UNIFAC terms, γ_s^C and γ_s^R in eq 3.1, are calculated by the UNIFAC model, in which the values of group volume parameters R_k and group surface area parameters Q_k for the ions are taken from Macedo et al.,[202] and the group interaction parameters between the solvent groups have not been changed.

In the model of Kikic et al., the group interaction parameters were estimated between ions (Li$^+$, Na$^+$, K$^+$, Ca^{2+}, Ba^{2+}, Sr^{2+}, Cu^{2+}, Ni^{2+}, Hg^{2+}, F$^-$, Cl$^-$, Br$^-$, I$^-$, NO$_3^-$, and CH$_3$COO$^-$) and solvent groups (CH$_2$, OH, CH$_3$OH, H$_2$O, and CH$_3$CO). The group interaction parameters between the solvent groups are the same as those in the UNIFAC model. It was shown that the model of Kikic et al. represents VLE for solvent−water−salt mixtures with an average accuracy of the total pressures around 9% and the vapor-phase mole fractions around 4%. Since it is a predictive group-contribution method, it has a much broader range of applicability than the model of Sander et al..

3.1.2. Model of Achard et al.

Achard et al.[204] developed a model in which the excess Gibbs energy is assumed to result from two terms: one resulting from SR interactions and the second from LR electrostatic interactions. Thus,

$$\ln \gamma_i = \ln \gamma_i^{SR} + \ln \gamma_i^{LR} \quad (3.9)$$

which is suitable for the solvents and ions.

An extended form of the Debye−Hückel law given by Pitzer[205,206] is used to account for LR electrostatic forces, whereas the UNIFAC model is for SR physical interactions. Additionally, the solvation equations accounting for hydration of ions ion aqueous solution (formation of water clusters) are incorporated into the UNIFAC model.

Structural parameters for hydrated components for aqueous solution are the following:

$$R_k^H = R_k + Nh_k R_1 \quad (3.10)$$

$$Q_k^H = Q_k + Nh_k Q_1 \quad (3.11)$$

where R_1 and Q_1 refer to water, and Nh_k represents the infinite dilution hydration number of group k.

The ions in the mixture are considered to be hydrated by water (1), except for organic solvents, whose hydration numbers are set to be zero. Moreover, it is also assumed that solvation phenomena between organic solvents and ions are nonexistent. In this case, the mole fractions of water and ionic components are, respectively,

$$x_1^H = \frac{x_1 - \sum_{j=2}^{N} Nh_j x_j}{1 - \sum_{j=2}^{N} Nh_j x_j} \quad (3.12)$$

$$x_i^H = \frac{x_i}{1 - \sum_{j=2}^{N} Nh_j x_j} \quad (3.13)$$

Activity coefficients of water and ionic components are, respectively,

$$\gamma_1^{SR} = \gamma_1^{SR,H} \frac{x_1^H}{x_1} \quad (3.14)$$

$$\gamma_i^{SR} = \gamma_i^{SR,H} \frac{x_i^H}{x_i} (\gamma_1^{SR,H} x_1^H)^{-Nh_i} \quad (3.15)$$

where $\gamma_1^{SR,H}$ and $\gamma_i^{SR,H}$ are calculated with the UNIFAC model using mole fractions and structural parameters of hydrated components given above. There is no influence of hydration on activity coefficients of organic solvents.

The model of Achard et al. only adds the ion−solvent interaction parameters and hydration number on the basis of the UNIFAC model, neglecting the difference between ion−ion interaction parameters, which, however, are considered in the model of Kikic et al., in order to reduce the number of required parameters.

The group interaction parameters were estimated between ions (Li$^+$, Na$^+$, K$^+$, Mg^{2+}, Ca^{2+}, Co^{2+}, Ba^{2+}, Sr^{2+}, NH$_4^+$, Cl$^-$, Br$^-$, F$^-$, NO$_3^-$, and SO$_4^{2-}$) and solvent groups (CH$_2$, OH, CH$_3$OH, H$_2$O, and CH$_3$CO). The group interaction parameters between the solvent groups are the same as those in the UNIFAC model. It was shown that the model of Achard et al. represents VLE for solvent−water−salt mixtures with an average accuracy of the total pressures around 4% and the vapor-phase mole fractions around 4%. So the calculated results with the model of Achard et al. are more accurate than those with the model of Kikic et al..

3.1.3. Model of Yan et al.

The model of Yan et al.[207] (also called LIFAC model) is put forwarded on the basis of the LIQUAC model. The difference between this model and the LIQUAC model[208−210] is that the UNIQUAC equation in the LIQUAC model has been substituted by the UNIFAC equation. The excess Gibbs energy consists of three terms: (1) a Debye−Hückel term, which represents the LR interactions caused by the Coulomb electrostatic forces; (2) a virial term, which accounts for the MR interactions caused by the ion−dipole effects; and (3) a UNIFAC term, which represents the SR interactions. That is to say,

$$G^E = G_{LR}^E + G_{MR}^E + G_{SR}^E \quad (3.16)$$

Thus,

$$\ln \gamma_s = \ln \gamma_s^{LR} + \ln \gamma_s^{MR} + \ln \gamma_s^{SR} \quad (3.17)$$

for the solvents for which the concentration scale is mole

fraction, and

$$\ln \gamma_j = \ln \gamma_j^{LR} + \ln \gamma_j^{MR} + \ln \gamma_j^{SR} - \ln(M_s/M + M_s \sum_{\text{ion}} m_{\text{ion}}) \quad (3.18)$$

for the ions for which the concentration scale is molality.

The LR interaction contribution to activity coefficients, $\ln \gamma_s^{LR}$ and $\ln \gamma_j^{LR}$, can be expressed by eqs 3.2 and 3.3 for solvents and ions, respectively.

The MR interaction contribution to activity coefficients for solvent s and ions, $\ln \gamma_s^{MR}$ and $\ln \gamma_j^{MR}$, is given as follows:

$$\ln \gamma_k^{MR} = \sum_{\text{ion}} B_{k,\text{ion}}(I)m_{\text{ion}} - \frac{M_k \sum_k \sum_i \nu_k^{(i)} x_i'}{M} \times \\ \sum_k \sum_{\text{ion}} [B_{k,\text{ion}}(I) + IB_{k,\text{ion}}'(I)]x_k' m_{\text{ion}} - \\ M_k \sum_c \sum_a [B_{c,a}(I) + IB_{c,a}'(I)]m_c m_a \quad (3.19)$$

$$\ln \gamma_s^{MR} = \sum_k \nu_k^{(s)} \ln \gamma_k^{MR} \quad (3.20)$$

$$\ln \gamma_j^{MR} = \frac{1}{M} \sum_k B_{j,k}(I)x_k' + \frac{z_j^2}{2M} \sum_k \sum_j B_{k,\text{ion}}'(I)x_k' m_{\text{ion}} + \\ \sum_c B_{c,a}(I)m_c + \frac{z_a^2}{2} \sum_{c<\text{bu}>} \sum_a B_{c,a}'(I)m_c m_a \quad (3.21)$$

where x_k' is the salt-free mole fraction of solvent group k, M_k is the molecular weight of solvent group k, M is the molecular weight of the mixed solvent, $B_{i,j}'$ is equal to $dB_{i,j}/dI$, $\nu_k^{(s)}$ is the number of groups of type k in the solvent s, and γ_k^{MR} is the activity coefficient of group k in the mixture for the MR contribution.

The second virial coefficient, $B_{i,j}$, is the interaction coefficient between species i and j (ion or solvent groups). For ion–ion interaction parameter $B_{c,a}$ and ion–solvent group interaction parameter $B_{k,\text{ion}}$, one obtains

$$B_{c,a} = b_{c,a} + c_{c,a} \exp(-I^{1/2} + 0.13I) \quad (3.22)$$

$$B_{k,\text{ion}} = b_{k,\text{ion}} + c_{k,\text{ion}} \exp(-1.2I^{1/2} + 0.13I) \quad (3.23)$$

where $b_{i,j}$ and $c_{i,j}$ are the MR interaction parameters ($b_{i,j} = b_{j,i}$, $c_{i,j} = c_{j,i}$, and $b_{i,i} = c_{i,i} = 0$) which are determined from a large number of experimental VLE data. Therefore, the group interaction parameters have been introduced into the MR term.

The SR interaction contribution to activity coefficients for solvents and ions, $\ln \gamma_s^{SR}$ and $\ln \gamma_j^{SR}$, is described by the UNIFAC model in which the group interaction parameters between the solvent groups remain constant, but the ion–ion and ion–solvent group interaction parameters are set to zero to reduce the number of required parameters because these parameters have a minor influence on the activity coefficients of the solvents.

The group interaction parameters were estimated between ions (Li^+, Na^+, K^+, NH_4^+, Ca^{2+}, Mg^{2+}, Ba^{2+}, Sr^{2+}, Cu^{2+}, Zn^{2+}, Co^{2+}, Ni^{2+}, Hg^{2+}, F^-, Cl^-, Br^-, I^-, NO_3^-, CH_3COO^-,

and SCN^-) and solvent groups (CH_2, OH, CH_3OH, H_2O, CH_2CO, CCOO, and CH_2O). It was shown that the deviations of vapor-phase mole fractions and temperatures in the model of Kikic et al. are generally twice as large as those in the model of Yan et al. under the same number of parameters used. So the calculated results with the model of Yan et al. are more accurate than those with the model of Kikic et al..

Unfortunately, the comparison of the model of Yan et al. with that of Achard et al. has not been done yet. But it should be mentioned that the group interaction parameters in the model of Yan et al. is more complete than those in the model of Achard et al., which would lead to a wide application in the VLE prediction for solvent–solid salt systems.

It is evident that in these three kinds of models (i.e., the extended UNIFAC models), the UNIFAC model, in principle, may be replaced by the ASOG model, as proposed by Correa et al.[211] Therefore, the ASOG model is combined with a Debye–Hückel term to account for salt effects. In addition, there are some other predictive models suitable for solvent–solid salt systems, as proposed by Huh and Bae (based on the modified double-lattice theory)[212,213] and by Lee et al.[214] (based on a plausible scheme of superposing electrostatic interaction on the short-range nonelectrostatic interactions). But the group interaction parameters provided by them are too limited, and thus, they are rarely used. Additionally, as mentioned in section 2.9 (Group Contribution Equations of State), the PR/UNIFAC model also can be extended for prediction of phase equilibria with strong electrolytes using the available VTPR (volume translated Peng–Robinson) parameters[215–220] and the group interaction parameters in the model of Yan et al..

The group-contribution methods for solvent–solid salt systems can be applied to CAMD so as to screen the suitable salt rapidly for a given separation task, as those for solvent–solvent systems. As a simplified presumption, a salt is thought to be composed of one positive ion and one negative ion, which are regarded as the groups of salts. It is consequently easy to assemble the ions into molecules in the same way as liquid solvents. These ions are collected in a CAMD program by Lei et al.[95] The combination rule is simply that the chemical valence of a salt must be zero, which is impossible to lead to a combination explosion because most molecules are composed of just two groups: one positive ion and the other negative ion. Therefore, both liquid solvents and solid salts can be designed in one CAMD program, and this goes an additional step in the application of CAMD. Similarly, there are still so many group interaction parameters missing because no experimental data are available for these groups. This is where CAMD for solvent–solid salt systems is limited.

3.2. Scaled Particle Theory

3.2.1. Description of Theory

By far, there are many theories[221–224] about salt effect, such as the electrostatic theory of Debye–McAulay in dilute electrolyte solutions, internal pressure theory of McDevit–Long, salt effect nature of Huangziqing, electrolyte solution theory of Pitzer, and scaled particle theory, in which the first four theories require the experimental data to correlate the model parameters or make some simplification with a limited accuracy or have no wide range to apply. But the scaled particle theory, which is deduced from thermodynamics and statistical physics, has defined physical meaning, and the required molecular parameters are readily available. Espe-

cially in the recent years, the study of scaled particle theory[225−232] has been further explored, since it is an a priori predictive method, and no experimental data are needed.

For a vapor and liquid phase in equilibrium, for the solute we know,

$$\mu_1^V = \mu_1^L \tag{3.24}$$

In terms of the grand canonical ensemble in statistical thermodynamics, the chemical potential of the solute in the gas phase is given by

$$\mu_1^V = kT \ln\left(\frac{\Lambda_1^3}{kT}\right) + kT \ln f_1^V \tag{3.25}$$

where

$$\Lambda_1 = \left(\frac{h^2}{2\pi m_1 kT}\right)^{1/2}$$

and f_1^V is the gas-phase fugacity of the solute.

The chemical potential of the solute in the liquid phase is given by

$$\mu_1^L = kT \ln \rho_1 \Lambda_1^3 + \bar{g}_1^h + \bar{g}_1^s \tag{3.26}$$

where $\bar{g}_1^h = \partial G_h/\partial\bar{N}_1$, representing the free energy of introducing a hard sphere of diameter σ_1 into the solvent (electrolyte solution), and $\bar{g}_1^s = \partial G_s/\partial\bar{N}_1$, representing the free energy needed to introduce the solute into the cavity due to the soft part of the chemical potential.

Incorporating eqs 3.25 and 3.26 into eq 3.24 and rearranging,

$$\ln\left(\frac{f_1^V}{\rho_1}\right) = \frac{\bar{g}_1^h}{kT} + \frac{\bar{g}_1^s}{kT} + \ln kT \tag{3.27}$$

The mole fraction of the solute gas in the solution is

$$x_1 = \frac{\rho_1}{\sum_j \rho_j} \tag{3.28}$$

Therefore, eq 3.27 can be written as

$$\ln\left(\frac{f_1^G}{x_1}\right) = \frac{\bar{g}_1^h}{kT} + \frac{\bar{g}_1^s}{kT} + \ln\left(kT\sum_j \rho_j\right) \tag{3.29}$$

At low pressure, the fugacity in eq 3.29 can be replaced by partial pressure. According to the Henry equation, the gas solubility at low solute concentration is described by the following equation:

$$P_1 = H_1 x_1 = H_1' c_1 \tag{3.30}$$

After eq 3.29 is combined with eq 3.30, we obtain

$$\ln H_1 = \frac{\bar{g}_1^h}{kT} + \frac{\bar{g}_1^s}{kT} + \ln\left(kT\sum_j \rho_j\right) \tag{3.31}$$

The solubility of a nonelectrolyte in a salt solution with low salt concentration is given by the Setschenow equation,

$$\log\frac{c_0}{c} = k_s c_s \tag{3.32}$$

where c_0 is the solubility in pure solvent; c is the solubility in a salt solution of concentration c_s; and k_s is the salting coefficient, which has a characteristic value for a given salt−nonelectrolyte pair. A positive value of k_s corresponds to salting-out ($c_0 > c$); a negative value of k_s, salting-in ($c_0 < c$).

Differentiating eq 3.32 with respect to c, we can write in an ordinary expression,

$$\lim_{c_s \to 0} \log\frac{c_0}{c} = k_s c_s \tag{3.33}$$

From eqs 3.30, 3.31, and 3.33, the following equation is derived:

$$-\left(\frac{\partial \log c}{\partial c_s}\right) = k_s = \left[\frac{\partial(\bar{g}_1^h/2.3kT)}{\partial C_s}\right]_{c_s \to 0} +$$
$$\left[\frac{\partial(\bar{g}_1^s/2.3kT)}{\partial C_s}\right]_{c_s \to 0} + [\partial(\ln\sum_{j=1}^{m}\rho_j)/\partial C_s]_{c_s \to 0} = k_\alpha + k_\beta + k_\gamma \tag{3.34}$$

where $\bar{g}_1^h$ is the free energy change when a cavity large enough to hold the nonelectrolyte molecule is formed in the solution, $\bar{g}_1^s$ is the free energy change when the nonelectrolyte is introduced into the cavity, and ρ_j is the number density of a solution species. k_α, k_β, and k_γ represent the contributions to the salting coefficient of each of the three terms on the right-hand side of eq 3.34. The problem now becomes one of deriving general expression for k_α, k_β, and k_γ in terms of parameters characteristic of the nonelectrolyte and the ions of the salts.

To find k_s for a particular system, it is necessary to know (1) the apparent molar volume, ϕ, of the salt at infinite dilution;[233,234] (2) the diameters (σ_3, σ_4) and polarizabilities (α_3, α_4) of cation and anion; and (3) the diameters (σ_1, σ_2) and polarizabilities (α_1, α_2) of the nonelectrolyte and solvent molecules.

3.2.2. Salt Effect on Relative Volatility at Infinite Dilution

In separation processes, it is advisable to have theoretical guidance in the selection of a suitable solid salt.[235] For this purpose, scaled particle theory is recommended to elucidate the effect of solid salt on separation factor (or selectivity and relative volatility).

An important state to select and evaluate solvents is at infinite dilution of the nonelectrolyte in the separation processes. It is assumed that the system is composed of the solvent, salt, and components A and B, both of which are nonelectrolyte. But when components A and B are in the case of infinite dilution, it is known that component B has no influence on the system composed of the solvent, salt, and component A. On the other hand, component A has also no influence on the system composed of the solvent, salt and component B. Therefore, even though scaled particle theory in most cases applies to a ternary system, it can extend to the systems containing more components when all nonelectrolytes are at finite dilution.

According to the deduction of establishing fundamental equations in scaled particle theory, the vapor partial pressures of nonelectrolytes in the solutions are always constant under the same temperature in the case of salt and no salt.

Assume that the system is composed of solvent and components A and B with low concentrations. The liquid molar fractions of components A and B are, respectively, x_{01} and x_{02}, corresponding to concentrations c_{01} and c_{02} (mol L^{-1}). When the system attains the state of vapor–liquid equilibrium, the vapor molar fractions of component A and component B are, respectively, y_{01} and y_{02}, corresponding to vapor pressure P_{01} and P_{02}. The total pressure is P_0, and component A is more volatile than component B in the solvent. It is required that the temperature and solute vapor partial pressure, P_{01} and P_{02}, be kept constant when adding salt to the system. In the case of adding salt, it is assumed that the liquid molar fractions of components A and B are, respectively, x_1 and x_2, corresponding to concentrations c_1 and c_2 (mol L^{-1}) and vapor partial pressure $P_1 = P_{01}$ and $P_2 = P_{02}$. The total pressure of the system with salt is P. Therefore, we can write

$$\frac{c_{01}/c_1}{c_{02}/c_2} = \frac{x_{01}/x_1}{x_{02}/x_2} = \frac{y_{02}x_{01}}{y_{01}x_{02}}\frac{y_1/x_1}{y_2/x_2}\frac{y_{01}y_2}{y_{02}y_1} = \frac{\alpha_s}{\alpha_0}\frac{P_{01}P_2}{P_{02}P_1} = \frac{\alpha_s}{\alpha_0}$$

(3.35)

where α_s and α_0 are relative volatilities of components A and B at finite dilution with salt and without salt, respectively. From eq 3.32, for components A and B,

$$\log \frac{c_{01}}{c_1} = k_{s1}c_s$$

(3.36)

$$\log \frac{c_{02}}{c_2} = k_{s2}c_s$$

(3.37)

In terms of the definition of relative volatility (see eq 2.27) and eqs 3.35, 3.36 and 3.37, we obtain

$$\frac{a_s}{a_0} = 10^{(k_{s1}-k_{s2})c_s}$$

(3.38)

When components A and B are at infinite dilution, it becomes

$$\frac{a_s^\infty}{a_0^\infty} = 10^{(k_{s1}-k_{s2})c_s}$$

(3.39)

where a_s^∞ and a_0^∞ represent relative volatilities at infinite dilution with salt and without salt, respectively.

Equation 3.39 discloses the relationship of salting coefficients and relative volatilities at infinite dilution and constructs a bridge between microscale and macroscale. Even if the calculated salting coefficients are not accurate due to the current limitation of scaled particle theory, it is not difficult to judge the magnitude of k_{s1} and k_{s2} by conventional thermodynamics knowledge and decide whether it is advantageous to improve the relative volatilities with salt. From eq 3.39, it is concluded that if $k_{s1} > k_{s2}$ with low salt concentration, the relative volatilities of components to be separated will be increased by adding salt; the greater the difference between k_{s1} and k_{s2}, the more apparent the effect of improving the relative volatility.

Table 4. Comparison of Relative Volatilities at Infinite Dilution between Calculated and Experimental Values for the System of DMF/C4 with Solid Salt at $T_1 = 303.15$ K and $T_2 = 323.15$ K

	a_{s15}^∞		a_{s25}^∞		a_{s35}^∞		a_{s45}^∞	
	T_1	T_2	T_1	T_2	T_1	T_2	T_1	T_2
calcd value	4.43	3.75	2.50	2.26	2.05	1.87	1.74	1.66
exptl value	4.53	3.73	2.55	2.28	2.11	1.94	1.85	1.76
rel error, %	2.21	0.54	1.96	0.88	2.84	3.61	5.95	5.68

Table 5. Comparison of Relative Volatilities at Infinite Dilution between Calculated and Experimental Values for the System of ACN/C3 with Solid Salt at Different Temperatures

				α_{s12}^∞		
T (K)	k_{s1}	k_{s2}	α_{012}^∞	calcd value	exptl value	rel error (%)
289.7	0.6053	0.5483	1.69	1.92	2.01	4.47
298.2	0.6034	0.5462	1.67	1.90	1.96	3.06
303.2	0.6000	0.5450	1.65	1.87	1.90	1.58
312.2	0.6000	0.5428	1.64	1.86	1.84	1.09
324.2	0.5977	0.5399	1.62	1.84	1.79	2.79

The value of α_0^∞ can be derived from experiment or calculation using a vapor pressure equation and liquid activity coefficient equation. According to eq 3.39, it is convenient to obtain the values of α_s^∞ just by calculating salting coefficients in terms of scaled particle theory.

3.2.3. Case Study

(1) The System of DMF/C4. The investigated system is composed of DMF, the solid salt NaSCN with weight fraction 10% in DMF, and a C4 mixture.[236] We use the numbers 1, 2, 3, 4, and 5 and s to represent *n*-butane, butene-1, *trans*-2-butene, *cis*-2-butene, 1,3-butadiene, and solid salt, respectively.

In terms of scaled particle theory, the three terms k_γ, k_β, and k_α were calculated, and the sequence of salting coefficients is $k_{s1} > k_{s2} > k_{s3} > k_{s4}$, which is reasonable because the fluidity of the electron cloud of the C4 mixture is different, and thus, the interaction between salt and C4 component is in the following order: butane < butene < butadiene < butyne. Furthermore, k_{s1}, k_{s2}, k_{s3}, and k_{s4} are larger than zero, which means that the salt effect of the C4 mixture is salting out.

The relative volatilities at infinite dilution of the C4 mixture with salt were calculated by using eq 3.39. To evaluate the accuracy, the calculated values were compared with the experimental values, as given in Table 4. It can be seen that the calculated values are in good agreement with the experimental values. This indicates that scaled particle theory can be successfully applied for this system.

(2) The System of ACN/C3. The investigated system is composed of ACN (acetonitrile), the solid salt NaSCN with weight fraction 10% in ACN, and a C3 (propane and propylene). The expressions of k_α, k_β, k_γ are deduced in the same way.

The salt coefficients, k_{s1} and k_{s2}, and relative volatilities at infinite dilution at different temperatures are given in Table 5, where we use the numbers 1 and 2 and s to represent propane, propylene, and salt, respectively. It can be seen that the calculated results from scaled particle theory are reliable for the system of ACN/C3 with solid salt with a relative error of <5%. Formerly, the solvents ACN and DMF were optimized by adding a little water to improve the relative volatilities of the nonelectrolytes. But we know that ACN

and DMF are prone to hydrolyze, which limits their use in industry. The solid salts do not bring this problem and, thus, can substitute for water to increase the separation ability of solvents.

(3) The System of Ethylene Glycol/Ethanol/Water. The investigated system is composed of ethylene glycol, solid salt potassium acetate (KAc) with weight fraction 10% in ethylene glycol, ethanol (1), and water (2). In many industrial plants, the mixture of ethanol and water are separated, with ethylene glycol added KAc as entrainer. In terms of scaled particle theory, the reason can be explained. Because the interactions between water and KAc are stronger than between alcohol and KAc, $k_{s1} > k_{s2}$. Therefore, it is derived from eq 3.39 that adding KAc should enhance the separation ability of ethylene glycol. But formerly, the interpretation of the phenomena was very vague.[237-239]

However, at present, the three terms of salt coefficients in scaled particle theory are not related to the hydrogen bond force between the solutes and solvents. Therefore, it is difficult to calculate salt coefficients precisely in terms of scaled particle theory for the polar solute systems, but we can qualitatively predict the salt effect according to eq 3.39. This also holds for other systems, such as ethylene glycol/potassium acetate (KAc)/acetone/methanol, in which the salt KAC is added to enhance the separation ability of ethylene glycol.[240,241]

Therefore, the relationship between microscale salt coefficients and macroscale relative volatilities at infinite dilution is established in terms of scaled particle theory. For the separation of a nonpolar system (e.g., DMF/C4 and ACN/C3), the relative volatilities at infinite dilution with salt correspond well to experimental values. The reason may be that C4 and C3 are nonpolar components and their sizes are not large, which lead to the accurate results. It is interesting to compare the relative contribution of the three terms k_α, k_β, and k_γ to the salting coefficient k_s. It is found that k_γ is very small; therefore, the salting coefficient k_s mainly depends upon the relative magnitudes of k_α and k_β.

However, for separating polar solute systems, salt coefficients are not easy to calculate accurately in terms of scaled particle theory. But this does not influence our analysis of whether it is advantageous to add salt to a system, because in most cases, it is not difficult for us to qualitatively judge the relative values of the salt coefficient of each component.

Although the application of scaled particle theory to the calculation of salt effect has the great advantages that the required molecular parameters are readily available, it is limited in some degree. For polar solutes, the scaled particle theory can only provide qualitative analysis according to eq 3.39. The reason may be that the hydrogen bonding between polar solutes and polar solvent is very complicated and greater than van der Waals bonding. By far, only van der Waals bonding is considered in scaled particle theory. Consequently, quantitative calculation for polar solutes is very difficult and inaccurate. Anyway, scaled particle theory is extended to solve the problem of theoretical prediction of the salt effect and promote the development of chemical technology. We know any theory has its own deficiency, but we believe that with the development of the scaled particle theory, the problem will be solved in the near future.

4. Solvent–Polymer Systems

A typical problem in polymer processing involves the determination of thermodynamic properties of mixtures of polymers, solvents, plasticizers, antiplasticizers, and diluents. Predictive thermodynamic models for describing phase equilibria of polymer–solvent systems can be classified into two general categories: activity coefficient models (e.g., UNIFAC-FV,[242-248] entropic-FV,[249,250] FH/Hansen,[251] GK-FV[249] and UNIFAC-ZM[252-254]) and equations of state (e.g., PSRK,[255] GC-Flory EOS[256-259] and GCLF EOS[260-268]). Equations of state are preferred over activity coefficient models in that equations of state can disclose the dependence of phase volume on pressure, which is especially important in estimating the swelling degree of polymers in polymer processing. Moreover, the thermodynamic properties such as density, enthalpy, entropy, heat capacity, and so on can also be calculated using equations of state.

4.1. Description of the Models

Table 6 presents an overview of the predictive models suitable for solvent–polymer systems, illustrating how the various physical effects are represented and which parameters are required in each of the models. Among them, UNIFAC-FV and GCLE EOS are the most commonly used in the activity coefficient models and equations of state, respectively, and thus will be emphasized here.

The UNIFAC-FV model is a group-contribution method and developed on the basis of the UNIFAC model. The UNIFAC model is known to underestimate experimental solvent activities in polymer solutions. At the end of the 1970s, Oishi and Prausnitz[242] extended the UNIFAC model to polymer solutions by adding a free-volume contribution deduced from the Prigogine–Flory–Patterson theory.[243] The arisen UNIFAC-FV model represents a group-contribution method, which can be fairly applied to polymer solutions, since the difference in thermal expansion behavior of polymer and solvent is explicitly taken into account by the free-volume contribution. According to UNIFAC-FV model, the solvent activity consists of three contributions: a combinatorial part a_i^C, a residual part a_i^R, and a free-volume contribution a_i^{FV},

$$\ln a_i = \ln a_i^C + \ln a_i^R + \ln a_i^{FV} \qquad (4.1)$$

where $\ln a_i^C$ and $\ln a_i^R$ are taken from the UNIFAC model. The free-volume term, $\ln a_i^{FV}$, is given by

$$\ln a_i^{FV} = 3c_i \ln\left[\frac{\tilde{v}_i^{1/3} - 1}{\tilde{v}_M^{1/3} - 1}\right] - c_i\left[\left(\frac{\tilde{v}_i}{\tilde{v}_M} - 1\right)\left(1 - \frac{1}{\tilde{v}_i^{1/3}}\right)^{-1}\right] \qquad (4.2)$$

The reduced volumes of solvent, $\tilde{v}_i$, are given by

$$\tilde{v}_i = \frac{v_i M_i}{15.17 b r_i} \qquad (4.3)$$

$$\tilde{v}_M = \frac{\sum_i w_i v_i}{15.17 b \sum_i r_i w_i / M_i} \qquad (4.4)$$

where v_i is the volume of component i per gram, $3c_i$ is the number of external degrees of freedom per solvent molecule, r_i is the volume parameter, w_i is the weight fraction, M_i is the molar mass of component i, and b is a proportionality

Table 6. Predictive Thermodynamic Models Used to Predict Multicomponent VLE for Solvent−Polymer Systems (a Schematic Overview of the Representation of Various Physical Effects and of the Parameters Used in Each Model)

model	combinatorial effects	free-volume effects	energetic effects	group parameters	group-interaction parameters
entropic-FV/UNIFAC	derived from the generalized van der Waals partition function		UNIFAC	R_k, Q_k	a_{mn} and a_{nm} obtained from binary VLE data for low molecular weight compounds
GK-FV	an empirical Staverman−Guggenheim correction added to the combinatorial and free-volume terms in the entropic FV model		UNIFAC	R_k, Q_k	a_{mn} and a_{nm} obtained from binary VLE data for low molecular weight compounds
UNIFAC-FV	UNIFAC	obtained from Flory's equation of state	UNIFAC	R_k, Q_k	a_{mn} and a_{nm} obtained from binary VLE data for low molecular weight compounds
UNIFAC-ZM	UNIFAC	included in the combinatorial term	UNIFAC	R_k, Q_k	a_{mn} and a_{nm} obtained from binary VLE data for low molecular weight compounds
FH/Hansen	Flory−Huggins	not accounted for	Hansen solubility parameters	molar volumes and Hansen solubility parameters are required for each component	
PSRK	combine the SRK equation of state with the UNIFAC model in the mixing rule		UNIFAC	R_k, Q_k	a_{mn} and a_{nm} obtained from binary VLE data for low molecular weight compounds
GC-Flory EOS	derived from the generalized van der Waals partition function; modification of the Flory EOS, which reduces to the ideal gas in the limit of zero pressure and accounts for nonrandom mixing		group contribution expressions	R_k, Q_k, $C_{k,1}$, $C_{k,2}$, C_k^0	ϵ_{mm}, ϵ_{mn} and $\Delta\epsilon$ obtained from $1/V(\partial V/\partial T)_p$, ΔH^{vap}, and binary VLE data for low molecular weight compounds
revised GC-Flory EOS	revision of the GC-Flory EOS, in which the extra binary entropic interaction parameters are not used and some new group parameters are replenished		group contribution expressions	R_k, Q_k, $C_{k,1}$, $C_{k,2}$, C_k^0	ϵ_{mm}, ϵ_{mn} and $\Delta\epsilon_{mn}$ obtained from PVT, ΔH^{vap}, and binary VLE data for low molecular weight compounds
GCLF EOS	derived from Guggenheim's statistical combinatorial formula		quasichemical theory	v_k^*, e_{kk}	α_{mn} obtained from binary VLE data for low molecular weight compounds

factor of order unity. Oishi and Prausnitz found that the agreement between the calculated and experimental activities for solvents in polymer solutions is the best when $b = 1.28$ and c (for many solvents) is set to 1.1.

In the UNIFAC-FV model, the UNIFAC model, in principle, may be replaced by the ASOG model. Thus, the ASOG-FV model was proposed by Tochigi et al.[195,269] But the UNIFAC-FV model is built upon the extensive UNIFAC work for small molecules and, thus, has a relatively large number of group parameters available.

We have evaluated the potential of UNIFAC-FV to predict VLE in dendrimer−solvent and hyperbranched polymer−solvent systems.[248] The dendritic polymers, hydroxyl-functional macromolecules, are present, and their solutions in polar solvents are studied. The hydrodynamic radius of a dendritic polymer depends mainly on the solvent polarity, as well as the nature and number of functional polymer groups. The investigated hydroxyl-functional hyperbranched polyethers and polyesters dissolved in strongly polar solvents such as water and ethanol represent soft globular structures with a comparatively large hydrodynamic volume, allowing for penetration of the solvent molecules and, therefore, interactions between the solvent and all polymer structural units, so a polymer solution should be described in such a way that a model considers the contribution of all structural units to the solvent residual activities. It was confirmed that the calculated results from the UNIFAC-FV model are in good agreement with those from experiments.

Wibawa et al.[253,254] revised the UNIFAC group interaction in the UNIFAC-FV model, since the nature of molecular

energy interactions of solvent−polymer systems is different from that of the low molecular weight compounds. A total of 142 binary systems that consisted of 16 polymers and 36 solvents over a wide range of concentrations were collected to correlate 46 pairs of group interaction parameters. A significant improvement of prediction results was achieved by the UNIFAC-FV model from 20.0 to 10.8% absolute average deviation (AAD) in solvent activities for the systems containing polar solvents and from 16.7 to 10.9% AAD for overall systems. Compared with other predictive models, such as entropic-FV, GK-FV, and UNIFAC-ZM models, the UNIFAC-FV model gave the best results.

But it should be noted that the activity coefficient models for solvent−polymer systems (e.g., UNIFAC-FV, entropic-FV, GK-FV, and UNIFAC-ZM) require pure component and mixture densities. It is sometimes difficult to find accurate density data for both solvent and polymer at the temperatures of the system, and prediction results from these models are rather sensitive to the pure component and mixture densities. From this viewpoint, equations of state (e.g., GCLF EOS), in which only the molecular structures are inputted, are more convenient. Another advantage of equations of state is that they can declare the effect of pressure on phase equilibria.

4.2. GCLF EOS

Among the equations of state for polymer−solvent systems, the group-contribution lattice-fluid equation of state (GCLF EOS) has unique features. The only input required for this model is the molecular structures of polymer and solvent in terms of their functional groups. At extreme conditions (very high pressure and very low temperature), it is very difficult to carry out an experiment, and thus, a predictive model is indispensable. Unfortunately, the number of group parameters available for the GCLF EOS is somewhat limited and involves only 24 main groups and 47 subgroups. There are many gaps in the group interaction parameter table provided by Lee and Danner.[263]

We have tried to fill the missing group interaction parameters of the GCLF EOS on the basis of the principle that all the group parameters can be obtained using only pure component and binary equilibrium properties of low molecular weight components, and PVT data of polymers are not needed. In other words, the group interaction energy ($e_{0,k}$, $e_{1,k}$, $e_{2,k}$) and reference volume parameters ($R_{0,k}$, $R_{1,k}$, $R_{2,k}$) may be derived by means of an equations of state (EOS); for example, Peng−Robinson (PR) EOS or its modification.[197] The group binary interaction parameters, α_{mn}, may be derived using activity coefficient models; for example, the UNIFAC model. The accuracy and reliability of the PR EOS or its modifications for predicting $P-V-T$ behavior of low molecular weight pure compounds and the UNIFAC model for predicting the activity coefficient of a low molecular weight binary system have already been accepted.

Of course, one possibility to obtain the necessary information is to carry out experimental measurements for the pure component and the mixture of interest, but measurements are often very time-consuming and expensive. For example, for 10 newly added groups (assuming that they belong to different main groups), there are 105 group parameters to be correlated. If an average number of 10 data points is required to determine one group parameter, in total there are 1050 data points to be measured. However, the existing parameter matrix of the UNIFAC model is developed to include 64 main groups and over 100 subgroups. That is to

say, to fill the gap of missing group parameters, the amount of experimental work is apparently too large, since all the data cannot be found in the literature. Therefore, it is possible to extend the group parameter matrix of the GCLF EOS when the experiments are time-consuming and expensive under extreme conditions.

4.2.1. Equation of State

The GCLF EOS is derived on the basis of the Panayiotou−Vera EOS[270,271] and is of the form

$$\frac{\tilde{P}}{\tilde{T}} = \ln\left(\frac{\tilde{v}}{\tilde{v}-1}\right) + \frac{z}{2}\ln\left(\frac{\tilde{v}+q/r-1}{\tilde{v}}\right) - \frac{\theta^2}{\tilde{T}} \quad (4.5)$$

where $\tilde{P}$, $\tilde{T}$, and $\tilde{v}$ are the reduced pressure, temperature, and molar volume, respectively, and defined by

$$\tilde{P} = \frac{P}{P^*}, \quad T = \frac{T}{T^*} \quad v = \frac{v}{v^*}, \quad \theta = \frac{q/r}{\tilde{v}+q/r-1} \quad (4.6)$$

$$P^* = \frac{z\epsilon^*}{2v_h}, \quad T^* = \frac{z\epsilon^*}{2R}, \quad v^* = v_h r \quad (4.7)$$

$$zq = (z-2)r + 2 \quad (4.8)$$

$$z = 10, \quad R = 8.314 \text{ J mol}^{-1} \text{ K}^{-1},$$
$$v_h = 9.75 \times 10^{-3} \text{m}^3 \text{ kmol}^{-1}$$

where q is the interaction surface area parameter; r is the number of lattice sites occupied by a molecule; z is the coordination number; R is the universal gas constant; v_h is the volume of a lattice site; and P^*, T^* and v^* are referred to as scaling parameters.

This equation of state contains two adjustable parameters: the molecular interaction energy, ϵ^*, and the molecular reference volume, v^*. Once these two parameters are known, all of the remaining parameters in eq 4.5 can be determined from eqs 4.6−4.8 at a given temperature and pressure. Properties of a system can then be determined by solving eq 4.5 with respect to reduced volume.

For pure components, the molecular interaction energy between like molecules, ϵ_i^*, is obtained from the following mixing rule,

$$\epsilon_i^* = \sum_k \sum_m \Theta_k^{(i)} \Theta_m^{(i)} (e_{kk} e_{mm})^{1/2} \quad (4.9)$$

where e_{kk} is the group interaction energy between like groups k,

$$e_{kk} = e_{0,k} + e_{1,k}\left(\frac{T}{T_0}\right) + e_{2,k}\left(\frac{T}{T_0}\right)^2 \quad (4.10)$$

T (K) is the system temperature, and T_0 is arbitrarily set to 273.15 K. The group surface area fractions, $\Theta_k^{(i)}$, are expressed by

$$\Theta_k^{(i)} = \frac{n_k^{(i)} Q_k}{\sum_n n_n^{(i)} Q_n} \quad (4.11)$$

where $n_k^{(i)}$ is the number of group k in component i, and Q_k is the dimensionless surface area parameter of group k, as

used in the UNIFAC model mentioned above. The molecular reference volume, v_i^*, is calculated from the group reference volume parameter, R_k, using the following mixing rule:

$$v_i^* = \sum_k n_k^{(i)} R_k \tag{4.12}$$

where R_k is given by

$$R_k = \frac{1}{10^3}\left[R_{0,k} + R_{1,k}\left(\frac{T}{T_0}\right) + R_{2,k}\left(\frac{T}{T_0}\right)^2\right] \tag{4.13}$$

For a binary mixture, the basic form of eq 4.5 is unchanged, and thus, the solving procedure is similar to that of pure components. But the following mixing rules are introduced:

$$\epsilon^* = \bar{\theta}_1\epsilon_{11} + \bar{\theta}_2\epsilon_{22} - \bar{\theta}_1\bar{\theta}_2\dot{\Gamma}_{12}\Delta\epsilon, \ \Delta\epsilon = \epsilon_{11} + \epsilon_{22} - 2\epsilon_{12} \tag{4.14}$$

$$\epsilon_{12} = (\epsilon_{11}\epsilon_{22})^{1/2}(1 - k_{12}) \tag{4.15}$$

$$\epsilon_{ii} = \sum_k \sum_m \Theta_k^{(i)}\Theta_m^{(i)}(e_{kk}e_{mm})^{1/2} \tag{4.16}$$

$$k_{12} = \sum_m \sum_n \Theta_m^{(M)}\Theta_n^{(M)}\alpha_{mn} \tag{4.17}$$

$$v^* = \sum x_i v_i^* \tag{4.18}$$

$$\Theta_k^{(i)} = \frac{n_k^i Q_k}{\sum_p n_p^{(i)} Q_p}, \quad \Theta_k^{(M)} = \frac{\sum_i n_k^{(i)} Q_k}{\sum_p \sum_i n_p^{(i)} Q_p} \tag{4.19}$$

where α_{mn} is the group binary interaction parameter; $\Theta_k^{(i)}$ and $\Theta_k^{(M)}$ are the surface area fraction of group k in the pure component i and in the mixture, respectively; and $\dot{\Gamma}_{12}$ is the nonrandomness parameter between molecules 1 and 2. The quasichemical approach gives the following relationship among the nonrandomness parameters:

$$\frac{\dot{\Gamma}_{11}\dot{\Gamma}_{22}}{\dot{\Gamma}_{12}^2} = \exp\left(\theta\frac{\Delta\epsilon}{RT}\right) \tag{4.20}$$

Other parameters are calculated from

$$r = \sum x_i r_i, \quad q = \sum x_i q_i, \quad \theta = \sum \theta_i \tag{4.21}$$

$$r_i = v_i^*/v_h, \ zq_i = (z - 2)r_i + 2 \tag{4.22}$$

$$\theta_i = \frac{zq_i N_i}{z(N_h + \sum q_j N_j)} = \frac{q_i N_i}{N_h + qN} = \frac{q_i/r_i}{\tilde{v}_i/r_i - r_i + q_i} \tag{4.23}$$

$$\bar{\theta}_i = \frac{zq_i N_i}{z\sum q_j N_j} = \frac{q_i N_i}{qN} = \frac{x_i q_i}{q} \tag{4.24}$$

$$\bar{\theta}_1\dot{\Gamma}_{11} + \bar{\theta}_2\dot{\Gamma}_{12} = \bar{\theta}_2\dot{\Gamma}_{22} + \bar{\theta}_1\dot{\Gamma}_{12} = 1 \tag{4.25}$$

where $\bar{\theta}_i$ is the molecular surface fraction of component i on a hole-free basis.

In GCLF EOS, the weight fraction activity coefficient (WFAC) of component i in the mixture is also given and expressed as

$$\ln \Omega_i = \ln \frac{a_i}{w_i} = \ln \varphi_i - \ln w_i + \ln \frac{\tilde{v}_i}{\tilde{v}} +$$
$$q_i \ln\left(\frac{\tilde{v}}{\tilde{v}-1}\frac{\tilde{v}_i-1}{\tilde{v}_i}\right) + q_i\left(\frac{2\theta_{i,p}-\theta}{\tilde{T}_i} - \frac{\theta}{\tilde{T}}\right) + \frac{zq_i}{2}\ln\dot{\Gamma}_i \tag{4.26}$$

$$\varphi_i = \frac{x_i v_i^*}{\sum_j x_j v_j^*} = \frac{x_i r_i}{\sum_j x_j r_j} \tag{4.27}$$

where the subscript i represents a pure component i; w_i and φ_i are the weight and volume fractions of component i in the mixture, respectively; and $\theta_{i,p}$ is the surface area fraction of the pure component i at the same temperature and pressure as the mixture. The activity coefficient defined by mole fraction is not appropriate to represent polymer solutions because the difference of molecular weight between solvent and polymer is usually too large.

Therefore, the group parameters ($e_{0,k}$, $e_{1,k}$, $e_{2,k}$, $R_{0,k}$, $R_{1,k}$, $R_{2,k}$, α_{mn}) should be given beforehand to solve the above equations. In principle, they can be derived from the properties of low molecular weight compounds.

Since eq 4.5 is of the form of transcendental equations, the calculation of densities (or molar volumes) is more complicated than that of common cubic equations of state (e.g., van der Waals, Redlich−Kwong, Peng−Robinson equations of state, etc.). It is known that cubic equations of state can be transformed into cubic polynomials with respect to molar volume. Unfortunately, even for these simple forms, we often get into trouble when solving them using the traditional Newton−Raphson method because unreasonable densities (or molar volumes) arise. As we know, most of the equations of state are of the characteristics of multiple peaks, and the Newton−Raphson method is valid only for solving local extremum. Thus, the converged results strongly depend on the initial values. The appropriate initial values are often in a very narrow range at high pressure. To find all of the meaningful roots, various initial values should be set by trial and error. For a one-stage equilibrium calculation, it may be possible to discard unmeaningful roots immediately, but for multistage equilibrium calculation, this would not be feasible. For this purpose, we have explored an algorithm for solving GCLF EOS from physical insight. The details about this algorithm are described in our previous publication.[267]

Lee and Danner[263] investigated the prediction results of activity coefficients of solvents in polymers at finite solvent concentrations for different predictive models. The systems of n-pentane/polyisobutylene, toluene/polystyrene, benzene/poly(vinyl acetate), methyl ethyl ketone/poly(methyl methacrylate), and benzene/poly(dimethyl siloxane) at a given temperature were concerned. It was found that GCLF EOS provides more accurate predictions than the UNIFAC-FV, the revised GC-Flory EOS, and the entropic FV models.

Later, Lee and Danner[264] also investigated the prediction results of activity coefficients of solvents in polymers at infinite dilution for different predictive models. A large amount of experimental data for various solvent−polymer
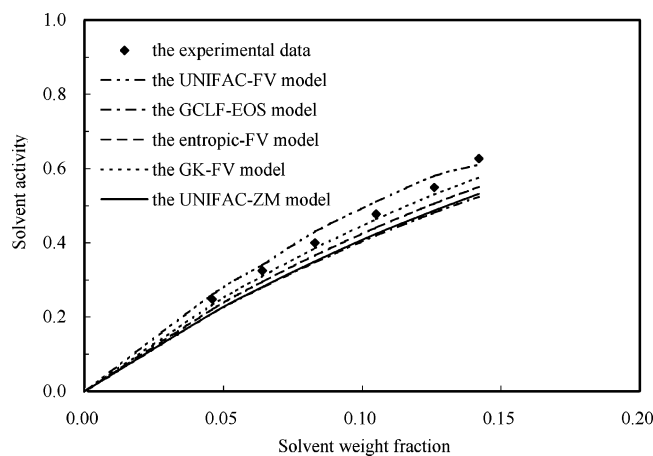
Figure 3. Solvent activity versus solvent weight fraction for the system of benzene/PIB (polyisobutylene) at 313.2 K. The calculated results from five kinds of models are compared with those from experiments.[334]

Figure 4. Solvent activity versus solvent weight fraction for the system of propanol/PVAc at 353.2 K. The calculated results from five kinds of models are compared with those from experiment.[335]

systems was collected, and extensive statistical analyses were performed. The prediction results of GCLF EOS were compared with those of the UNIFAC-FV, the revised GC-Flory EOS, and the entropic FV models. The GCLF gives the best predictions for nonpolar and weakly polar solvents, whereas the entropic FV model gives the best results for strongly polar solvents. As a whole, the GCLF EOS provides more accurate predictions that the UNIFAC-FV, the revised GC-Flory EOS, and the entropic FV models for solvent−polymer systems.

We selected two systems of benzene/PIB (polyisobutylene) and propanol/PVAc (poly(vinyl acetate)) to compare the predictive accuracy among the five models (UNIFAC-FV, GCLF EOS, entropic-FV, GK-FV, and UNIFAC-ZM), for which the group interaction parameters can be found in the open references.

For the system of benzene/PIB containing nonpolar solvent, the calculated results from these five models are all close to the experimental data, as shown in Figure 3. But it seems that the GK-FV model gives the best predictions for nonpolar solvents, since it is a revised version of the entropic-FV model for offsetting the underestimate of solvent activity.

For the system of propanol/PVAc containing polar solvent, a relatively large deviation between the experimental and calculated values was found, as shown in Figure 4, but both GCLF EOS and entropic-FV provide the best results; UNIFAC-ZM, the worst.

4.2.2. Extension of Group Parameters

Procedure for the Estimation of Group Parameters. The estimation of group interaction energy ($e_{0,k}$, $e_{1,k}$, $e_{2,k}$) and reference volume parameters ($R_{0,k}$, $R_{1,k}$, $R_{2,k}$) was carried out as follows:

(i) Using volume-translated PR EOS (VTPR EOS),[197] the densities at saturation were calculated for a series of normal alkanes, branched alkanes, cycloalkanes, aromatics, ethers, ketones, esters, acids, alcohols, water, amine, nitrified hydrocarbons, chlorinated hydrocarbons, fluoridated hydrocarbons, nitriles, tetrahydrofuran (THF), and other compounds. Calculations were carried out in the temperature range 250−500 K at 1 K intervals. This temperature range is far away from the triple and critical points of compounds selected in the parameter estimation in order to get reliable data by using the VTPR EOS. In the VTPR EOS, a volume
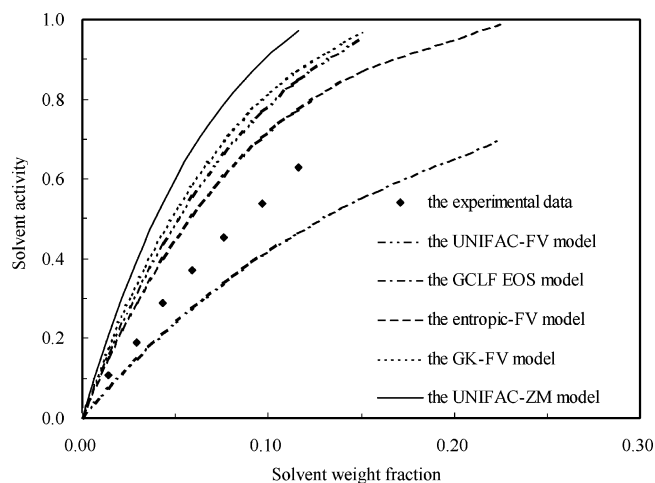
translation parameter is introduced to improve the description of saturated liquid densities, especially for polar components.

(ii) Fitting methods were used to minimize the deviations between the values from VTPR EOS and GCLF EOS so as to correlate the six parameters ($e_{0,k}$, $e_{1,k}$, $e_{2,k}$, $R_{0,k}$, $R_{1,k}$, $R_{2,k}$) simultaneously. The fitting procedure was done in a sequential fashion: normal alkanes, branched alkanes, cycloalkanes, aromatics, alcohols, ethers, ketones, esters, acids, etc. That is to say, the parameters for groups CH_3 and CH_2 were first regressed using only normal alkane data, then the parameters for groups CH and C using branched alkane data. These values were then used in conjunction with data for aromatics to obtain the ACH group parameters, and so forth.

Similarly, the group binary interaction parameters, α_{mn}, were obtained by means of the UNIFAC model (original version). Calculations were performed in the temperature range of 250−500 K with temperature steps of 5 K and a mole fraction of 0−1 at 10 mol % step.

Group Parameters. In this way, a number of new group parameters were derived, but the old group parameters that were fitted from the experimental data remained constant. The current GCLF EOS parameter matrix is illustrated in Figure 5, where the new 20 main groups are added. Since some group binary interaction parameters are not found in the UNIFAC table, a number of gaps still remain. Note that the group number coincides with the notation in the UNIFAC model and is a little different from that given by Lee and Danner.[263] The notation for the groups refers to the reference.[42]

4.3. Application of GCLF EOS

4.3.1. Solubility of Gas in Polymers

In foaming applications, properties such as carbon dioxide (CO_2) solubility in the polymer, polymer swelling, polymer density, and polymer crystallinity play an important role in the nature of the functional materials and affect the product's thermal conductivity, weight, impact strength, and finish. Therefore, property determination of polymers in the presence of dissolved gases can be viewed as essential for technological development of foamed polymer products.

The solubility of carbon dioxide (CO_2) in the amorphous polypropylene (PP) below T_m could be obtained with the GCLF EOS. As shown in Figure 6, at low temperatures,
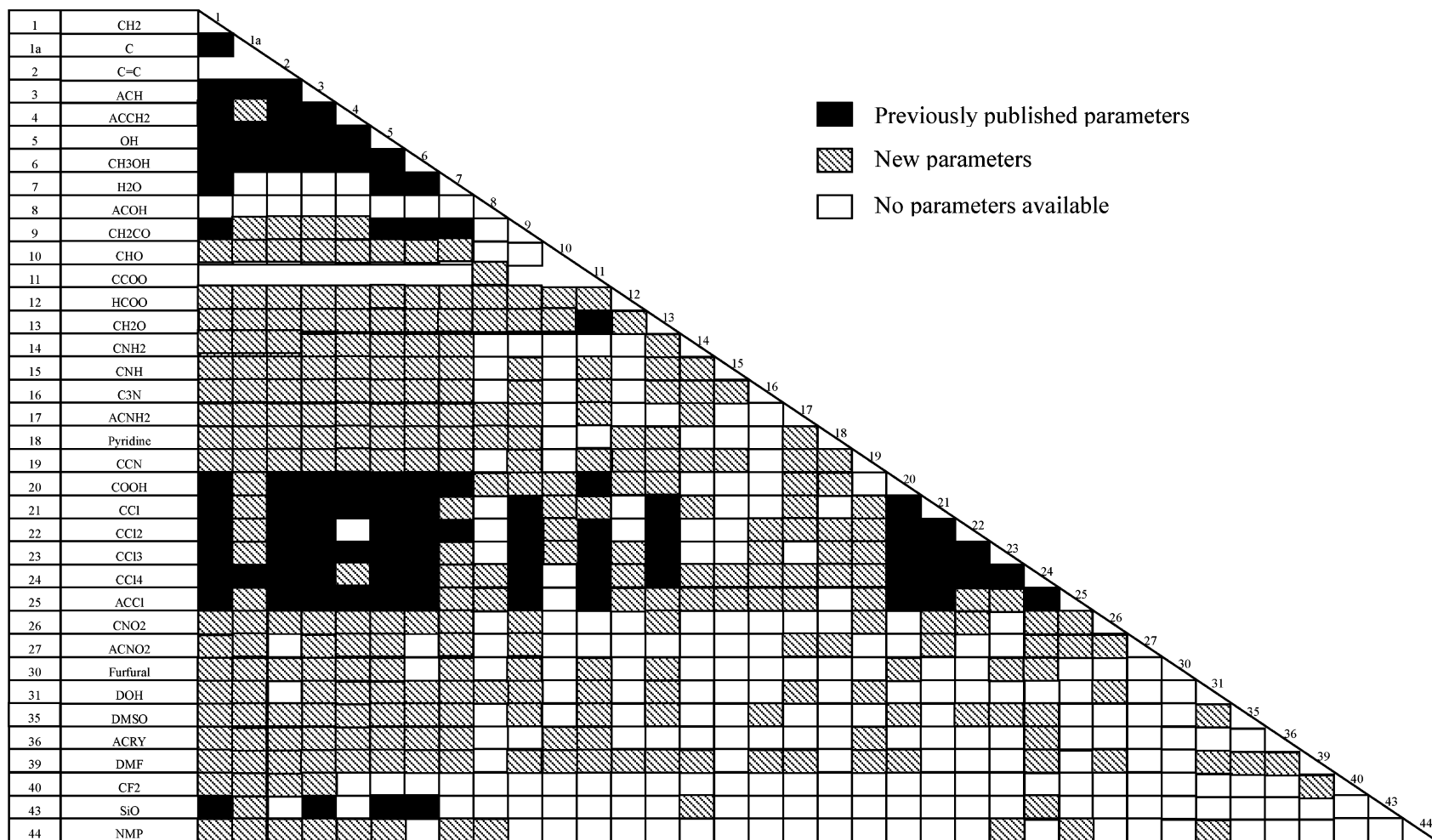
Figure 5. The GCLF EOS parameter matrix. New parameters are obtained by means of the VTPR EOS and UNIFAC model. Reprinted with permission from ref 337. Copyright 2006, Elsevier B. V.
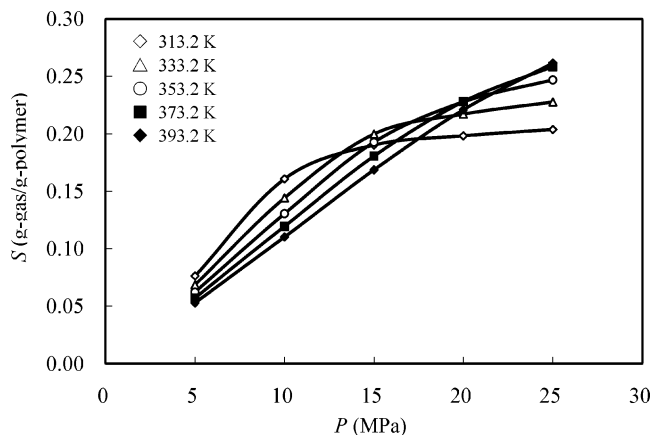
Figure 6. Solubility of CO_2 in rubbery state polypropylene with values estimated from the GCLF EOS. Symbols and lines refer to estimations made with the GCLF EOS. Reprinted with permission from ref 341. Copyright 2006, Elsevier B. V.

S-shaped isotherms were observed, whereas at high temperatures, the isotherms tended to become straight. At a given low pressure, below 10 MPa, the solubility decreased with increasing temperature, but at a given high pressure, above 10 MPa, the situation became somewhat complicated, which can be attributed to changes in sample crystallinity with temperature and pressure.

4.3.2. Crystallinity

The crystallinity change induced by a dissolved gas in glassy polymers was reported by several researchers.[272−276] Crystallinity (X_m, mass fraction) of polymer in its rubbery state can be calculated from

$$X_m = 1 - \frac{S^{exp}}{S^{cal}(X_m = 0)} \quad (4.28)$$

which assumes that the contribution of gas solubility in the polymer depends mainly on the amorphous region of the polymer and the crystalline region has negligible contribution.[277−280] The denominator in the last term of eq 4.28 refers to the solubility of CO_2 in the amorphous polymer. Thus, it is possible to estimate the crystallinity of polymer in the rubbery state in the presence of CO_2 by using interaction parameters from the GCLF EOS that have been extrapolated to rubbery state temperatures from those parameters determined from the molten state PP solubility data.

From the experimental data of the molten state PP, the GCLF EOS parameters can be extrapolated with temperature for a given pressure. Equation 4.28 was applied to estimate changes in crystallinity. Crystallinity of PP in the rubbery state in the presence of CO_2 is shown in Figure 7. It can be seen that at a given pressure, as temperature increases, crystallinity of the rubbery state first tends to remain constant and then decreases rapidly in the vicinity of 373.2 K. This behavior is consistent with the change of solubility and swelling degree, because crystallization tends to reduce the solubility and swelling degree. CO_2 lowers the melting temperature of the crystallinity polymer regions,[281] and as temperature increases, the crystallinity should decrease. At a given temperature, the crystallinity at 10 MPa is higher than that at 5 MPa. This may be due to some extent to the hydrostatic pressure effect but also possibly due to induced crystallinity caused by CO_2.
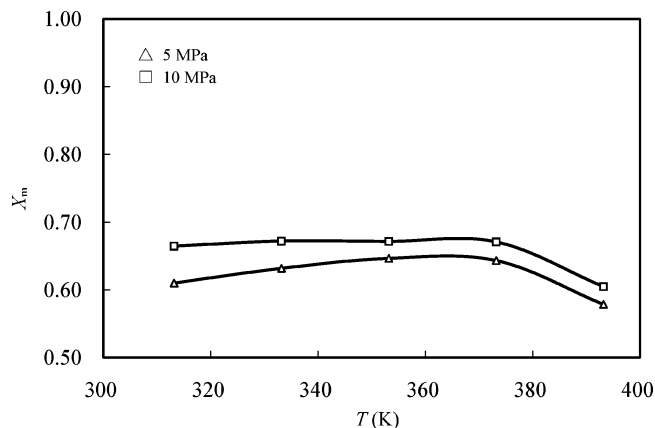

Figure 7. Effect of temperature on crystallinity of polypropylene in the presence of CO_2. Reprinted with permission from ref 341. Copyright 2006, Elsevier B. V.
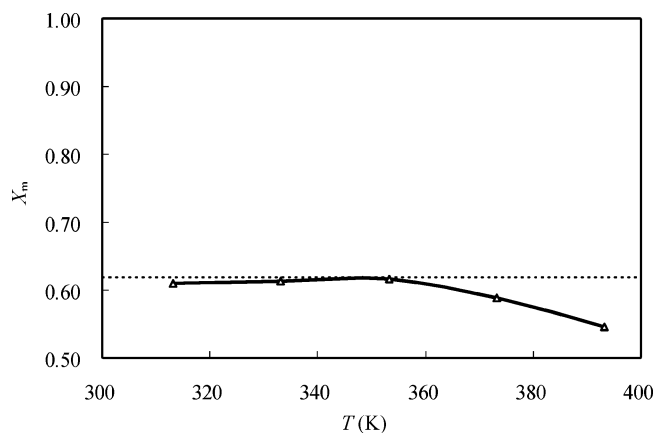

Figure 8. Effect of temperature on crystallinity based on extrapolation of high-pressure values to zero CO_2 content; the dashed line denotes the experimental crystallinity at room temperature. Reprinted with permission from ref 341. Copyright 2006, Elsevier B. V.

Methods for measuring the crystallinity of a polymer in various forms in the presence of CO_2 are limited. To test the reliability of crystallinity values estimated, the values were extrapolated to zero content CO_2 using linear extrapolation. The results are shown in Figure 8, where the dashed line denotes the experimental crystallinity at room temperature determined by the DSC technique ($X_m = 0.62$). At low temperatures, the crystallinity values tend to remain constant, but at high temperatures, the crystallinity values decrease sharply. This tendency is consistent with the results of Braun and Guillet,[282,283] which means that it is likely that the crystallinity values extrapolated to room temperature are close to the experimental crystallinity values. The crystallinity values calculated by this procedure using GCLF EOS are rough estimations for the changes in crystallinity of PP induced by CO_2. However, more detailed theoretical (simulation) and experimental techniques are required to understand the trends.

4.3.3. Specific Volume of Pure Polymers

On the basis of the extended group parameter matrix, the specific volume of pure polymers can be calculated by using GCLF EOS to check the reliability of some new group parameters.

The specific volumes of poly(vinyl acetate), poly(tetrahydrofuran) (PTHF), poly(styrene/acrylonitrile 3 wt %) (SAN3),
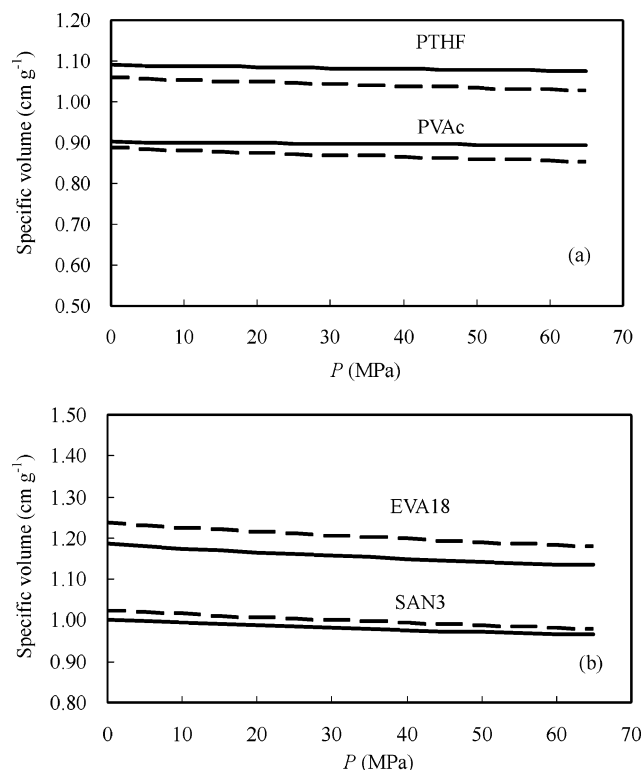
Figure 9. Prediction of specific volumes (cm g^{-1}) as a function of pressure, P (MPa). The solid lines represent the calculated values by GCLF EOS, and the dashed lines represent the calculated values by the Tait equation. (a) PVAc at 373.15 K and PTHF (poly-(tetrahydrofuran)) at 353.15 K; (b) SAN3 at 473.15 K and EVA18 at 423.15 K. Reprinted with permission from ref 337. Copyright 2006, Elsevier B. V.

and poly(ethylene/vinyl acetate 18 wt %) (EVA18) were calculated. The results were compared with values calculated with the Tait equation.[284] It can be seen from Figure 9 that the results from GCLF EOS and the Tait equation are in good agreement, and the average relative deviation (ARD) is <5%. Note that the calculations were performed assuming that the polymers are in the molten state. At low temperatures, however, these polymers are possibly not amorphous and exhibit some crystallinity. The GCLF EOS does not take into account crystallinity yet, and thus, significant errors may be expected for semicrystalline polymers.

Additionally, it was found that for homopolymers, the specific volume of the polymer is almost independent of its molecular weight. But for random copolymers, it seems that above a certain molecular weight, the molecular weight has no influence on specific volume.

4.3.4. Weight Fraction Activity Coefficients

The change of weight fraction activity coefficient (WFAC) Ω_i with weight fraction of solvent in the mixture, w_i, was investigated for the systems of water/polyethyleneimine (PEI) and acetonitrile (ACN)/polystyrene (PS).[337] For the system of water/PEI, the calculated values are in good agreement with the experimental values[285] with ARD 4.85%, except that at $w = 0.019$, the relative deviation is somewhat high. The reason may be that at very low solvent concentration, the accuracy of both experiment and calculation is not so sufficient.

For the system of ACN/PS, there is a relatively large deviation between the calculated and experimental values;[269] however, as pointed out by Danner et al.,[260] the GCLF EOS

gives the best predictions for the nonpolar and weakly polar systems. For the systems containing strongly polar solvents (e.g., ACN), the predictions are sometimes less good but as accurate as or better than other models (e.g., UNIFAC-FV model). However, the GCLF EOS can still predict the tendency of Ω_i with w_i. At a given temperature, Ω_i decreases with increasing w_i; at a given w_i, Ω_i decreases with increasing temperature. Moreover, it was also found that Ω_i of the solvent in the mixture is almost independent of molecular weight of the polymer.

As in the case of the UNIFAC model, the applicability of GCLF EOS largely depends on the availability and reliability of the group parameters. Since some group binary interaction parameters are missing in the UNIFAC table, the same gaps remain in the GCLF EOS matrix, and the proximity effect of groups is not considered in the GCLF EOS. in addition, the isomers or compounds with conjugated double bonds are not accurately described, although they are considered in other nonpredictive EOS.[286−289] Therefore, there is still some potential to improve GCLF EOS in the future.

5. Solvent–Ionic Liquid Systems

In recent years, room temperature ionic liquids have been very popular for their potential as "designer solvents". Ionic liquids show very unique properties, such as

(1) A low melting point (<373 K) and a wide liquid range (∼300 K);

(2) A suitable viscosity;

(3) Stability up to high temperature;

(4) High solubility for both polar and nonpolar organic and inorganic substances; and

(5) In particular, negligible vapor pressure and, therefore, nonflammability.

This means that they can be applied as replacements for conventional toxic, flammable, and volatile organic solvents. Because of the above-mentioned properties, they are very interesting solvents for industrial applications (chemical reactions, separation processes, batteries, electrochemistry, etc.).[290−303]

Typical ionic liquids are composed of a large organic cation and an inorganic polyatomic anion. Since a large number of cations and anions can be combined, there is virtually no limit to the number of feasible ionic liquids. Therefore, they are referred to as "designer solvents" for biphasic reactions or as selective solvents (entrainers) for separation processes.

However, a large number of possible ionic liquids are of little use for separation science if no systematic approach for the tailor-making of these substances for specific separation tasks is provided. Additionally, the mechanisms that lead to an efficient ionic liquid entrainer are not yet completely understood. Therefore, the design of ionic liquids as entrainers can only be based upon the separate examination of the influence of different kinds of structural variations. The structures and mechanisms that result in effective ionic liquid additives for a given separation task can be derived from the results of such a study. Since the experimental work would be too time-consuming and cost-intensive, it is necessary to employ an appropriate a priori method. The common structure-interpolating group-contribution methods (GCMs), such as UNIFAC models, are not desirable for the considered solvent−ionic liquid systems, because only a very limited number of interaction parameters resulting from some experimental data can be found.[310,338] Nevertheless, the
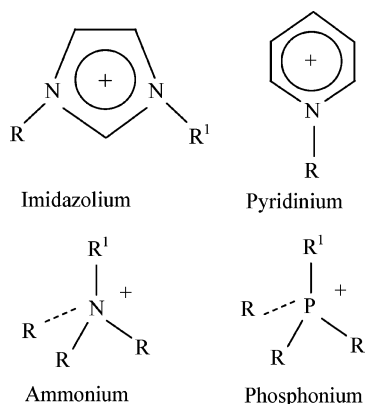
Figure 10. Common cations in ionic liquids; typical 1-alkyl-3-methylimidazolium cations and the abbreviations used to refer to them. R = Me, R^1 = Et: [emim]$^+$; R = Me, R^1= n-Bu: [bmim]$^+$; R = Me, R^1 = n-hexyl: [hmim]$^+$; R = Me, R^1 = n-octyl: [omim]$^+$.

number of published equilibrium data for solvent−ionic liquid systems is still very limited. Therefore, in this case, we would like to select the conductor-like screening for real solvents (COSMO-RS) model to predict the thermodynamic properties of solvent−ionic liquid systems and, thus, to identify the best suited structural composition of the ionic liquid for a given separation task.

Then, what are ionic liquids? Ionic liquids are salts consisting entirely of ions that exist in the liquid state at ambient temperature; , that is, they are salts that do not normally need to be melted by means of an external heat source.

The most common ionic liquids in use are those with alkylammonium, alkylphosophonium, N-alkylpyridinium, and N,N-dialkylimidazolium cations (see Figure 10); however, many more ionic liquids are synthesized on the basis of 1,3-dialkylimidazolium cations, with 1-butyl-3-methylimidazolium [bmim]$^+$ being probably the most common cation. The most common anions are [PF$_6$]$^-$, [BF$_4$]$^-$, [SbF$_6$]$^-$, [CF$_3$SO$_3$]$^-$, [CuCl$_2$]$^-$, [AlCl$_4$]$^-$, [AlBr$_4$]$^-$, [AlI$_4$]$^-$, [AlCl$_3$Et]$^-$, [NO$_3$]$^-$, [NO$_2$]$^-$, and [SO$_4$]$^{2-}$. Ionic liquids of this type have displayed the useful combination of low melting point along with high thermal and chemical stability. Detailed information about the synthesis and application of ionic liquids is available in the references.[293]

5.1. COSMO-RS Model

The COSMO-RS model, developed since 1994,[304−311] is a novel and efficient method for the priori prediction of thermophysical data It is based on a physically founded model and, unlike GCMs, uses only atom-specific parameters, which can be used to predict the thermodynamic properties of solvent−ionic liquid systems. Therefore, it is anticipated that this model is, at least qualitatively, able to describe structural variations correctly.

The extension of COSMO (conductor-like screening) model to real fluids is the COSMO-RS model. Instead of assuming the surrounding molecules in focus (solutes) to be an electrical conductor, the RS method separates the surface of the solute molecule into portions of given area and compares the screening charges with those of a second molecule (the solvent), which is treated in the same manner. The screening charges represent the electrostatic interaction potential of the molecules and enable the calculation of one component's chemical potential using a statistical mechanics approach.

A liquid in COSMO-RS is considered to be an ensemble of almost closely packed ideally screened molecules, and the interactions of the molecules are expressed as pairwise interactions of the screening charges. This includes electrostatic interactions as well as hydrogen bonding. By this reduction of molecular interactions to surface contacts, the statistical thermodynamics is reduced to a simple set of equations, which are similar to, but even somewhat more accurate than, the UNIQUAC type of equations used in the UNIFAC models.

This model assumes that ideal behavior means a complete neutrality of the charges of both molecules. Every deviation from this (called a "misfit") leads to activity coefficients differing from unity. Furthermore, the energy to transport a molecule into an electrical conductor is a measure of the vapor pressure. As a result, all kinds of thermodynamical data can be calculated. The model even works for multi-component systems. This method treats preferred enthalpy, , that is, interaction effects, but also includes a great deal of the solvation entropy, as recently shown in a study on the mutual solubilities of hydrocarbons and water.

The accuracy of COSMO-RS depends strongly on the quantum chemical method used. Furthermore, the method carries internal parameters because only electrostatic interactions are taken into account. The following atom-based internal constants are obtained using this method:

(1) Radius of the elements (used for cavity construction; only 17% larger than bond radii);

(2) Dispersion constants (one per element; vdW energy contributions expressed by element-specific parameters);

(3) Effective contact area (determines the number of independent neighbors for a molecule);

(4) Electrostatic misfit energy coefficient ("self" energy of a single segment of a surface divided by the surface charge density);

(5) Hydrogen-bonding constants c_{hb} and σ_{hb} (σ_{hb} is the threshold for hydrogen bonding and c_{hb}, the strength coefficient);

(6) Ring correction coefficient, ω;

(7) Coefficient, λ, for the combinatorial part of the chemical potential; and

(8) Transfer constant, η (connects reference states in gas and solution).

These constants have been determined once and have since been improved in several revisions. The activity coefficient of component i is related to chemical potential and given as follows:

$$\gamma_i = \frac{1}{x_i} \exp\left(\frac{\mu_i - \mu_i^0}{RT}\right) \tag{5.1}$$

where μ_i is the chemical potential of component i in the mixture, μ_i^0 is the chemical potential in the pure liquid substance, R is the gas constant, and T is the system temperature. The chemical potential can be solved by using the exact equations resulting from statistical thermodynamics.

The COSMO-RS model can be used to evaluate the separation ability of ionic liquids for a given separation task. It is composed of three steps: conformational analysis, COSMO calculation, and COSMO-RS calculation. The details about the calculation procedure of COSMO-RS model are described in the references.[312,313]

5.1.1. Conformations and Conformational Analysis

A molecule prefers to occupy the minimum points of the potential energy and arranges its atoms accordingly. By rotation around single bonds, molecules with the same molecular formula can form geometrical isomers by arranging their atoms in different, nonequivalent positions to each other, the so-called minimum energy conformations or stable conformations. To identify the stable conformations of a molecule, a conformational analysis is performed. Although it is desirable to find all minimum energy conformations, the complexity of the potential energy surface renders it impossible for all but the smallest molecules to have a complete result. To reduce the effort, algorithms have been developed to make the conformational search more effective and less time-consuming. An overview of various methods of conformational analysis is presented by Howard and Kollman.[314]

The conformational analysis is normally carried out using the molecular modeling program (e.g., HyperChem, ChemOffice, et al.), which is used to generate the molecular structures. It is assumed that single molecules and ions are in a vacuum, and their potential energies are calculated with the semiempirical PM3 methods. The semiempirical method has to be carefully chosen because the accuracy of its results depends on the components considered.

5.1.2. COSMO and COSMO-RS Model

For further considerations in a subsequent COSMO-RS model, the screening charges of molecular structures obtained from the conformational analysis have to be available. For this purpose, quantum chemical continuum solvation models (CSMs) are applied. Since the dielectric boundary conditions for arbitrarily shaped cavities are very complex, the COSMO model employs an ideal conductor as the dielectric medium. Compared with other CSMs, this approach results in simplified boundary conditions and therefore highly efficient algorithms. So far, the COSMO model is implemented in the programs Turbomole, Gaussian, DMOL3, and MOPAC and many other programs, such as GAMESS, PQS, ADF, and MOLPRO, applying either density functional theory or semiempirical methods. The calculation of molecular energies is accomplished using the TZVP basis set and BP function.[315−317] As the result of COSMO calculation, a "COSMO" file is generated. This file delivers all information of the respective molecular or ionic structure that is necessary for subsequent calculations of chemical potentials and activity coefficients.

The subsequent calculations using the COSMO-RS method that consists mainly of statistical thermodynamics are performed with the COSMOtherm software (Eckert, F. COSMOtherm Users Manual, 2002). The parametrization, BP-TZVP-C21-0104, which is required for the calculation of physicochemical data and contains intrinsic parameters of COSMOtherm and element-specific parameters, is adopted.

The influence of the conformations of solvents and ionic liquids on activity coefficients has been investigated by Jork et al.[312] and by Lei et al.,[313] respectively, and similar results were observed. For the separation of nonpolar solvents, the influence of the conformations of solvents and ionic liquids is not so apparent, and activity coefficients slightly fluctuate along a dashed line, which is referred to as the reference state. But for the separation of polar solvents, the influence of the conformations of solvents cannot be neglected.
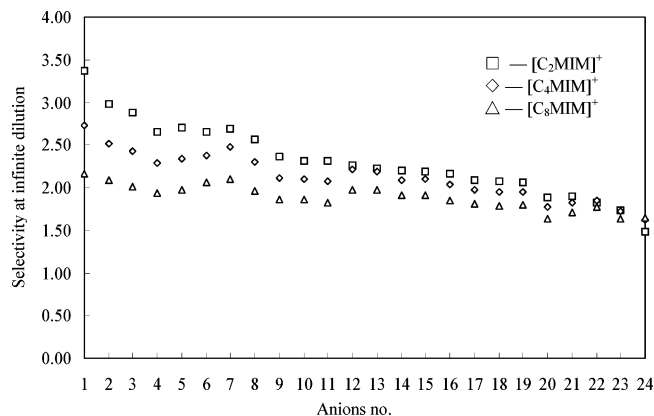

Figure 11. Influence of alkyl chain length of the cations on the selectivity of *n*-hexane to 1-hexene at infinite dilution at 333.15 K. □, [C$_2$MIM]$^+$; ◇, [C$_4$MIM]$^+$; △, [C$_8$MIM]$^+$. The corresponding no. of anions (1−24) is 1, [PF$_6$]$^-$; 2, [BOB]$^-$; 3, [B(CN)$_4$]$^-$; 4, [BTA]$^-$; 5, [CF$_3$SO$_3$]$^-$; 6, [BMB]$^-$; 7, [BF$_4$]$^-$; 8, [N(CN)$_2$]$^-$; 9, [BBB]$^-$; 10, [BSB]$^-$; 11, [Sal]$^-$; 12, [SCN]$^-$; 13, [HSO$_4$]$^-$; 14, [BMA]$^-$; 15, [CH$_3$SO$_4$]$^-$; 16, [C$_2$H$_5$SO$_4$]$^-$; 17, [MAcA]$^-$; 18, [TOS]$^-$; 19, [MDEGSO$_4$]$^-$; 20, [C$_8$H$_{17}$SO$_4$]$^-$; 21, [DMPO$_4$]$^-$; 22, [CH$_3$SO$_3$]$^-$; 23, [OAc]$^-$; 24, [Cl]$^-$. Reprinted with permission from ref 313. Copyright 2006, Elsevier B. V.

5.2. Prediction for Nonpolar Systems

5.2.1. Identifying the Best Suited Chemical Structure of Ionic Liquids

Separation of olefins and paraffins is a specific problem in the field of hydrocarbon processing. Since the boiling points of olefins and paraffins lie within narrow temperature ranges, it is difficult and expensive to separate them by conventional distillation. An additional solvent (namely entrainer) is normally required to add into the mixture to alter the selectivity of the components to be separated.

1-Hexene and *n*-hexane have been taken on as the representation of nonpolar systems, since the separation mechanism between 1-hexene/*n*-hexane and other hydrocarbons is consistent on the basis of the different mobilities of the electron cloud of C−C (no double bond) and C=C (double bond), and thus, different interactions between the entrainer and the component to be separated, and 1-hexene is a high-value-added product in industry. The goal is to identify a relation between the chemical structure of ionic liquids and the impact on separation factor (i.e., selectivity).

Figure 11 shows the influence of the alkyl chain length of the cations on the selectivity of *n*-hexane to 1-hexene at infinite dilution at 333.15 K by using the COSMO-RS model. The meaning of the abbreviations for all ionic liquids is given in the Nomenclature section. The series of [RMIM]$^+$ cations, , that is, [C$_2$MIM]$^+$, [C$_4$MIM]$^+$ and [C$_8$MIM]$^+$, are concerned, as well as 24 kinds of anions. The alkyl chain varies from ethyl group, butyl group, to octyl group. It can be seen that at a given anion, a long alkyl chain length of cations is unfavorable for increasing the selectivity, except for [CH$_3$SO$_3$]$^-$ and [Cl]$^-$. In addition, at a given cation, a long alkyl chain length of anions is also unfavorable for increasing the selectivity, since the selectivity decreases according to the sequence [HSO$_4$]$^-$, [CH$_3$SO$_4$]$^-$, [C$_2$H$_5$SO$_4$]$^-$, [C$_8$H$_{17}$SO$_4$]$^-$. Therefore, in general, the shorter the alkyl chain length, the higher the selectivity of *n*-hexane to 1-hexene.

On the other hand, it seems that in the series of [RMIM]$^+$ the anion affects the selectivity more strongly than the cation because the change of selectivity in the horizontal direction
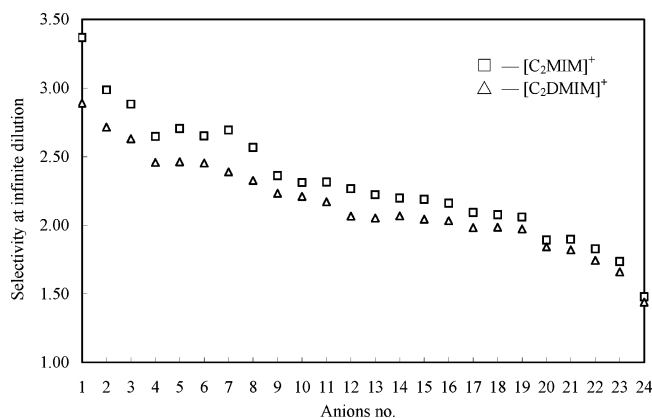
Figure 12. Influence of group substitution between [C$_2$MIM]$^+$ and [C$_2$DMIM]$^+$ on the selectivity of n-hexane to 1-hexene at infinite dilution at 333.15 K. □, [C$_2$MIM]$^+$; △, [C$_2$DMIM]$^+$. The corresponding no. of anions (1−24) is 1, [PF$_6$]$^-$; 2, [BOB]$^-$; 3, [B(CN)$_4$]$^-$; 4, [BTA]$^-$; 5, [CF$_3$SO$_3$]$^-$; 6, [BMB]$^-$; 7, [BF$_4$]$^-$; 8, [N(CN)$_2$]$^-$; 9, [BBB]$^-$; 10, [BSB]$^-$; 11, [Sal]$^-$; 12, [SCN]$^-$; 13, [HSO$_4$]$^-$; 14, [BMA]$^-$; 15, [CH$_3$SO$_4$]$^-$; 16, [C$_2$H$_5$SO$_4$]$^-$; 17, [MAcA]$^-$; 18, [TOS]$^-$; 19, [MDEGSO$_4$]$^-$; 20, [C$_8$H$_{17}$SO$_4$]$^-$; 21, [DMPO$_4$]$^-$; 22, [CH$_3$SO$_3$]$^-$; 23, [OAc]$^-$; 24, [Cl]$^-$. Reprinted with permission from ref 313. Copyright 2006, Elsevier B. V.

is higher than in the vertical direction, as shown in Figure 11. Moreover, the favorable anions are those in which the sterical shielding effect around their charge centers exists: for example, [PF$_6$]$^-$, [BOB]$^-$, [B(CN)$_4$]$^-$, [BTA]$^-$, [CF$_3$SO$_3$]$^-$, [BMB]$^-$, etc. On the contrary, the unfavorable anions are those in which the sterical shielding effect around their charge centers does not exist; for example, [DMPO$_4$]$^-$, [CH$_3$SO$_3$]$^-$, [OAc]$^-$, [Cl]$^-$, etc.

The influence of group substitution on the selectivity of n-hexane to 1-hexene at infinite dilution has also been investigated by using the COSMO-RS model, as shown in Figure 12. The 2-hydrogen of [C$_2$MIM]$^+$ is substituted by a methyl group to become [C$_2$DMIM]$^+$ and, thus, increases the degree of group branch. It can be seen that at a given anion, the selectivity of n-hexane to 1-hexene at infinite dilution is lower for [C$_2$DMIM]$^+$ than that for [C$_2$MIM]$^+$. This manifests that group substitution is unfavorable for increasing the selectivity.

So it can be deduced from the COSMO-RS model that the suitable ionic liquids for the separation of nonpolar systems are of small molecular volume, an unbranched group, and show a sterical shielding effect around the anion charge center. But it should be mentioned that in the COSMO-RS calculation, the state is at infinite dilution, and the demixing effect is not taken into account because prediction of liquid−liquid-phase splits and the associated tie lines in a ternary system requires an extensive and time-consuming computation.

To verify the reliability of the calculated results at infinite dilution by the COSMO-RS model, HSGC (headspace gas chromatography) experiments at finite dilution need to be done. Figure 13 shows the influence of feeding concentration of 1-hexene and n-hexane on the selectivity of n-hexane to 1-hexene for three kinds of ionic liquids at 333.15 K. The series of [RMIM]$^+$ cations, , that is, [C$_2$MIM]$^+$, [C$_4$MIM]$^+$, and [C$_8$MIM]$^+$, were concerned. It can be seen that at a given ionic liquid, as the feeding concentration increases, the selectivity of n-hexane to 1-hexene decreases. Moreover, at a given anion, that is, [BF$_4$]$^-$, at low feeding concentration, the long alkyl chain length of the cations is unfavorable for improving the selectivity, but at high feeding concentration,
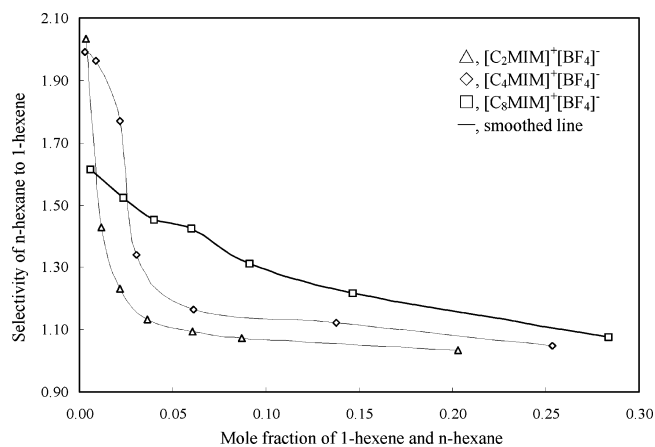

Figure 13. Influence of feeding concentration of 1-hexene and n-hexane on the selectivity of n-hexane to 1-hexene for three ternary systems containing ionic liquids at 333.15 K.

the opposite trend is exhibited. For these three kinds of ionic liquids, at low feeding concentration, the separation ability of ionic liquids is in the order of [C$_2$MIM]$^+$[BF$_4$]$^-$ > [C$_4$MIM]$^+$[BF$_4$]$^-$ > [C$_8$MIM]$^+$[BF$_4$]$^-$, whereas at high feeding concentration, the separation ability of ionic liquids is in the order of [C$_2$MIM]$^+$[BF$_4$]$^-$ < [C$_4$MIM]$^+$[BF$_4$]$^-$ < [C$_8$MIM]$^+$[BF$_4$]$^-$. We relate this effect to the formation of a liquid−liquid demixing. It may be deduced that the solubility of 1-hexene and n-hexane in ionic liquids is in the order of [C$_2$MIM]$^+$[BF$_4$]$^-$ < [C$_4$MIM]$^+$[BF$_4$]$^-$ < [C$_8$MIM]$^+$[BF$_4$]$^-$. Therefore, the ionic liquid with high solvent capacity is desirable in selecting the potential entrainer for the separation of a nonpolar system.

It is evident from the COSMO-RS model that at a low feeding concentration, the separation ability of ionic liquids is in the order of [C$_2$MIM]$^+$[BF$_4$]$^-$ > [C$_4$MIM]$^+$[BF$_4$]$^-$ > [C$_8$MIM]$^+$[BF$_4$]$^-$, which is consistent with the experimental results, because this is the region of miscibility. But at high feeding concentration, it is not consistent with the experimental results, because in this case, the solution is immiscible. This means that the COSMO-RS model is suitable for making a rapid screening of potential ionic liquids for nonpolar systems at low feeding concentration.

5.2.2. Demixing Effect on the Selectivity

Care should be taken to consider the demixing effects at high feeding concentration. Figure 14 shows the demixing effect on the selectivity of n-hexane to 1-hexene for the ternary system 1-hexene/n-hexane/[C$_8$MIM]$^+$[BTA]$^-$ at $T =$ 333.15 K. It was found that as the feeding concentration increases, the selectivity also decreases but without an apparent slope, as compared to [C$_2$MIM]$^+$[BF$_4$]$^-$, [C$_4$MIM]$^+$[BF$_4$]$^-$ and [C$_8$MIM]$^+$[BF$_4$]$^-$. This may be due to a higher solvent capacity of [C$_8$MIM]$^+$[BTA]$^-$.

As we know, a suitable entrainer should possess both a high selectivity and a high solvent capacity for the components to be separated. Therefore, it is necessary to compare the solvent capacity among the ionic liquids investigated. The calculated and experimental results of selectivity versus solvent capacity at infinite dilution are shown in Figure 15. Both exhibit a similar trend.

The ionic liquid [C$_8$MIM]$^+$[BTA]$^-$ has the highest solvent capacity but the lowest selectivity at infinite dilution among all the ionic liquids investigated (note that the selectivity is in the following order: [C$_2$MIM]$^+$[BF$_4$]$^-$ > [C$_4$MIM]$^+$[BF$_4$]$^-$
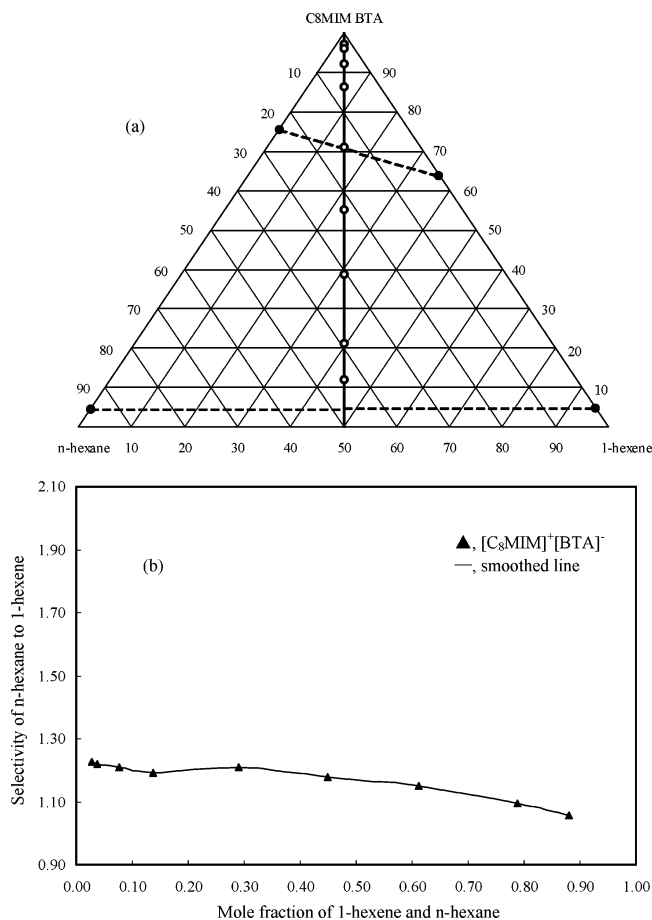
Figure 14. Demixing effect on the selectivity of *n*-hexane to 1-hexene for the ternary system 1-hexene/*n*-hexane/[C$_8$MIM]$^+$-[BTA]$^-$ at 333.15 K. (a) The triangular phase diagram of solubility; ○, experimental point at different feeding concentrations; (b) the selectivity of *n*-hexane to 1-hexene at different feeding concentrations.
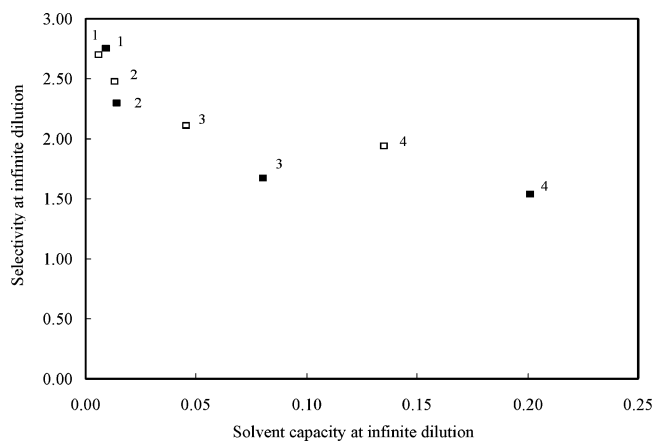

Figure 15. Selectivity versus solvent capacity at infinite dilution for the 1-hexene/*n*-hexane/ionic liquid systems at 333.15 K. 1, [C$_2$MIM]$^+$[BF$_4$]$^-$; 2, [C$_4$MIM]$^+$[BF$_4$]$^-$; 3, [C$_8$MIM]$^+$[BF$_4$]$^-$; 4, [C$_8$MIM]$^+$[BTA]$^-$; □, the calculated results by the COSMO-RS model; ■, the experimental results from the references.[310,344]

> [C$_8$MIM]$^+$[BF$_4$]$^-$ > [C$_8$MIM]$^+$[BTA]$^-$, which is consistent with the experimental results at low feeding concentration as shown in Figures 13 and 14). However, it has been proven by the HSGC experiment that [C$_8$MIM]$^+$[BTA]$^-$ also has the largest selectivity at high feeding concentration. This indicates that solvent capacity could affect selectivity at finite dilution.
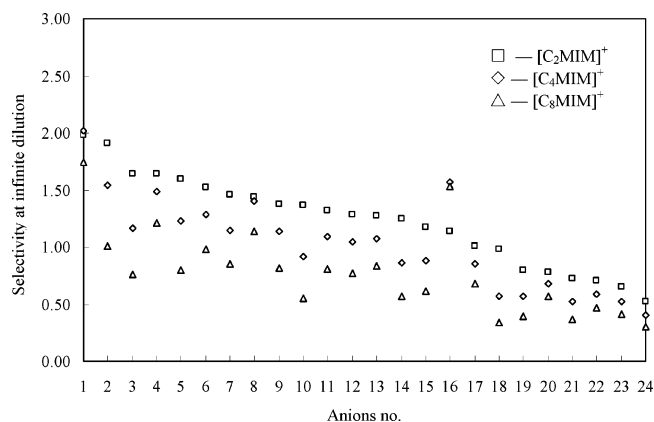

Figure 16. Influence of alkyl chain length of the cations on the selectivity of ethanol to water at infinite dilution at 353.15 K. □, [C$_2$MIM]$^+$; ◇, [C$_4$MIM]$^+$; △, [C$_8$MIM]$^+$. The corresponding no. of anions (1−24) is 1, [OAc]$^-$; 2, [HSO$_4$]$^-$; 3, [N(CN)$_2$]$^-$; 4, [DMPO]$^-$; 5, [SCN]$^-$; 6, [MAcA]$^-$; 7, [Sal]$^-$; 8, [CH$_3$SO$_3$]$^-$; 9, [CH$_3$SO$_4$]$^-$; 10, [BF$_4$]$^-$; 11, [BMA]$^-$; 12, [C$_2$H$_5$SO$_4$]$^-$; 13, [TOS]$^-$; 14, [CF$_3$SO$_3$]$^-$; 15, [BMB]$^-$; 16, [Cl]$^-$; 17, [MDEGSO$_4$]$^-$; 18, [PF$_6$]$^-$; 19, [BOB]$^-$; 20, [C$_8$H$_{17}$SO$_4$]$^-$; 21, [B(CN)$_4$]$^-$; 22, [BSB]$^-$; 23, [BBB]$^-$; 24, [BTA]$^-$.

Jork et al.[312] investigated the separation of the non-polar system of methylcyclohexane and toluene with ionic liquids as entrainers. The following ionic liquids were tested: [C$_8$Chin]$^+$[BTA]$^-$, [C$_8$Chin]$^+$[BBB]$^-$, [CABHEM]$^+$-[CH$_3$SO$_4$]$^-$, and [C$_4$MIM]$^+$[BTA]$^-$. It was found that the ionic liquids with the anion [BTA]$^-$ bring out high solvent capacity and selectivity, and the ionic liquid [C$_8$Chin]$^+$[BTA]$^-$ is the most favorable entrainer. The VLE data measured from HSGC experiments qualitatively confirmed the COSMO-RS calculations. In addition, a large number of experimental data are available from the references to validate the consistency between the experimental and calculated results.[345−365]

5.3. Prediction for Polar Systems

Ethanol and water are taken on as the representation of a polar system since anhydrous ethanol is used not only as a chemical reagent and organic solvent but also as the raw material of many important chemical products and intermediates.[318−323] The separation mechanism for polar systems is consistent on the basis of different interactions between entrainer and the component to be separated.

Figure 16 shows the influence of alkyl chain length of the cations on the selectivity of ethanol to water at infinite dilution at 353.15 K by using the COSMO-RS model. The series of [RMIM]$^+$ cations, , that is, [C$_2$MIM]$^+$, [C$_4$MIM]$^+$, and [C$_8$MIM]$^+$, are concerned, as well as 24 kinds of anions. The alkyl chain varies from ethyl group, butyl group, to octyl group. Similarly, at a given anion, a long alkyl chain length of cations is unfavorable for increasing the selectivity, except for [OAc]$^-$ and [Cl]$^-$. In addition, at a given cation, a long alkyl chain length of anions is also unfavorable for increasing the selectivity, since the selectivity decreases according to the sequence [HSO$_4$]$^-$, [CH$_3$SO$_4$]$^-$, [C$_2$H$_5$SO$_4$]$^-$, [C$_8$H$_{17}$SO$_4$]$^-$. Therefore, in general, the shorter the alkyl chain length, the higher the selectivity of ethanol to water. However, this also holds for the separation of nonpolar systems.

On the other hand, it seems that in the series of [RMIM]$^+$, the anion affects the selectivity more strongly than the cation because the change of selectivity in the horizontal direction is higher than in the vertical direction, as shown in Figure 16. Moreover, the favorable anions are those in which no
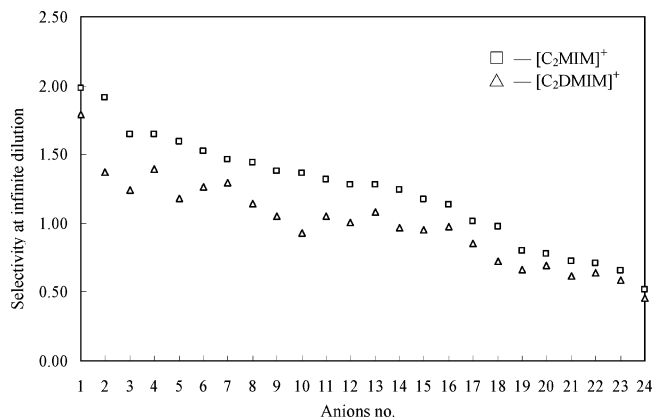
Figure 17. Influence of group substitution between $[C_2MIM]^+$ and $[C_2DMIM]^+$ on the selectivity of ethanol to water at infinite dilution at 353.15 K. □, $[C_2MIM]^+$; △, $[C_2DMIM]^+$. The corresponding no. of anions (1−24) is 1, $[OAc]^-$; 2, $[HSO_4]^-$; 3, $[N(CN)_2]^-$; 4, $[DMPO_4]^-$; 5, $[SCN]^-$; 6, $[MAcA]^-$; 7, $[Sal]^-$; 8, $[CH_3SO_3]^-$; 9, $[CH_3SO_4]^-$; 10, $[BF_4]^-$; 11, $[BMA]^-$; 12, $[C_2H_5SO_4]^-$; 13, $[TOS]^-$; 14, $[CF_3SO_3]^-$; 15, $[BMB]^-$; 16, $[Cl]^-$; 17, $[MDEGSO_4]^-$; 18, $[PF_6]^-$; 19, $[BOB]^-$; 20, $[C_8H_{17}SO_4]^-$; 21, $[B(CN)_4]^-$; 22, $[BSB]^-$; 23, $[BBB]^-$; 24, $[BTA]^-$.

sterical shielding effect around their charge centers exists; for example, $[OAc]^-$, $[HSO_4]^-$, $[DMPO_4]^-$, $[SCN]^-$, $[Cl]^-$, etc. On the contrary, the unfavorable anions are those in which sterical shielding effect around their charge centers does exist; for example, $[PF_6]^-$, $[BOB]^-$, $[B(CN)_4]^-$, $[BMB]^-$, $[BBB]^-$, $[BTA]^-$, etc. However, this is contrary to the results from the separation of nonpolar systems.

The influence of group substitution on the selectivity of ethanol to water at infinite dilution has also been investigated by using the COSMO-RS model, as shown in Figure 17. The 2-hydrogen of $[C_2MIM]^+$ is substituted by a methyl group to become $[C_2DMIM]^+$ and, thus, to increase the degree of group branch. It can be seen that at a given anion, the selectivity of ethanol to water at infinite dilution is lower for $[C_2DMIM]^+$ than that for $[C_2MIM]^+$. This manifests that group substitution is unfavorable for increasing the selectivity. However, this also holds for the separation of nonpolar systems. So it can be deduced from the COSMO-RS model that the suitable ionic liquids for the separation of ethanol and water are of small molecular volume, an unbranched group, and show no sterical shielding effect around the anion charge center. But it should be mentioned that although in the COSMO-RS calculation the state is at infinite dilution, the demixing effect sometimes is not so important because a large miscible region often exists for the polar systems (especially aqueous solutions) containing ionic liquids.

To verify the reliability of the calculated results by the COSMO-RS model, we compared the results from experiment[324] and calculation. Figure 18 shows the selectivity of ethanol to water at atmospheric pressure (101.32 kPa) for the two ternary systems ethanol/water/$[C_1MIM]^+[DMPO_4]^-$ and ethanol/water/$[C_2MIM]^+[DEPO_4]^-$, in which the feeding concentration of ethanol and water is up to 80 wt %. Evidently, a short alkyl chain length of cations and anions is favorable for increasing the selectivity. Both the calculated and experimental results agree quite well. The influence of the sterical shielding effect around their charge centers has also been investigated for the two ternary systems ethanol/water/$[C_2MIM]^+[Cl]^-$ and ethanol/water/$[C_2MIM]^+[PF_6]^-$ (see Figure 19). As mentioned before, the absence of a sterical shielding effect around their charge centers is
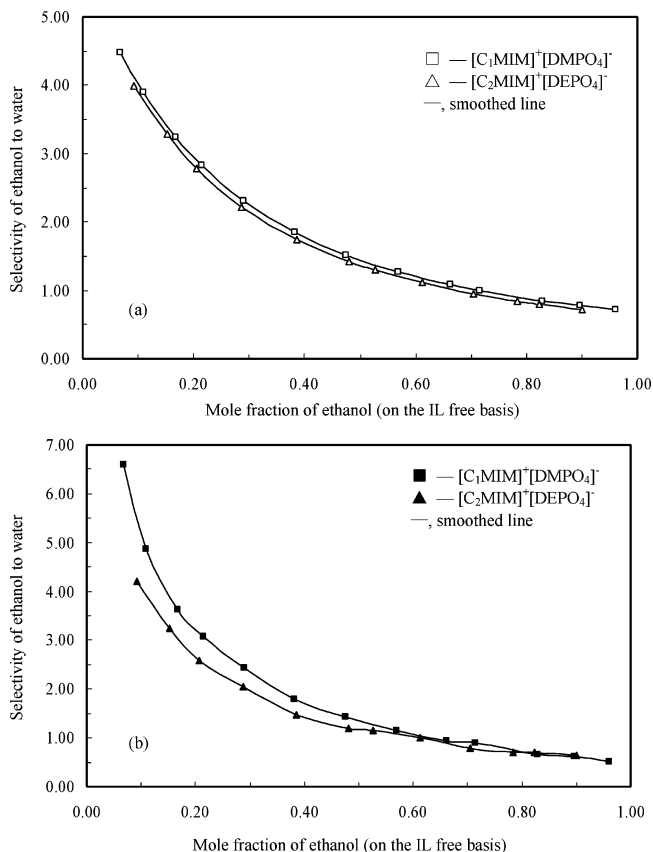

Figure 18. Selectivity of ethanol to water at atmospheric pressure (101.32 kPa) for the two ternary systems ethanol/water/$[C_1MIM]^+$-$[DMPO_4]^-$ and ethanol/water/$[C_2MIM]^+[DEPO_4]^-$ containing 20 wt % $[C_1MIM]^+[DMPO_4]^-$ or $[C_2MIM]^+[DEPO_4]^-$. (a) The calculated results by the COSMO-RS model; (b) the experimental results from the reference.[324] Reprinted with permission from ref 342. Copyright 2007, Elsevier Ltd.

favorable for increasing the selectivity, since the separation ability of $[C_2MIM]^+[Cl]^-$ is higher than that of $[C_2MIM]^+$-$[PF_6]^-$; however, it is noted that there is a difference between the values of selectivity from experiment and calculation, as shown in Figures 18 and 19. This is attributed to the drawback of COSMOS-RS model that it is not able to account for long-range forces (e.g., coulomb forces). As a consequence, this model does not meet the Debye−Hückel limiting law in diluted solutions, which is an indispensable property of any consistent molecular theory dealing with electrolyte solutions, but they exhibit a similar trend. That is to say, the calculated results by the COSMO-RS model are qualitatively consistent with the experimental results.

For the separation of ethanol and water, one ionic liquid, , that is, $[C_2MIM]^+[BF_4]^-$, was selected as entrainer for process simulation by Seiler et al.[290] It has been confirmed that this ionic liquid shows a remarkable separation performance and, therefore, enables an extractive distillation process that requires less energy than the conventional process using 1,2-ethanediol as entrainer. The maximum energy saving is up to 24%.

Jork et al.[312] investigated the separation of tetrahydrofuran (THF) and water with ionic liquids as entrainers. The tested ionic liquids consisted of the cations $[C_2MIM]^+$ and $[C_4MIM]^+$ combined with the anions $[OAc]^-$, $[Cl]^-$, $[HSO_4]^-$, $[C_2H_5SO_4]^-$, $[Sal]^-$, $[SCN]^-$, $[TOS]^-$, $[N(CN)_2]^-$, $[CH_3SO_4]^-$, $[MDEGSO_4]^-$, $[C_8H_{17}SO_4]^-$, $[CF_3SO_3]^-$, $[BF_4]^-$, $[BOB]^-$, $[PF_6]^-$, and $[BTA]^-$. It was found from the HSGC data that
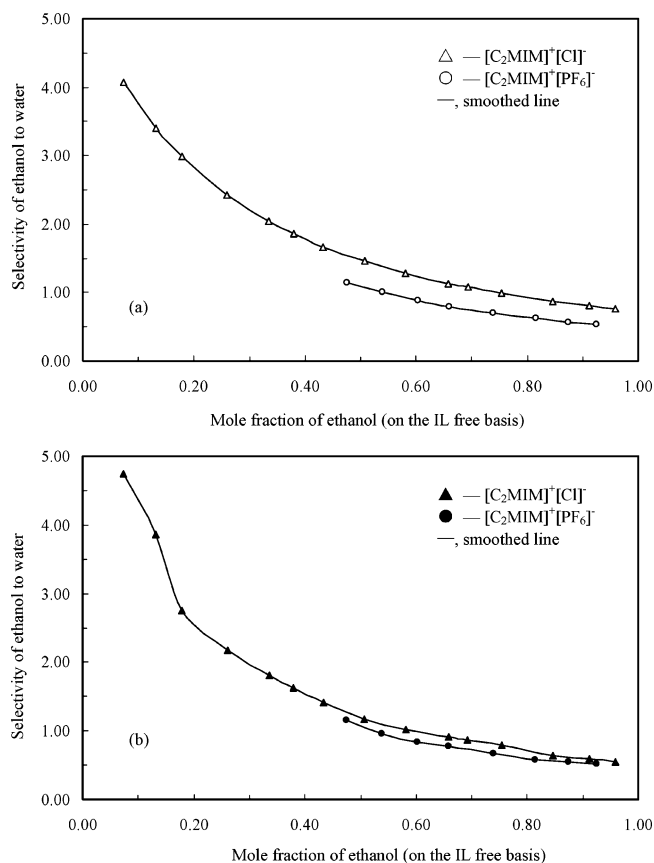
Figure 19. Selectivity of ethanol to water at atmospheric pressure (101.32 kPa) for the two ternary systems ethanol/water/$[C_2MIM]^+$-$[Cl]^-$ and ethanol/water/$[C_2MIM]^+[PF_6]^-$ containing 20 wt % $[C_1MIM]^+[Cl]^-$ or $[C_2MIM]^+[PF_6]^-$. (a) The calculated results by the COSMO-RS model; (b) the experimental results from the reference.[324] Reprinted with permission from ref 342. Copyright 2007, Elsevier Ltd.

the ionic liquids $[C_4MIM]^+[OAc]^-$ and $[C_2MIM]^+[Cl]^-$ ($[C_2MIM]^+[OAc]^-$ not tested) exhibit a higher selectivity than other ionic liquids, which is consistent with the results from the COSMO-RS model. This indicates that the COSMO-RS model can be used as a tool to tailor the suitable ionic liquid so as to reduce the amount of experimental work.

5.4. Prediction for Polar–Weakly Polar Systems

The COSMO-RS model was used to make a priori prediction of the extraction of stimulants from aqueous solution with ionic liquids as entrainers. The composition of stimulants in aqueous solution is at infinite dilution, sometimes up to the detecting limitation of analytical apparatus.[325−332]

The stimulants prohibited by the World Anti-Doping Agency (WADA) in the year 2006 are adrafinil, amfepramone, amiphenazole, amphetamine, amphetaminil, benzphetamine, bromantan, carphedon, cathine, clobenzorex, cocaine, dimethylamphetamine, ephedrine, etilamphetamine, etilefrine, famprofazone, fencamfamin, fencamine, fenetylline, fenfluramine, fenproporex, furfenorex, mefenorex, mephentermine, mesocarb, methamphetamine, methylamphetamine, methylenedioxy, methylephedrine, methylphenidate, modafinil, nikethamide, norfenfluramine, parahydroxyamphetamine, pemoline, phendimetrazine, phenmetrazine, phentermine, prolintane, selegiline, strychnine, and other substances with a similar chemical structure or similar biological effects, as
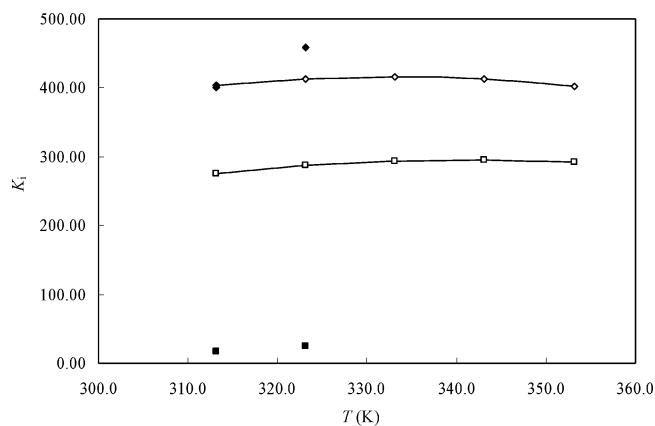
Figure 20. Partition coefficients, K_i, of C9N and C10N between the aqueous phase and supercritical fluid phase (or MTBE phase) at different temperatures. ◇, C9N with SC CO$_2$ and $[C_2MIM]^+[OAc]^-$ as the entrainer; □, C10N with SC CO$_2$ and $[C_2MIM]^+[OAc]^-$ as the entrainer; ◆, C9N with MTBE as the entrainer; ■, C10N with MTBE as the entrainer. Reprinted with permission from ref 342. Copyright 2007, Elsevier Ltd.

well as ethanol, which is listed separately for some specified sports (see http://www.wada-ama.org). The common characteristics for these stimulants is that they are polar substances with carbon chains.

The drugs amphetamine (C9N) and nikethamide (C10N) were selected as the simulated stimulants. It was found that the suitable ionic liquids for the extraction of C9N and C10 from aqueous phase are of small molecular volume, an unbranched group, and show no sterical shielding effect around the anion charge center.[342] That is to say, the same conclusion is attained between polar and polar−weakly polar systems, and thus, it seems that $[C_2MIM]^+[OAc]^-$ is the best among all the ionic liquids investigated.

Partition coefficients of C9N and C10N between the aqueous phase and the supercritical fluid phase (by the double actions of supercritical carbon dioxide (SC CO$_2$) and ionic liquid) at different temperatures were predicted by using the COSMO-RS model, as shown in Figure 20. In the calculation, the ionic liquid $[C_2MIM]^+[OAc]^-$ was selected, and the concentration was 0.10 mole fraction in aqueous phase. It was found that both C9N and C10N exhibit very high partition coefficients in the case that SC CO$_2$ and $[C_2MIM]^+$-$[OAc]^-$ are used as the entrainer, and the temperature has almost no influence on the partition coefficient under supercritical conditions. As a comparison, partition coefficients of C9N and C10N between the aqueous phase and the traditional organic phase (i.e., methyl *tert*-butyl ether (MTBE) phase) are also included in Figure 20. For C9N, a high partition coefficient is obtained, which is similar as the double actions of SC CO$_2$ and $[C_2MIM]^+[OAc]^-$. But for C10N, the partition coefficient is too small. This indicates that the separation efficiency of traditional liquid−liquid extraction is lower than that of supercritical extraction with an ionic liquid for the separation of stimulants from an aqueous solution.

5.5. Comparison between the COSMO-RS and UNIFAC Models

Among the wide range of applications of predictive molecular thermodynamic models, a nonpolar system and a system containing a polar component have been chosen. Figure 21 shows the VLE (vapor−liquid equilibria) of the
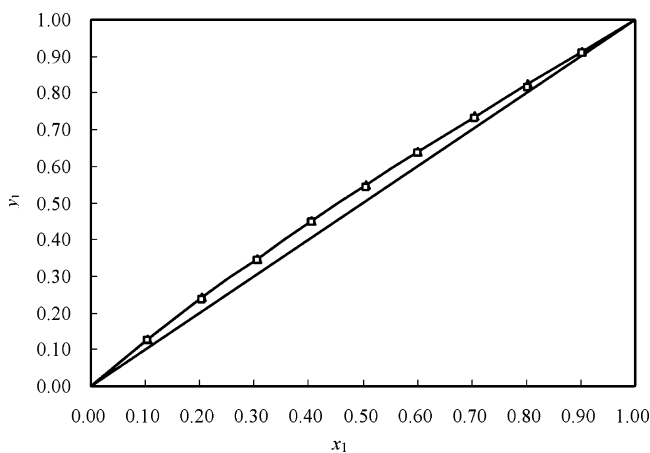
Figure 21. VLE of 1-hexene (1) and *n*-hexane (2) at 333.15 K. □, Experimental data; △, calculated results by the COSMO-RS model; −, calculated results by the UNIFAC model. Reprinted with permission from ref 336. Copyright 2006, Elsevier B. V.
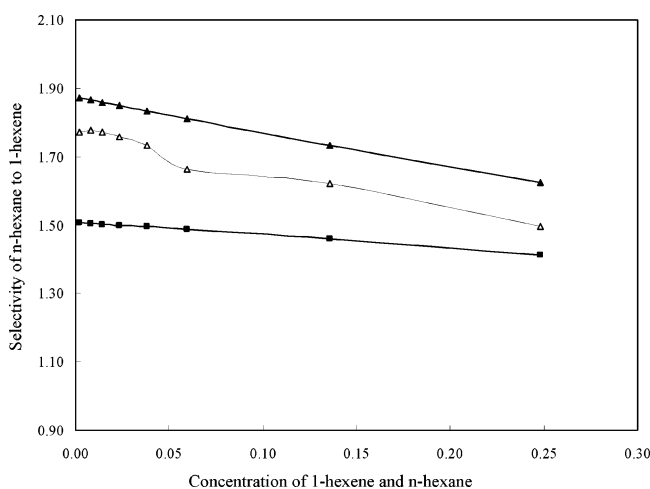

Figure 22. Influence of feeding concentration of 1-hexene and *n*-hexane on the selectivity of *n*-hexane to 1-hexene for the 1-hexene/*n*-hexane/NMP system at $T = 333.15$ K. △, experimental results; ■, calculated results by the COSMO-RS model; ▲, calculated results by the UNIFAC model; −, smoothed line. Reprinted with permission from ref 336. Copyright 2006, Elsevier B. V.

1-hexene (1)/*n*-hexane (2) system, where x_1 and y_1 are the molar fraction of 1-hexene in the liquid and vapor phases, respectively. The experimental data were compared with predictions of the COSMO-RS and UNIFAC models, and good agreement was found. For the ternary system of 1-hexene (1)/*n*-hexane (2)/NMP (*N*-methyl-2-pyrrolidone) in which NMP is used as the entrainer, the most important data, selectivity, is shown in Figure 22. It is evident that the COSMO-RS model underestimates the selectivity of *n*-hexane to 1-hexene, whereas the UNIFAC model overestimates it. In other words, the calculated results by the COSMO-RS and UNIFAC models may not agree well for the systems containing polar components.

Both the COSMO-RS model and the UNIFAC model are predictive models. For predicting thermodynamic behavior of nonpolar systems, they agree quite well. But for predicting thermodynamic behavior of polar systems, the situation may be different. In some cases, the calculated results by the COSMO-RS model may be quantitatively worse than the results of UNIFAC model, but we do not always need to obtain the accurate values. What is most import is that we

should know the influence of structural variations of ionic liquids on the calculated results qualitatively for rapid screening of potential ionic liquids.

In addition, the applicable systems for both models are also different, and the COSMO-RS model seems more universal. Contrary to the UNIFAC model, the COSMO-RS model can resolve the differences among isomers. At the same time, the main weaknesses of the COSMO-RS model are (1) the dispersive interactions are neglected, which leads to very poor results for systems such as *n*-hexane−perfluorohexane; (2) hydrogen-bonding effects are not properly taken into account; (3) isomer and proximity effects are not properly described; and (4) the temperature dependence is only qualitatively correct.[343] But the COSMO-RS model can be used to make a priori prediction for suitable ionic liquids, and no experimental data are needed. However, more experimental data have to be measured to see whether the UNIFAC model can be developed for the description of systems with ionic liquids, since ionic liquids as "designer solvents" are very attractive in the separation processes.

6. Conclusions

Predictive molecular thermodynamics models are the types of models for which phase equilibria can be described without binary interaction parameters being inputted. In separation processes, predictive molecular thermodynamic models can be used for identifying the relation between the molecular structure of the solvent and the separation performance and, thus, screening the best suited entainer rapidly so as to largely reduce the amount of experimental work. In polymer processing, predictive molecular thermodynamic models are used for predicting the solubility of gas in polymers, polymers' crystallinity, specific volume of pure polymers, weight fraction activity coefficients, etc. so as to control the nature of the functional materials in the PGSS process and foaming processing.

The predictive molecular thermodynamic models also can be classified into two categories: the models with relation to experimental data (e.g., the UNIFAC model) and the models without relation to experimental data (or called priori predictive models; e.g., the COSMO-RS model). The former is suitable for solvent−solvent systems with low molecular weight, solvent−solid salt systems and solvent−polymer systems, whereas the latter is for solvent−ionic liquid systems. The models and their applications are given in an in-depth review. By means of the predictive molecular thermodynamic models, CAMD can be used for screening the best suited entrainer rapidly for solvent−solvent systems with low molecular weight and solvent−solid salt systems in separation processes. For solvent−polymer systems, GCLF EOS is more emphasized because it is preferred over activity coefficient models (e.g., the UNIFAC-FV model), and the only input required for this model is the molecular structures of the polymer and solvent in terms of their functional groups. We have filled the missing group interaction parameters of the GCLF EOS for 20 main groups and 33 subgroups. The COSMO-RS model is a novel and efficient method for priori prediction, especially suitable for solvent−ionic liquid systems. A systematic variation of the cations and anions has been performed to preliminarily obtain first trends for the separation of nonpolar systems, polar systems, and polar−weakly polar systems. Following these results, experimental evidence was achieved. Then it is required for the chemists to synthesize the ionic liquid with optimum

molecular structures. Therefore, by means of predictive molecular thermodynamic models, the materials (including liquid solvents, solid salts, polymers and ionic liquids) can be regarded as "designer solvents" for a given task in the fields of separation processes, polymer processing, etc.

7. Nomenclature

ASOG = analytical solution of groups
CAMD = computer-aided molecular design
COSMO = conductor-like screening model
COSMO-RS = conductor-like screening model for real solvents
DISQUAC = dispersive-quasichemical
entropic-FV = entropic free volume
EOS = equation of state
FH/Hansen = Flory−Huggins model based on the Hansen solubility
GCEOS = group-contribution equation of state
GC-Flory EOS = group-contribution Flory equation of state
GCLF EOS = group-contribution lattice-fluid equation of state
GCMs = group-contribution methods
GK-FV = G. M. Kontogeorgis free volume
HSGC = headspace-gas chromatography
LCVM = linear combination of Vidal and Michelsen mixing rules
LLE = liquid−liquid equilibria
MHV1 = modified Huron−Vidal first order
MHV2 = modified Huron−Vidal second order
MOSCED = modified separation of cohesive energy density
NRTL = nonrandom two liquids
PGSS = particles from gas-saturated solutions
PR = Peng−Robinson
PSRK = predictive Soave−Redlich−Kwong
RST = regular solution theory
SLE = solid−liquid equilibria
SPACE = solvatochromic parameters for activity coefficient estimation
SRK = Soave−Redlich−Kwong
UNIFAC = UNIQUAC functional group activity coefficient
UNIFAC-FV = UNIFAC free volume
UNIFAC-ZM = UNIFAC Zhong−Masuoka
UNIQUAC = universal quasichemical
UNIWAALS = UNIFAC + van der Waals
VLE = vapor−liquid equilibria
VTPR = volume translated Peng−Robinson
W−S = Wong−Sandler

Cations

[CABHEM] = tridecylpentaethoxymethylammonium
$[C_8Chin]^+$ = 1-octylquinolinium
$[C_1MIM]^+$ = 1,3-dimethylimidazolium
$[C_1DMIM]^+$ = methyl methyl methylimidazolium
$[C_2MIM]^+$ = 1-ethyl-3-methylimidazolium
$[C_2DMIM]^+$ = 1-ethyl-2,3-dimethylimidazolium
$[C_4MIM]^+$ = 1-butyl-3-methylimidazolium
$[C_4DMIM]^+$ = 1-butyl-2,3-dimethylimidazolium
$[C_5MIM]^+$ = 1-methyl-3-pentylimidazolium
$[C_8MIM]^+$ = 1-methyl-3-octylimidazolium
$[C_4MPy]^+$ = 1-butyl-4-methylpyridinium
$[EMDiPAm]^+$ = ethyldiisopropylmethylammonium

Anions

$[OAc]^-$ = acetate
$[BBB]^-$ = bis[1,2-benzenediolato(2-)−O,O′]-borate
$[B(CN)_4]^-$ = tetracyanoborate
$[BF_4]^-$ = tetrafluoroborate
$[BMA]^-$ = bis(methylsulfonyl)amide
$[BMB]^-$ = bis(malonato(2-))borate
$[BOB]^-$ = bis(oxalato(2-))borate
$[BSB]^-$ = bis(salicylato(2-))borate
$[BTA]^-$ = bis(trifluoromethylsulfonyl)amide
$[CF_3SO_3]^-$ = trifluoromethylsulfonate

$[CH_3SO_3]^-$ = methylsulfonate
$[CH_3SO_4]^-$ = methylsulfate
$[C_2H_5SO_4]^-$ = ethylsulfate
$[C_8H_{17}SO_4]^-$ = octylsulfate
$[Cl]^-$ = chloride
$[DMPO_4]^-$ = dimethylphosphate
$[DEPO_4]^-$ = diethylphosphate
$[HSO_4]^-$ = hydrogensulfate
$[MAcA]^-$ = N-methylsulfonylacetamide
$[MDEGSO_4]^-$ = 2-(2-methoxyethoxy)ethylsulfate
$[N(CN)_2]^-$ = dicyanamide
$[BMA]$ = bis(methylsulfonyl)amide
$[PF_6]^-$ = hexafluorophosphate
$[SCN]^-$ = thiocyanate
$[TOS]^-$ = p-toluenesulfonate
$[Sal]^-$ = salicylate

8. Acknowledgment

9. References

(1) Lei, Z. G.; Li, C. Y.; Chen, B. H. *Sep. Purif. Rev.* **2003**, *32*, 121.
(2) Lei, Z. G.; Chen, B. H.; Ding, Z. W. *Special Distillation Processes*; Elsevier: Amsterdam, 2005.
(3) Cooper, A. I. *J. Mater. Chem.* **2000**, *10*, 207.
(4) Tomasko, D. L.; Li, H.; Liu, X.; Wingert, M. J.; Lee, L. J.; Koelling, K. W. *Ind. Eng. Chem. Res.* **2003**, *42*, 6431.
(5) Caskey, T.; Lesser, A. J.; McCarthy, T. J. *Polym. Eng. Sci.* **2001**, *41*, 2259.
(6) Kishimoto, Y.; Ishii, R. *Polymer* **2000**, *41*, 3483.
(7) Varma-Nair, M.; Handa, P. Y.; Mehta, A. K.; Agarwal, P. *Thermochim. Acta* **2003**, *396*, 57.
(8) Jung, J.; Perrut, M. *J. Supercrit. Fluids* **2001**, *20*, 179.
(9) Sproule, T. L.; Lee, J. A.; Li, H.; Lannutti, J. J.; Tomasko, D. L. *J. Supercrit. Fluids* **2004**, *28*, 241.
(10) Yeo, S. D.; Kiran, E. *J. Supercrit. Fluids* **2005**, *34*, 287.
(11) Dai, X.; Li, Z.; Wang, Y.; Yang, G.; Xu, J.; Han, B. *J. Supercrit. Fluids* **2005**, *33*, 259.
(12) Seader, J. D.; Henley, E. J. *Separation Process Principles*; Wiley: New York, 1998.
(13) Richardson, J. F.; Harker, J. H.; Backhurst, J. R. *Chemical Engineering Particle Technology and Separation Process*; Butterworth-Heinemann: Oxford, 2002.
(14) Tong, J. S.; Gao, G. H.; Liu, Y. P. *Chemical Engineering Thermodynamics*; Tsinghua University Press: Beijing, 1995.
(15) Zhu, Z. Q. *Supercritical Fluid Technology*; Chemical Industry Press: Beijing, 2001.
(16) Prausnitz, J. M. *Molecular Thermodynamics of Fluid-Phase Equilibria*; Prentice Hall: New Jersey, 1969.
(17) Smith, J. M.; Van Ness, H. C. *Introduction to Chemical Engineering Thermodynamics*; McGraw-Hill: New York, 1975.
(18) Malanowski, S.; Anderko, A. *Modelling Phase Equilibria: Thermodynamic Background and Practical Tools*; Wiley: New York, 1992.
(19) Sandler, S. I. *Chemical Engineering Thermodynamics*; Wiley: New York, 1989.
(20) Reed, T. M.; Gubbins, K. E. *Applied Statistical Mechanics: Thermodynamic and Transport Properties of Fluids*; McGraw-Hill: New York, 1973.
(21) Scatchard, G. *Chem. Rev.* **1931**, *8*, 321.
(22) Hildebrand, J. H.; Wood, S. E. *J. Chem. Phys.* **1933**, *1*, 817.

(23) Hildebrand, J. H.; Scott, R. L. *The Solubility of Nonelectrolytes*; Reingold: New York, 1950.

(24) Hansen, C. M. *J. Paint Technol.* **1967**, *39*, 505.

(25) Karger, B.; Snyder, L. R.; Eon, C. *J. Chromatogr.* **1976**, *125*, 71.

(26) Tijssen, R.; Billiet, H. A. H.; Schoenmakers, P. J. *J. Chromatogr.* **1976**, *122*, 185.

(27) Novak, J. P.; Matous, J.; Pick, J. *Liquid-Liquid Equilibria*; Elsevier: Amsterdam, 1987.

(28) Derr, E. L.; Deal, C. H. *Inst. Chem. Eng. Symp. Ser.* **1969**, *3*, 40.

(29) Wilson, G. M.; Deal, C. H. *Ind. Eng. Chem. Fundam.* **1962**, *1*, 20.

(30) Kojima, K.; Tochigi, K. *Prediction of Vapor-Liquid Equilibria by the ASOG Method*; Elsevier: Tokyo, 1979.

(31) Tochigi, K.; Minami, S.; Kojima, K. *J. Chem. Eng. Jpn.* **1977**, *10*, 349.

(32) Tochigi, K.; Tiegs, D.; Gmehling, J.; Kojima, K. *J. Chem. Eng. Jpn.* **1990**, *23*, 453.

(33) Fredenslund, A.; Jones, R. L.; Prausnitz, J. M. *AIChE J.* **1975**, *21*, 1086.

(34) Jorgensen, S. S.; Kolbe, B.; Gmehling, J.; Rasmussen, P. *Ind. Eng. Chem. Process Des. Dev.* **1979**, *18*, 714.

(35) Gmehling, J.; Rasmussen, P.; Fredenslund, A. *Ind. Eng. Chem. Process Des. Dev.* **1982**, *21*, 118.

(36) Macedo, E. A.; Weidlich, U.; Gmehling, J.; Rasmussen, P. *Ind. Eng. Chem. Process Des. Dev.* **1983**, *22*, 676.

(37) Tiegs, D.; Gmehling, J.; Rasmussen, P.; Fredenslund, A. *Ind. Eng. Chem. Res.* **1987**, *26*, 159.

(38) Hansen, H. K.; Rasmussen, P.; Fredenslund, A.; Schiller, M.; Gmehling, J. *Ind. Eng. Chem. Res.* **1991**, *30*, 2352.

(39) Gmehling, J. *Fluid Phase Equilib.* **1995**, *107*, 1.

(40) Gmehling, J. *Fluid Phase Equilib.* **1998**, *144*, 37.

(41) Bondi, A. *Physical Properties of Molecular Liquids, Crystals and Glasses*; Wiley: New York, 1968.

(42) Gmehling, J.; Li, J.; Schiller, M. *Ind. Eng. Chem. Res.* **1993**, *32*, 178.

(43) Lohmann, J.; Gmehling, J. *J. Chem. Eng. Jpn.* **2001**, *34*, 43.

(44) Gmehling, J.; Lohmann, J.; Jakob, A.; Li, J.; Joh, R. *Ind. Eng. Chem. Res.* **1998**, *37*, 4876.

(45) Gmehling, J.; Wittig, R.; Lohmann, J.; Joh, R. *Ind. Eng. Chem. Res.* **2002**, *41*, 1678.

(46) Wittig, R.; Lohmann, J.; Gmehling, J. *Ind. Eng. Chem. Res.* **2003**, *42*, 183.

(47) Bastos, J. C.; Soares, M. E.; Medina, A. G. *Ind. Eng. Chem. Res.* **1988**, *27*, 1269.

(48) Thomas, E. R.; Eckert, L. R. *Ind. Eng. Chem. Process Des. Dev.* **1984**, *23*, 194.

(49) Yang, Z. S.; Li, C. L.; Wu, J. Y. *Petrochem. Technol. (China)* **2001**, *30*, 285.

(50) Wu, Y. Z.; Wang, S. K.; Hwang, D. R.; Shi, J. *Can. J. Chem. Eng.* **1992**, *70*, 398.

(51) Howell, W. J.; Karachewski, A. M.; Stephenson, K. M.; Eckert, C. A.; Park, J. H.; Carr, P. W.; Rutan, S. C. *Fluid Phase Equilib.* **1989**, *52*, 151.

(52) Park, J. H.; Carr, P. W. *Anal. Chem.* **1987**, *59*, 2596.

(53) Lazzaroni, M. J.; Bush, D.; Eckert, C. A.; Frank, T. C.; Gupta, S.; Olson, J. D. *Ind. Eng. Chem. Res.* **2005**, *44*, 4075.

(54) Hait, M. J.; Eckert, C. A.; Bergmann, D. L.; Karachewski, A. M.; Dallas, A. J.; Eikens, D. I.; Li, J. J.; Carr, P. W.; Poe, R. B.; Rutan, S. C. *Ind. Eng. Chem. Res.* **1993**, *32*, 2905.

(55) Poe, R. B.; Rutan, S. C.; Hait, M. J.; Eckert, C. A.; Carr, P. W. *Anal. Chim. Acta* **1993**, *277*, 223.

(56) Castells, C. B.; Carr, P. W.; Eikens, D. I.; Bush, D.; Eckert, C. A. *Ind. Eng. Chem. Res.* **1999**, *38*, 4104.

(57) Kamlet, M. J.; Abboud, J. L. M.; Abraham, M. H.; Taft, R. W. *J. Org. Chem.* **1983**, *48*, 2877.

(58) Li, J.; Zhang, Y.; Dallas, A. J.; Carr, P. W. *J. Chromatogr.* **1991**, *550*, 101.

(59) Li, J.; Zhang, Y.; Carr, P. W. *Anal. Chem.* **1992**, *64*, 210.

(60) Li, J.; Zhang, Y.; Ouyang, H.; Carr, P. W. *J. Am. Chem. Soc.* **1992**, *114*, 9813.

(61) Brignole, E. A.; Bottini, S.; Gani, R. *Fluid Phase Equilib.* **1986**, *29*, 125.

(62) Stephanopoulos, G.; Townsend, D. W. *Chem. Eng. Res. Des.* **1986**, *64*, 160.

(63) Macchietto, S.; Odele, O.; Omatsone, O. *Chem. Eng. Res. Des.* **1990**, *68*, 429.

(64) Nielsen, B.; Gani, R.; Fredenslund, A. In: *Computer Applications in Chemical Engineering*; Bussemaker, H. T., Iedema, P. D., Eds.; Elsevier: Amsterdam, 1990; pp 227–232.

(65) Foucher, E. R.; Doherty, M. F.; Malone, M. F. *Ind. Eng. Chem. Res.* **1991**, *30*, 760.

(66) Porter, K. E.; Sitthiosoth, S.; Jenkins, J. D. *Chem. Eng. Res. Des.* **1991**, *69*, 229.

(67) Naser, S. F.; Fournier, R. L. *Comput. Chem. Eng.* **1991**, *15*, 397.

(68) Odele, O.; Macchietto, S. *Fluid Phase Equilib.* **1993**, *82*, 47.

(69) Bieker, T.; Simmrock, K. H. *Comput. Chem. Eng.* **1994**, *18*, 25.

(70) Meniai, A. H.; Newsham, D. M. T. *Trans. IChemE* **1996**, *74*, 695.

(71) Mathias, P. M.; Cheng, H.; Cook, S. J.; Klotz, H. C.; Parekh, V. S. *Fluid Phase Equilib.* **1996**, *116*, 225.

(72) Venkatasubramanian, V.; Chan, K.; Caruthers, J. M. *ACS Symp. Ser.* **1995**, *589*, 396.

(73) Joback, K. G.; Stephanopoulos, G. *Adv. Chem. Eng.* **1995**, *21*, 257.

(74) Churi, N.; Achenie, L. E. K. *Ind. Eng. Chem. Res.* **1996**, *53*, 3788.

(75) Marcoulaki, E. C.; Kokossis, A. C. *Comput. Chem. Eng.* **1998**, *22*, S11.

(76) Mavrovouniotis, M. L. *Comput. Chem. Eng.* **1998**, *22*, 713.

(77) Meniai, A. H.; Newsham, D. M. T.; Khalfaoui, B. *Trans. IChemE* **1998**, *76(A11)*, 942.

(78) Ourique, J. E.; Telles, A. S. *Comput. Chem. Eng.* **1998**, *22*, S615.

(79) Pistikopoulos, E. N.; Stefanis, S. K. *Comput. Chem. Eng.* **1998**, *22*, 717.

(80) Raman, V. S.; Maranas, C. D. *Comput. Chem. Eng.* **1998**, *22*, 747.

(81) Sinha, M.; Achenie, L. E. K.; Ostrovsky, G. M. *Comput. Chem. Eng.* **1999**, *23*, 1381.

(82) Harper, P. M.; Gani, R.; Ishikawa, T.; Kolar, P. *Fluid Phase Equilib.* **1999**, *158–160*, 337.

(83) Hostrup, M.; Harper, P. M.; Gani, R. *Comput. Chem. Eng.* **1999**, *23*, 1395.

(84) Franklin, J. L. *Ind. Eng. Chem. Res.* **1949**, *41*, 1070.

(85) Gani, R.; Brignole, E. A. *Fluid Phase Equilib.* **1983**, *13*, 331.

(86) Gani, R.; Fredenslund, A. A. *Fluid Phase Equilib.* **1993**, *82*, 39.

(87) Gani, R.; Nielsen, B.; Fredenslund, A. *AIChE J.* **1991**, *37*, 1318.

(88) Pretel, E. J.; Lopez, P. A.; Bottini, S. B.; Brignole, E. A. *AIChE J.* **1994**, *40*, 1349.

(89) Joback, K. G.; Reid, R. C. *Chem. Eng. Comm.* **1987**, *57*, 233.

(90) Reid, R. C.; Prausnitz, J. M.; Poling, B. E. *The Properties of Gases and Liquids*; McGraw-Hill: New York, 1987.

(91) Poling, B. E.; Prausnitz, J. M.; O'Connell, J. P. *The Properties of Gases and Liquids*; McGraw-Hill: New York, 2000.

(92) Tong, J. S. *Fluid Thermodynamic Properties*; Petrochemical Technology Press: Beijing, 1996.

(93) Lai, W. Y.; Chen, D. H.; Maddox, R. N. *Ind. Eng. Chem. Res.* **1987**, *26*, 1072.

(94) Lyman, W. J.; Reehl, W. F.; Rosenblatt, D. H. *Handbook of Chemical Property Estimation Methods*; McGraw-Hill: New York, 1982.

(95) Lei, Z. G.; Wang, H. Y.; Zhou, R. Q.; Duan, Z. T. *Comput. Chem. Eng.* **2002**, *26*, 1213.

(96) Chen, B. H.; Lei, Z. G.; Li, Q. S.; Li, C. Y. *AIChE J.* **2005**, *51*, 3114.

(97) Liao, B.; Lei, Z. G.; Xu, Z.; Zhou, R. Q.; Duan, Z. T. *Chem. Eng. J.* **2001**, *84*, 581.

(98) Lei, Z. G.; Zhou, R. Q.; Duan, Z. T. *Chem. Eng. J.* **2002**, *85*, 379.

(99) Lei, Z. G.; Zhou, R. Q.; Duan, Z. T. *J. Chem. Eng. Jpn.* **2002**, *35*, 211.

(100) Lei, Z. G.; Chen, B. H.; Li, J. W. *Chin. J. Chem. Eng.* **2003**, *11*, 297.

(101) Lei, Z. G.; Li, C. Y.; Chen, B. H. *Korean J. Chem. Eng.* **2003**, *20*, 1077.

(102) Chen, B. H.; Lei, Z. G.; Li, C. Y. *J. Chem. Eng. Jpn.* **2003**, *36*, 20.

(103) Braam, V. D.; Izak, N. *Ind. Eng. Chem. Res.* **2000**, *39*, 1423.

(104) Cesar, R.; Jose, C.; Aurelio, V.; Fernando, V. D. *Ind. Eng. Chem. Res.* **1997**, *36*, 4934.

(105) Lei, Z. G.; Wang, H. Y.; Zhou, R. Q.; Duan, Z. T. *Chem. Eng. J.* **2002**, *87*, 149.

(106) Lei, Z. G.; Zhang, J. C.; Chen, B. H. *J. Chem. Technol. Biotechnol.* **2002**, *77*, 1251.

(107) Li, J. W.; Lei, Z. G.; Ding, Z. W.; Li, C. Y.; Chen, B. H. *Sep. Purif. Rev.* **2005**, *34*, 87.

(108) Dahmani, O.; Wichterle, I.; Ait-Kaci, A. *Fluid Phase Equilib.* **1997**, *132*, 15.

(109) Figurski, G.; Emmerling, U.; Nipprasch, D.; Kehiaian, H. V. *Fluid Phase Equilib.* **1997**, *137*, 173.

(110) Delitala, C.; Marongiu, B.; Porcedda, S. *Fluid Phase Equilib.* **1998**, *142*, 1.

(111) Marongiu, B.; Porcedda, S.; Valenti, R. *Fluid Phase Equilib.* **1998**, *145*, 99.

(112) Reference deleted in revision.

(113) Alessandra, C.; Marongiu, B.; Porcedda, S. *Thermochim. Acta* **1998**, *311*, 1.

(114) Herraiz, J.; Shen, S.; Fernandez, J.; Coronas, A. *Fluid Phase Equilib.* **1999**, *155*, 327.

(115) Domanska, U.; Gonzalez, J. A. *Fluid Phase Equilib.* **1997**, *129*, 139.

(116) Gonzalez, J. A.; Fuente, I. G.; Cobos, J. C. *Fluid Phase Equilib.* **1997**, *135*, 1.

(117) Domanska, U.; Gonzalez, J. A. *Fluid Phase Equilib.* **1998**, *147*, 251.

(118) Gonzalez, J. A.; Carmona, J.; Fuente, I. G.; Cobos, J. C. *Thermochim. Acta* **1999**, *326*, 53.

(119) Gonzalez, J. A.; Fuente, I. G.; Cobos, J. C. *Fluid Phase Equilib.* **1999**, *154*, 11.
(120) Gonzalez, J. A.; Fuente, I. G.; Cobos, J. C. *Fluid Phase Equilib.* **2000**, *168*, 31.
(121) Domanska, U.; Szurgocinska, M.; Gonzalez, J. A. *Fluid Phase Equilib.* **2001**, *190*, 15.
(122) Gonzalez, J. A.; Szurgocinska, M.; Domanska, U. *Fluid Phase Equilib.* **2002**, *200*, 349.
(123) Gonzalez, J. A.; Villa, S.; Riesco, N.; Fuente, I. G.; Cobos, J. C. *Thermochim. Acta* **2002**, *381*, 103.
(124) Domanska, U.; Szurgocinska, M.; Gonzalez, J. A. *Ind. Eng. Chem. Res.* **2002**, *41*, 3253.
(125) Domanska, U.; Gonzalez, J. A. *Fluid Phase Equilib.* **2003**, *205*, 317.
(126) Gonzalez, J. A.; Cobos, J. C.; Fuente, I. G. *Fluid Phase Equilib.* **2004**, *224*, 169.
(127) Gonzalez, J. A.; Mozo, I.; Fuente, I. G.; Cobos, J. C. *Ind. Eng. Chem. Res.* **2004**, *43*, 7622.
(128) Domanska, U.; Lachwa, J.; Gonzalez, J. A. *Fluid Phase Equilib.* **2005**, *235*, 182.
(129) Gonzalez, J. A.; Domanska, U.; Lachwa, J. *Ind. Eng. Chem. Res.* **2005**, *44*, 5795.
(130) Domanska, U.; Gloskowska, M. *Fluid Phase Equilib.* **2004**, *216*, 135.
(131) Domanska, U.; Marciniak, M. *Ind. Eng. Chem. Res.* **2004**, *43*, 7647.
(132) Gonzalez, J. A.; Carmona, J.; Riesco, N.; Fuente, I. G.; Cobos, J. C. *Can. J. Chem.* **2001**, *79*, 1447.
(133) Gonzalez, J. A.; Fuente, I. G.; Cobos, J. C.; Casanova, C. *Fluid Phase Equilib.* **1992**, *78*, 61.
(134) Gonzalez, J. A.; Fuente, I. G.; Cobos, J. C.; Casanova, C. *Ber. Bunsenges. Phys. Chem.* **1991**, *95*, 1658.
(135) Gonzalez, J. A.; Fuente, I. G.; Cobos, J. C.; Casanova, C. *Fluid Phase Equilib.* **1994**, *94*, 167.
(136) Gonzalez, J. A.; Fuente, I. G.; Cobos, J. C.; Casanova, C. *Thermochim. Acta* **1992**, *217*, 57.
(137) Gonzalez, J. A.; Garcia, I.; Cobos, J. C.; Casanova, C. *Thermochim. Acta* **1991**, *189*, 115.
(138) Gonzalez, J. A.; Cobos, J. C.; Garcia, I.; Casanova, C. *Thermochim. Acta* **1990**, *171*, 153.
(139) Kehiaian, H. V.; Grolier, J. P. E.; Benson, G. C. *J. Chim. Phys.* **1978**, *75*, 1031.
(140) Kehiaian, H. V. *Fluid Phase Equilib.* **1983**, *13*, 243.
(141) Kehiaian, H. V. *Pure Appl. Chem.* **1983**, *13*, 243.
(142) Kehiaian, H. V. *Pure Appl. Chem.* **1985**, *57*, 15.
(143) Kehiaian, H. V.; Guieu, R.; Faradjzadeh, A.; Carbonnel, L. *Ber. Bunsenges. Phys. Chem.* **1981**, *85*, 132.
(144) Pierotti, G. J.; Deal, C. H.; Derr, E. L. *Ind. Eng. Chem.* **1959**, *51*, 95.
(145) Duan, Z. T. *Petrochem. Technol.* (*China*) **1978**, *7*, 177.
(146) Momoh, S. O. *Sep. Sci. Technol.* **1991**, *26*, 729.
(147) Weimer, R. F.; Prausnitz, J. M. *Hydro. Proc. Petro. Ref.* **1965**, *44*, 237.
(148) Helpinstill, J. G.; Winkle, M. V. *Ind. Eng. Chem.* **1968**, *7*, 213.
(149) Gould, R. F. *Extractive and Azeotropic Distillation*; American Chemical Society: Washington, DC, 1972.
(150) Hoffman, E. J. *Azeotropic and Extractive Distillation*; Wiley: New York, 1964.
(151) Nam, S. J. *J. KIChE* **1974**, *12*, 65.
(152) Briggs, G. G. *J. Agric. Food. Chem.* **1981**, *29*, 1050.
(153) Tsonopoulos, C.; Prausnitz, J. M. *Ind. Eng. Chem. Fundam.* **1971**, *10*, 593.
(154) Medir, M.; Giralt, F. *AIChE J.* **1982**, *28*, 341.
(155) Dutt, N. V. K.; Prasad, D. H. L. *Fluid Phase Equilib.* **1989**, *45*, 1.
(156) Yalkowsky, S. H.; Valvani, S. C. *J. Chem. Eng. Data* **1979**, *24*, 127.
(157) Mackay, D.; Shiu, W. Y. *J. Chem. Eng. Data* **1977**, *22*, 399.
(158) Prausnitz, J. M.; Anderson, R. *AIChE J.* **1961**, *7*, 96.
(159) Yi, B.; Xu, Z.; Lei, Z. G.; Liu, Y. X.; Zhou, R. Q.; Duan, Z. T. *J. Chem. Ind. Eng.* (*China*) **2001**, *52*, 549.
(160) Lei, Z. G.; Li, C. Y.; Chen, B. H. *Chin. J. Chem. Eng.* **2003**, *11*, 515.
(161) Lei, Z. G.; Li, C. Y.; Li, Y. X.; Chen, B. H. *Sep. Purif. Technol.* **2004**, *36*, 131.
(162) King, J. W.; List, G. R. *Supercritical Fluid Technology in Oil and Lipid Chemistry*; AOCS Press: Champaign, Illinois, 1996.
(163) Huron, M. J.; Vidal, J. *Fluid Phase Equilib.* **1979**, *3*, 255.
(164) Holderbaum, T.; Gmehling, J. *Fluid Phase Equilib.* **1991**, *70*, 251.
(165) Horstmann, S.; Jabloniec, A.; Krafczyk, J.; Fischer, K.; Gmehling, J. *Fluid Phase Equilib.* **2005**, *227*, 157.
(166) Chen, J.; Fischer, K.; Gmehling, J. *Fluid Phase Equilib.* **2002**, *200*, 411.
(167) Yang, Q. Y.; Zhong, C. L. *Fluid Phase Equilib.* **2001**, *192*, 103.
(168) Guilbot, P.; Theveneau, P.; Baba-Ahmed, A.; Horstmann, S.; Fischer, K.; Richon, D. *Fluid Phase Equilib.* **2000**, *170*, 193.
(169) Horstmann, S.; Fischer, K.; Gmehling, J.; Kolar, P. *J. Chem. Thermodyn.* **2000**, *32*, 451.
(170) Horstmann, S.; Fischer, K.; Gmehling, J. *Fluid Phase Equilib.* **2000**, *167*, 173.
(171) Keshtkar, A.; Jalali, F.; Moshfeghian, M. *Fluid Phase Equilib.* **1998**, *145*, 225.
(172) Li, J.; Fischer, K.; Gmehling, J. *Fluid Phase Equilib.* **1998**, *143*, 71.
(173) Gmehling, J.; Li, J.; Fischer, K. *Fluid Phase Equilib.* **1997**, *141*, 113.
(174) Kiepe, J.; Horstmann, S.; Fischer, K.; Gmehling, J. *Ind. Eng. Chem. Res.* **2004**, *43*, 6607.
(175) Fischer, K.; Gmehling, J. *Fluid Phase Equilib.* **1996**, *121*, 185.
(176) Michelsen, M. L. *Fluid Phase Equilib.* **1990**, *60*, 213.
(177) Michelsen, M. L. *Fluid Phase Equilib.* **1990**, *60*, 47.
(178) Dahl, S.; Michelsen, M. L. *AIChE J.* **1990**, *36*, 1829.
(179) Lermite, C.; Vidal, J. *Fluid Phase Equilib.* **1992**, *72*, 111.
(180) Boukouvalas, C.; Spiliotis, N.; Coutsikos, P.; Tzouvaras, N.; Tassios, D. *Fluid Phase Equilib.* **1994**, *92*, 75.
(181) Wong, D. S. H.; Orbey, H.; Sandler, S. I. *Ind. Eng. Chem. Res.* **1992**, *31*, 2033.
(182) Gupte, P. A.; Rasmussen, P.; Fredenslund, A. *Ind. Eng. Chem. Fundam.* **1986**, *25*, 636.
(183) Skjold-Jorgensen, S. *Fluid Phase Equilib.* **1984**, *16*, 317.
(184) Skjold-Jorgensen, S. *Ind. Eng. Chem. Res.* **1988**, *27*, 110.
(185) Gros, H. P.; Bottini, S. B.; Brignole, E. A. *Fluid Phase Equilib.* **1996**, *116*, 535.
(186) Bottini, S. B.; Fornari, T.; Brignole, E. A. *Fluid Phase Equilib.* **1999**, *158−160*, 211.
(187) Haruki, M.; Shimoyama, Y.; Iwai, Y.; Arai, Y. *Fluid Phase Equilib.* **2003**, *205*, 103.
(188) Haruki, M.; Iwai, Y.; Arai, Y. *Fluid Phase Equilib.* **2001**, *189*, 13.
(189) Ishizuka, E.; Sarashina, E.; E.; Arai, Y.; Saito, S. *J. Chem. Eng. Jpn.* **1980**, *13*, 90.
(190) Espinosa, S.; Foco, G. M.; Bermudez, A.; Fornari, T. *Fluid Phase Equilib.* **2000**, *172*, 129.
(191) Tochigi, K.; Kurihara, K.; Kojima, K. *Ind. Eng. Chem. Res.* **1990**, *29*, 2142.
(192) Soave, G. *Chem. Eng. Sci.* **1972**, *4*, 1197.
(193) Mathias, P. M.; Copeman, T. W. *Fluid Phase Equilib.* **1983**, *13*, 91.
(194) Tochigi, K. *Fluid Phase Equilib.* **1998**, *144*, 59.
(195) Tochigi, K.; Futakuchi, H.; Kojima, K. *Fluid Phase Equilib.* **1998**, *152*, 209.
(196) Yu, Y. X.; Chen, Z.; Gao, G. H. *J. Tsinghua Univ. (Sci. & Technol.)* **2002**, *42*, 595.
(197) Ahlers, J.; Gmehling, J. *Fluid Phase Equilib.* **2001**, *191*, 177.
(198) Sander, B.; Fredenslund, A.; Rasmussen, P. *Chem. Eng. Sci.* **1986**, *41*, 1171.
(199) Kikic, I.; Fermeglia, M.; Rasmussen, P. *Chem. Eng. Sci.* **1991**, *46*, 2775.
(200) Cardoso, M.; O'Connell, J. P. *Fluid Phase Equilib.* **1987**, *33*, 315.
(201) Aznar, M.; Telles, A. S. *Braz. J. Chem. Eng.* **2001**, *18*, 127.
(202) Macedo, E. A.; Skovborg, P.; Rasmussen, P. *Chem. Eng. Sci.* **1990**, *45*, 875.
(203) Franks, F. *Water, A Comprehensive Treatise*; Plenum: New York, 1973.
(204) Achard, C.; Dussap, C. G.; Gros, J. B. *Fluid Phase Equilib.* **1994**, *98*, 71.
(205) Pitzer, K. S. *J. Phys. Chem.* **1973**, *77*, 268.
(206) Pitzer, K. S. *J. Am. Chem. Soc.* **1980**, *102*, 2902.
(207) Yan, W.; Topphoff, M.; Rose, C.; Gmehling, J. *Fluid Phase Equilib.* **1999**, *162*, 97.
(208) Li, J.; Polka, H. M.; Gmehling, J. *Fluid Phase Equilib.* **1994**, *94*, 89.
(209) Polka, H. M.; Li, J.; Gmehling, J. *Fluid Phase Equilib.* **1994**, *94*, 115.
(210) Li, J.; Lin, Y. Z.; Gmehling, J. *Ind. Eng. Chem. Res.* **2005**, *44*, 1602.
(211) Correa, A.; Comesana, J. F.; Correa, J. M.; Sereno, A. M. *Fluid Phase Equilib.* **1997**, *129*, 267.
(212) Huh, J. Y.; Bae, Y. C. *Chem. Eng. Sci.* **2002**, *57*, 2747.
(213) Joo, J. H.; Bae, Y. C.; Sun, Y. K. *Polymer* **2006**, *47*, 211.
(214) Lee, C. S.; Park, S. B.; Shim, Y. S. *Ind. Eng. Chem. Res.* **1996**, *35*, 4772.
(215) Collinet, E.; Gmehling, J. *Fluid Phase Equilib.* **2006**, *246*, 111.
(216) Collinet, E.; Gmehling, J. *Fluid Phase Equilib.* **2005**, *230*, 131.
(217) Ahlers, J.; Gmehling, J. *Ind. Eng. Chem. Res.* **2002**, *41*, 3489.
(218) Ahlers, J.; Gmehling, J. *Ind. Eng. Chem. Res.* **2002**, *41*, 5890.
(219) Wang, L. S.; Ahlers, J.; Gmehling, J. *Ind. Eng. Chem. Res.* **2003**, *42*, 6205.
(220) Ahlers, J.; Yamaguchi, T.; Gmehling, J. *Ind. Eng. Chem. Res.* **2004**, *43*, 6569.
(221) Li, Y. *Thermodynamics of Metal Extraction*; Tsinghua University Press: Beijing, 2003.
(222) Shoor, S. K.; Gubbins, K. E. *J. Phys. Chem.* **1969**, *73*, 498.
(223) Masterton, W. L.; Lee, T. P. *J. Phys. Chem.* **1970**, *74*, 1776.
(224) Pierotti, R. A. *Chem. Rev.* **1976**, *76*, 717.

(225) O'Connor, T. F.; Debenedetti, P. G.; Carbeck, J. D. *Biophys. Chem.* **2007**, *127*, 51.

(226) Graziano, G. *Chem. Phys. Lett.* **2006**, *432*, 84.

(227) Graziano, G.; Lee, B. *Biophys. Chem.* **2003**, *105*, 241.

(228) Brusatori, M. A.; Van Tassel, P. R. *J. Colloid Interface Sci.* **1999**, *219*, 333.

(229) Siderius, D. W.; Corti, D. S. *Ind. Eng. Chem. Res.* **2006**, *45*, 5489.

(230) Graziano, G. *J. Phys. Chem. B* **2006**, *110*, 11421.

(231) Heying, M.; Corti, D. S. *J. Phys. Chem. B* **2004**, *108*, 19756.

(232) Kodaka, M. *J. Phys. Chem. B* **2001**, *105*, 5592.

(233) Millero, F. J. *Chem. Rev.* **1971**, *71*, 147.

(234) Chen, L. L. *Handbook of Solvents*; Chemical Industry Press: Beijing, 1994.

(235) Lei, Z. G.; Wang, H. Y.; Xu, Z.; Zhou, R. Q.; Duan, Z. T. *Chem. Ind. Eng. Prog.* (*China*) **2001**, *20*, 6.

(236) Lei, Z. G.; Zhou, R. Q.; Duan, Z. T. *Fluid Phase Equilib.* **2002**, *200*, 187.

(237) Duan, Z. T.; Lei, L. H.; Zhou, R. Q. *Petrochem. Technol.* (*China*) **1980**, *9*, 350.

(238) Lei, L. H.; Duan, Z. T.; Xu, Y. F. *Petrochem. Technol.* (*China*) **1982**, *11*, 404.

(239) Zhang, Q. K.; Qian, W.; Jiang, W. J. *Petrochem. Technol.* (*China*) **1984**, *13*, 1.

(240) Zhao, C. P.; Zhao, C. M.; Chen, M. X. *Petrochem. Technol.* (*China*) **1989**, *18*, 236.

(241) Zhao, C. P.; Chen, M. X.; Zhao, C. M. *Chem. Eng.* (*China*) **1992**, *20*, 58.

(242) Oishi, T.; Prausnitz, J. M. *Ind. Eng. Chem. Process Des. Dev.* **1978**, *17*, 333.

(243) Prausnitz, J. M.; Lichtenthaler, R. N.; Azevedo, E. G. *Molecular Thermodynamics of Fluid-Phase Equilibria*; Prentice Hall: New Jersey 1999.

(244) Kouskoumvekaki, I. A.; Giesen, R.; Michelsen, M. L.; Kontogeorgis, G. M. *Ind. Eng. Chem. Res.* **2002**, *41*, 4848.

(245) Tande, B. M.; Deitcher, R. W.; Sandler, S. I.; Wagner, N. J. *J. Chem. Eng. Data* **2002**, *47*, 376.

(246) Kontogeorgis, G. M.; Coutsikos, P.; Tassios, D.; Fredenslund, A. *Fluid Phase Equilib.* **1994**, *92*, 35.

(247) Hansen, H. K.; Rasmussen, P.; Fredenslund, A.; Schiller, M.; Gmehling, J. *Ind. Eng. Chem. Res.* **1991**, *30*, 2352.

(248) Seiler, M.; Rolker, J.; Mokrushina, L. V.; Kautz, H.; Frey, H.; Arlt, W. *Fluid Phase Equilib.* **2004**, *221*, 83.

(249) Kontogeorgis, G. M.; Fredenslund, A.; Tassios, D. P. *Ind. Eng. Chem. Res.* **1993**, *32*, 362.

(250) Elbro, H. S.; Fredenslund, A.; Rasmussen, P. *Macromolecules* **1990**, *23*, 4707.

(251) Lindvig, T.; Michelsen, M. L.; Kontogeorgis, G. M. *Fluid Phase Equilib.* **2002**, *203*, 247.

(252) Zhong, C.; Sato, Y.; Masuoka, H.; Chen, X. *Fluid Phase Equilib.* **1996**, *123*, 97.

(253) Wibawa, G.; Takishima, S.; Sato, Y.; Masuoka, H. *Fluid Phase Equilib.* **2002**, *202*, 367.

(254) Wibawa, G.; Takishima, S.; Sato, Y.; Masuoka, H. *Fluid Phase Equilib.* **2003**, *205*, 353.

(255) Bertucco, A.; Mio, C. *Fluid Phase Equilib.* **1996**, *117*, 18.

(256) Holten-Andersen, J.; Rasmussen, P.; Fredenslund, A. *Ind. Eng. Chem. Res.* **1987**, *26*, 1382.

(257) Chen, F.; Fredenslund, A.; Rasmussen, P. *Ind. Eng. Chem. Res.* **1990**, *29*, 875.

(258) Bogdanic, G.; Fredenslund, A. *Ind. Eng. Chem. Res.* **1994**, *33*, 1331.

(259) Saraiva, A.; Bogdanic, G.; Fredenslund, A. *Ind. Eng. Chem. Res.* **1995**, *34*, 1835.

(260) Danner, R. P.; Hamedi, M.; Lee, B. C. *Fluid Phase Equilib.* **2002**, *194−197*, 619.

(261) High, M. S.; Danner, R. P. *AIChE J.* **1990**, *36*, 1625.

(262) Hamedi, M.; Muralidharan, V.; Lee, B. C.; Danner, R. P. *Fluid Phase Equilib.* **2003**, *204*, 41.

(263) Lee, B. C.; Danner, R. P. *AIChE J.* **1996**, *42*, 837.

(264) Lee, B. C.; Danner, R. P. *Fluid Phase Equilib.* **1997**, *128*, 97.

(265) Lee, B. C.; Danner, R. P. *Fluid Phase Equilib.* **1996**, *117*, 33.

(266) High, M. S.; Danner, R. P. *Fluid Phase Equilib.* **1989**, *53*, 323.

(267) Wang, C. Y.; Lei, Z. G. *Korean J. Chem. Eng.* **2006**, *23*, 102.

(268) Lindvig, T.; Economou, I. G.; Danner, R. P.; Michelsen, M. L.; Kontogeorgis, G. M. *Fluid Phase Equilib.* **2004**, *220*, 11.

(269) Choi, J. S.; Tochigi, K.; Kojima, K. *Fluid Phase Equilib.* **1995**, *111*, 143.

(270) Panayiotou, C.; Vera, J. H. *Polym. Eng. Sci.* **1982**, *22*, 345.

(271) Panayiotou, C.; Vera, J. H. *Polym. J.* **1982**, *14*, 681.

(272) Beckman, E.; Porter, R. S. *J. Polym. Sci., Part B: Polym. Phys.* **1987**, *25*, 1511.

(273) Chiou, J. S.; Barlow, J. W.; Paul, D. R. *J. Appl. Polym. Sci.* **1985**, *30*, 3911.

(274) Kazarian, S. G.; Brantley, N. H.; Eckert, C. A. *Vib. Spectrosc.* **1999**, *19*, 277.

(275) Fleming, O. S.; Chan, K. L. A.; Kazarian, S. G. *Vib. Spectrosc.* **2004**, *35*, 3.

(276) Fleming, O. S.; Kazarian, S. G. *Appl. Spectrosc.* **2004**, *58*, 390.

(277) Cooper, A. I. *J. Mater. Chem.* **2000**, *10*, 207.

(278) Sato, Y.; Yurugi, M.; Yamabiki, T.; Takishima, S.; Masuoka, H. *J. Appl. Polym. Sci.* **2001**, *79*, 1134.

(279) Shieh, Y. T.; Su, J. H.; Manivannan, G.; Lee, P. H. C.; Sawan, S. P. *J. Appl. Polym. Sci.* **1996**, *59*, 707.

(280) Shieh, Y. T.; Su, J. H.; Manivannan, G.; Lee, P. H. C.; Sawan, S. P.; Spall, W. D. *J. Appl. Polym. Sci.* **1996**, *59*, 695.

(281) Tomasko, D. L.; Li, H.; Liu, D.; Han, X.; Wingert, M. J.; Lee, L. J.; Koelling, K. W. *Ind. Eng. Chem. Res.* **2003**, *42*, 6431.

(282) Braun, J. M.; Guillet, J. E. *J. Polym. Sci. Polym. Chem.* **1975**, *13*, 1119.

(283) Braun, J. M.; Guillet, J. E. *Macromolecules* **1977**, *10*, 101.

(284) Rodgers, P. A. *J. Appl. Polym. Sci.* **1993**, *48*, 1061.

(285) Striolo, A.; Prausnitz, J. M. *Polymer* **2000**, *41*, 1109.

(286) Bicerano, J. *Prediction of Polymer Properties*; Marcel Dekker: New York, 1993.

(287) Boudouris, D.; Constantinou, L.; Panayiotou, C. *Fluid Phase Equilib.* **2000**, *167*, 1.

(288) Constantinou, L.; Gani, R. *AIChE J.* **1994**, *40*, 1697.

(289) Constantinou, L.; Prickett, S. E.; Mavrovouniotis, M. L. *Ind. Eng. Chem. Res.* **1993**, *32*, 1734.

(290) Seiler, M.; Jork, C.; Kavarnou, A.; Arlt, W.; Hirsch, R. *AIChE J.* **2004**, *50*, 2439.

(291) Kato, R.; Krummen, M.; Gmehling, J. *Fluid Phase Equilib.* **2004**, *224*, 47.

(292) Döker, M.; Gmehling, J. *Fluid Phase Equilib.* **2005**, *227*, 255.

(293) Wasserscheid, P.; Welton, T. *Ionic Liquids in Synthesis*; Wiley-VCH: Weinheim, 2003.

(294) Arlt, W.; Spuhl, O.; Klamt, A. *Chem. Eng. Process.* **2004**, *43*, 221.

(295) Welton, T. *Chem. Rev.* **1999**, *99*, 2071.

(296) Gordon, C. M. *Appl. Catal., A* **2001**, *222*, 101.

(297) Olivier, H. *J. Mol. Catal.* **1999**, *146*, 285.

(298) Hagiwara, R.; Ito, Y. *J. Fluorine Chem.* **2000**, *105*, 221.

(299) Zhao, D. B.; Wu, M.; Kou, Y.; Min, E. Z. *Catal. Today* **2002**, *74*, 157.

(300) Gregory, S. O.; Mahdi, M. A. O. *J. Mol. Catal. A: Chem.* **2002**, *187*, 215.

(301) Gusmao, K. B.; Queiroz, L. F. T.; de Souza, R. F.; Leca, F.; Loup, C.; Reau, R. *J. Catal.* **2003**, *219*, 59.

(302) Wang, B.; Kang, Y. R.; Yang, L. M.; Suo, J. S. *J. Mol. Catal. A: Chem.* **2003**, *303*, 19.

(303) Letcher, T. M.; Deenadayalu, N. *J. Chem. Thermodyn.* **2003**, *35*, 67.

(304) Klamt, A. *J. Phys. Chem.* **1995**, *99*, 2224.

(305) Klamt, A.; Jonas, V.; Burger, T.; Lohrenz, J. C. W. *J. Phys. Chem. A* **1998**, *101*, 5074.

(306) Klamt, A.; Eckert, F. *Fluid Phase Equilib.* **2000**, *172*, 43.

(307) Eckert, F.; Klamt, A. *Fluid Phase Equilib.* **2003**, *210*, 117.

(308) Klamt, A. *COSMO-RS: From Quantum Chemistry to Fluid Phase Thermodynamics and Drug Design*; Elsevier: Amsterdam, 2005.

(309) Spuhl, O.; Arlt, W. *Ind. Eng. Chem. Res.* **2004**, *43*, 852.

(310) Kato, R.; Gmehling, J. *J. Chem. Thermodyn.* **2005**, *37*, 603.

(311) Grensemann, H.; Gmehling, J. *Ind. Eng. Chem. Res.* **2005**, *44*, 7043.

(312) Jork, C.; Kristen, C.; Pieraccini, D.; Stark, A.; Chiappe, C.; Beste, Y. A.; Arlt, W. *J. Chem. Thermodyn.* **2005**, *37*, 537.

(313) Lei, Z.; Arlt, W.; Wasserscheid, P. *Fluid Phase Equilib.* **2006**, *241*, 290.

(314) Howard, A. E.; Kollman, P. A. *J. Med. Chem.* **1988**, *31*, 1669.

(315) Perdew, J. P. *Phys. Rev. B: Condens. Matter Mater. Phys.* **1986**, *33*, 8822.

(316) Perdew, J. P.; Chevary, J. A.; Vosko, S. H.; Jackson, K. A.; Pederson, M. R.; Singh, D. J.; Fiolhais, C. *Phys. Rev. B: Condens. Matter Mater. Phys.* **1992**, *46*, 6671.

(317) Schafer, A.; Huber, C.; Ahlrichs, R. *J. Chem. Phys.* **1994**, *100*, 5829.

(318) Fawzi, A. B.; Fahmi, A. A.; Jana, S. *Sep. Purif. Technol.* **2000**, *18*, 111.

(319) Fahmi, A. A.; Fawzi, A. B.; Rami, J. *Sep. Sci. Technol.* **1999**, *34*, 2355.

(320) Vane, L. M. *Sep. Purif. Technol.* **2002**, *27*, 83.

(321) Fahmi, A.; Datta, R. *Fluid Phase Equilib.* **1998**, *147*, 65.

(322) Lei, Z. G.; Zhang, J. C.; Chen, B. H. *J. Chem. Technol. Biotechnol.* **2002**, *77*, 1251.

(323) Jork, C.; Seiler, M.; Beste, Y. A.; Arlt, W. *J. Chem. Eng. Data* **2004**, *49*, 852.

(324) Zhao, J.; Dong, C.; Li, C.; Meng, H.; Wang, Z. *Fluid Phase Equilib.* **2006**, *242*, 147.

(325) Yagiuda, K.; Hemmi, A.; Ito, S.; Asano, Y.; Fushinuki, Y.; Chen, C. Y.; Karube, I. *Biosens. Bioelectron.* **1996**, *11*, 703.

(326) Williamson, S.; Gossop, M.; Powis, B.; Griffiths, P.; Fountain, J.; Strang, *J. Drug Alcohol Depend.* **1997**, *44*, 87.
(327) Kintz, P.; Samyn, N. *J. Chromatogr., B* **1999**, *733*, 137.
(328) Allen, D. L.; Oliver, J. S. *Forensic Sci. Int.* **2000**, *107*, 1.
(329) He, C.; Li, S.; Liu, H.; Li, K.; Liu, F. *J. Chromatogr., A* **2005**, *1082*, 143.
(330) Wu, J. C.; Lord, H.; Pawliszyn, J. *Talanta* **2001**, *54*, 655.
(331) Liu, H.; He, C.; Wen, D.; Liu, H.; Liu, F.; Li, K. *Anal. Chim. Acta* **2006**, *557*, 329.
(332) Yang, X. H.; Wang, X. C.; Zhang, X. M. *Anal. Chim. Acta* **2005**, *549*, 81.
(333) Liu, J. Q. *Chem. Eng. (China)* **1995**, *23*, 7.
(334) Wibawa, G.; Takahashi, M.; Sato, Y.; Takishima, S.; Masuoka, H. *J. Chem. Eng. Data* **2002**, *47*, 518.
(335) Wibawa, G.; Hatano, R.; Sato, Y.; Takishima, S.; Masuoka, H. *J. Chem. Eng. Data* **2002**, *47*, 1022.
(336) Lei, Z.; Arlt, W.; Wasserscheid, P. *Fluid Phase Equilib.* **2007**, *260*, 29.
(337) Li, J.; Lei, Z.; Chen, B.; Li, C. *Fluid Phase Equilib.* **2007**, *260*, 135.
(338) Nebig, S.; Bölts, R.; Gmehling, J. *Fluid Phase Equilib.* **2007**, *258*, 168.
(339) Weidlich, U.; Gmehling, J. *Ind. Eng. Chem. Res.* **1987**, *26*, 1372.
(340) Gmehling, J.; Möllmann, C. *Ind. Eng. Chem. Res.* **1998**, *37*, 3112.
(341) Lei, Z.; Ohyabu, H.; Sato, Y.; Inomata, H.; Smith, R. L. *J. Supercrit. Fluids* **2007**, *40*, 452.
(342) Lei, Z.; Chen, B.; Li, C. *Chem. Eng. Sci.* **2007**, *62*, 3940.
(343) Grensemann, H.; Gmehling, J. *Ind. Eng. Chem. Res.* **2005**, *44*, 1610.
(344) Foco, G. M.; Bottini, S. B.; Quezada, N.; de la Fuente, J. C.; Peters, C. J. *J. Chem. Eng. Data* **2006**, *51*, 1088.
(345) Heintz, A.; Verevkin, S. P. *J. Chem. Eng. Data* **2006**, *51*, 434.
(346) Heintz, A.; Kulikov, D. V.; Verevkin, S. P. *J. Chem. Eng. Data* **2002**, *47*, 894.
(347) Krummen, M.; Wasserscheid, P.; Gmehling, J. *J. Chem. Eng. Data* **2002**, *47*, 1411.

(348) Heintz, A.; Vasiltsova, T. V.; Safarov, J.; Bich, E.; Verevkin, S. P. *J. Chem. Eng. Data* **2006**, *51*, 648.
(349) Letcher, T. M.; Soko, B.; Ramjugernath, D.; Deenadayalu, N.; Nevines, A.; Naicker, P. K. *J. Chem. Eng. Data* **2003**, *48*, 708.
(350) David, W.; Letcher, T. M.; Ramjugernath, D.; Raal, J. D. *J. Chem. Thermodyn.* **2003**, *35*, 1335.
(351) Heintz, A.; Kulikov, D. V.; Verevkin, S. P. *J. Chem. Eng. Data* **2001**, *46*, 1526.
(352) Letcher, T. M.; Soko, B.; Reddy, P.; Deenadayalu, N. *J. Chem. Eng. Data* **2003**, *48*, 1587.
(353) Kato, R.; Gmehling, J. *Fluid Phase Equilib.* **2004**, *226*, 37.
(354) Deenadayalu, N.; Letcher, T. M.; Reddy, P. *J. Chem. Eng. Data* **2005**, *50*, 105.
(355) Letcher, T. M.; Domanska, U.; Marciniak, M.; Marciniak, A. *J. Chem. Thermodyn.* **2005**, *37*, 587.
(356) Letcher, T. M.; Reddy, P. *Fluid Phase Equilib.* **2005**, *235*, 11.
(357) Heintz, A.; Casas, L. M.; Nesterov, I. A.; Emel'yanenko, V. N.; Verevkin, S. P. *J. Chem. Eng. Data* **2005**, *50*, 1510.
(358) Heintz, A.; Verevkin, S. P. *J. Chem. Eng. Data* **2005**, *50*, 1515.
(359) Letcher, T. M.; Marciniak, A.; Marciniak, M.; Domanska, U. *J. Chem. Eng. Data* **2005**, *50*, 1294.
(360) Letcher, T. M.; Marciniak, A.; Marciniak, M.; Domanska, U. *J. Chem. Thermodyn.* **2005**, *37*, 1327.
(361) Mutelet, F.; Jaubert, J. N.; Rogalski, M.; Boukherissa, M.; Dicko, A. *J. Chem. Eng. Data* **2006**, *51*, 1274.
(362) Zhou, Q.; Wang, L. S. *J. Chem. Eng. Data* **2006**, *51*, 1698.
(363) Sumartschenkowa, I. A.; Verevkin, S. P.; Vasiltsova, T. V.; Bich, E.; Heintz, A.; Shevelyova, M. P.; Kabo, G. J. *J. Chem. Eng. Data* **2006**, *51*, 2138.
(364) Banerjee, T.; Khanna, A. *J. Chem. Eng. Data* **2006**, *51*, 2170.
(365) Deenadayalu, N.; Thango, S. H.; Letcher, T. M.; Ramjugernath, D. *J. Chem. Thermodyn.* **2006**, *38*, 542.